

Durham E-Theses

Late Quaternary glaciation of the continental shelf offshore of NW Ireland

PURCELL, CATRIONA,SHONA

How to cite:

PURCELL, CATRIONA,SHONA (2014) *Late Quaternary glaciation of the continental shelf offshore of NW Ireland*, Durham theses, Durham University. Available at Durham E-Theses Online:
<http://etheses.dur.ac.uk/10774/>

Use policy

The full-text may be used and/or reproduced, and given to third parties in any format or medium, without prior permission or charge, for personal research or study, educational, or not-for-profit purposes provided that:

- a full bibliographic reference is made to the original source
- a [link](#) is made to the metadata record in Durham E-Theses
- the full-text is not changed in any way

The full-text must not be sold in any format or medium without the formal permission of the copyright holders.

Please consult the [full Durham E-Theses policy](#) for further details.

Abstract

The continental shelf offshore of NW Ireland is an area where marine geological and chronological data pertaining to the advance and retreat of the last British-Irish Ice Sheet (BIIS) remains sparse and therefore ice sheet limits are poorly constrained. This is important because well constrained and well dated ice sheet limits are critical to developing accurate ice sheet models representative of the dynamics of the BIIS. The aim of this study is to reconstruct the timing, extent and nature of the last ice sheet advance and retreat across the NW Ireland continental shelf through the sedimentological analysis and radiocarbon dating of marine sediment cores.

A transect of thirteen cores from offshore of Donegal Bay, NW Ireland provide direct evidence for extensive glaciation of the continental shelf. Sedimentological and chronological evidence from the cores indicates that the ice sheet extended to the shelf edge at the last glacial maximum (LGM) and that subsequent retreat from this shelf edge position was underway by 23,700 cal. yr BP. Initial retreat from the shelf edge was rapid and associated with a large calving event. Retreat across the mid shelf was slow and punctuated by the formation of a series of moraines. The ice sheet was likely a grounded tidewater margin in which meltwater contributed strongly to both retreat and glacimarine sedimentation. The ice sheet had attained an inner shelf position, inshore of a prominent moraine in Donegal Bay (the 'Donegal Bay Moraine'), before 17,800 cal. yr BP, and therefore in contrast to previous work, it is inferred that this moraine pre-dates the Killard Point Stadial. Foraminiferal analysis from two cores (CE-08-003 and CE-08-010) shows the presence of a range of glacimarine taxa associated with ice sheet retreat across the shelf followed by the appearance of warmer Atlantic water taxa later in the cores. Collectively this suggests that ocean forcing did not drive initial retreat from the shelf and it emphasises the role of meltwater during deglaciation of the NW shelf.



Durham
University

Department of Geography

**Late Quaternary glaciation of the continental shelf offshore of
NW Ireland**

Catriona Purcell

Grey College

March 2014

Submitted for the degree of Masters by research

Table of Contents

Abstract	i
Table of contents	iii
Statement of copyright	vi
List of Tables	vii
List of Figures	viii
<i>Acknowledgements</i>	

Chapter 1

1	Introduction	1
	1.1 Introduction	1
	1.2 Aims and research questions	4
	1.3 Study area	4

Chapter 2

2	Synopsis of the conflicting views on the BILS extent during the LGM in NW Ireland	6
	2.1 Introduction	6
	2.2 Early studies prior to 1980	6
	2.3 Terrestrial investigations from 1980	9
	2.4 Timing of ice sheet retreat	12
	2.5 Recent marine geophysical investigations 2002-2012	14
	2.6 Summary	19

Chapter 3

3	Methods	20
	3.1 Introduction	20
	3.2 Core site selection	20
	3.3 Core sedimentology	23
	3.4 Shear strength	25
	3.5 Magnetic susceptibility and gamma density	25
	3.6 ¹⁴ C dating	25
	3.7 Biological analysis	26

3.7.1 Foraminiferal abundance	26
3.7.2 Sampling	27

Chapter 4

4	Results and interpretation	28
	4.1 Introduction	28
	4.2 Chronology	28
	4.3 Core sedimentology- Description	31
	4.3.1 Core CE-08-003	32
	4.3.2 Core CE-08-004	35
	4.3.3 Core CE-08-005	38
	4.3.4 Core CE-08-008	39
	4.3.5 Core CE-08-009	41
	4.3.6 Core CE-08-010	42
	4.3.7 Core CE-08-011	45
	4.3.8 Core CE-08-015	47
	4.3.9 Core CE-08-017	50
	4.3.10 Core CE-08-018	51
	4.3.11 Core CE-08-025	54
	4.3.12 Core CE-08-031	55
	4.3.13 Core CE-08-033	57
	4.4 Foraminifera abundance analysis	59
	4.5 Lithofacies Associations	62
	4.5.1 LFA 1: Brown diamict and mud association	62
	4.5.2 LFA 2: Mud and sand association	62
	4.5.3 LFA 3: Sand and gravel association	63
	4.5.4 LFA 4: Sand and gravel association	63
	4.6 Core sedimentology- Interpretation	65
	4.6.1 LFA 1: Brown diamict and mud association	65
	4.6.2 LFA 2: Mud and sand association	66
	4.6.3 LFA 3: Sand and gravel association	67
	4.6.4 LFA 4: Sand and gravel association	67
	4.7 Summary	68

Chapter 5

5	Discussion	69
	5.1 The sedimentary record of ice sheet advance and retreat on the NW continental shelf	69

5.2 Timing and nature of ice sheet retreat	71
5.3 Wider implications	73

Chapter 6

6	Conclusion	77
	6.1 Introduction	77
	6.2 Main findings	77
	6.2.1 BIS extended to the shelf edge during the LGM	77
	6.2.2 Initial retreat from the shelf edge was rapid and associated with a large calving event	77
	6.2.3 Mid shelf and inner shelf cores indicate the slow retreat of a tidewater ice margin	78
	6.2.4 The ice sheet had retreated to inner Donegal Bay by c.17,800 cal. yr BP	78
	6.2.5 The drivers of ice sheet retreat are still unclear	78
	6.3 Recommendations for future research	78
	6.3.1 Improving core chronologies for the continental shelf	78
	6.3.2 Improve our understanding on the forcing behind ice sheet collapse	79
	6.3.3 Reconstructing the dynamics of the BIIS	79
7	References	80
8	Appendices	86

Statement of copyright

“The copyright of this thesis rests with the author. No quotation from it should be published without the author's prior written consent and information derived from it should be acknowledged.”

List of tables

Chapter 3

Table 1	Details of the investigated cores	22
Table 2	Lithofacies identified in cores from the continental shelf offshore of northwest Ireland	23

Chapter 4

Table 3	NW Ireland continental shelf radiocarbon dates. Specific dates are discussed below within the section on sediment description	29
----------------	---	-----------

List of figures

Chapter 1

- Fig.1** Location map showing the study area 2
- Fig.2** Location map of the study area of the continental shelf off NW Ireland showing large-scale geomorphology, including a suite of moraines (blue, green, purple shading) and slope gullies (yellow lines). The locations of cores on the shelf (black dots) and slope (red dots) are also shown. The 13 vibrocores analysed in this thesis are numbers 3, 4, 5, 8, 9, 10, 11, 15, 17, 18, 25, 31 and 33. 3
- Fig. 3** Map showing onshore geology of Donegal 5

Chapter 2

- Fig. 4** Map of Northwest Ireland, showing the Lough Foyle–Bloody Foreland ice limit proposed by Stephens and Synge (1965). The map also shows the location of Malin Head. 8
- Fig. 5** Bathymetric map of NW Ireland shelf showing positions of cores collected and also interpreted moraines. The Donegal Bay moraine runs between cores 4 and 5 10
- Fig. 6** Map of the proposed ice sheet limits pre-LGM ~27 kyr 11
- Fig. 7** Map displaying the location of Belderg and Corvish. 13
- Fig. 8** Location map of the Rockall Trough, Rockall Bank, the continental slope and the Malin shelf. These sites have been the focus of extensive geophysical investigations. 15
- Fig. 9** Geomorphological interpretation of the Rockall Trough and continental slope established by Sacchetti *et al.*, (2012b). This map illustrates the maturity of the canyon systems distal to the Donegal Bay moraines. 18

Chapter 3

- Fig. 10** Location map showing cores collected in cruise CE-08 of the Celtic Explorer from the NW Irish continental shelf. The cores that are the focus of this study are indicated by boxes. 21

Chapter 4

- Fig. 11** Map showing the radiocarbon dates obtained from the continental shelf and the location of cores they were obtained from. 30
- Fig. 12 X-rays of various lithofacies. A)** Dmm with a few large clasts dispersed throughout (CE-08-011; 39-78 cm) **B)** Dmm with a clast rich layer (CE-08-010; 455-479 cm) **C)** Fl and Fm lithofacies and a few shells (CE-08-003; 442-472 cm) **D)** Fm lithofacies (CE-08-003; 150-190 cm) **E)** Suf and Sm lithofacies with a high abundance of shelly material (CE-08-033; 0-30 cm). 31
- Fig. 13 X-rays of various lithofacies. A)** Gms with a few large clasts (CE-08-010; 278-322 cm) **B)** Sm and a few shells (CE-08-015; 240-278 cm) **C)** Sh, Sm lithofacies and a shell (CE-08-003; 353-393 cm) **D)** Fl and bioturbated Fm with a few scattered pebbles (CE-08-010; 415-455 cm) **E)** Dmm with numerous clasts dispersed throughout but one particular large outsized clast (CE-08-008; 226-264 cm). 31
- Fig. 14** Sedimentology, magnetic susceptibility and gamma density of core CE-08-003. Core log, calibrated ¹⁴C dates and associated sedimentation rates and LFAs are shown on the left. 34

Fig. 15	Sedimentology, magnetic susceptibility and gamma density for core CE-08-004. Core log, calibrated 14C dates and LFAs are shown on the right. Magnetic susceptibility and gamma density values for the core are also shown.	37
Fig. 16	Sedimentology of core CE-08-005, with the core log and associated LFAs.	38
Fig. 17	Sedimentology, magnetic susceptibility, gamma density and shear strength values for core CE-08-008.	40
Fig. 18	Sedimentology for core CE-08-009, with the core log and associated LFAs.	41
Fig. 19	Sedimentology, magnetic susceptibility, gamma density and shear strength values for core CE-08-010, with calibrated 14C date.	44
Fig. 20	Sedimentology, magnetic susceptibility, gamma density and shear strength values for core CE-08-011.	46
Fig. 21	Sedimentology, magnetic susceptibility and gamma density for core CE-08-015, with calibrated 14C date.	49
Fig. 22	Sedimentology of core CE-08-017 and associated LFAs.	51
Fig. 23	Sedimentology, magnetic susceptibility and gamma density for core CE-08-018, with calibrated 14C date.	53
Fig. 24	Sedimentology of core CE-08-025 and associated LFAs.	54
Fig. 25	Sedimentology, magnetic susceptibility and gamma density of core CE-08-031.	56
Fig. 26	Sedimentology, magnetic susceptibility, gamma density and shear strength values for core CE-08-033.	58
Fig. 27	Foraminiferal assemblage from core CE-08-003, classified into two faunal assemblage zones. Also shown are mollusc data and 14C dates from core CE-08-003.	60
Fig. 28	Foraminiferal assemblage from core CE-08-010, classified into two faunal assemblage zones, the 14C date obtained this core is also shown.	61
Fig. 29	Colour coded core logs displaying lithofacies and associated LFAs.	64

Chapter 5

Fig. 30	Location map showing cores collected during cruise CE-08 of the Celtic Explorer from the NW Irish continental shelf, the prominent arcuate moraines (blue shading) including the Donegal Bay moraine and three of the obtained from radiocarbon dating in this study	69
Fig. 30	Map showing a selection of radiocarbon dates (from this study) plotted against the isochrones proposed by C. Clark et al. (2012).	74

Acknowledgements

I would like to express my deepest appreciation to my primary supervisor Prof Colm Ó Cofaigh who even on the other side of the world still managed to supply endless guidance, feedback and support. A special thank you to my secondary supervisor Dr Jerry Lloyd, for his invaluable insight into the world of benthic foraminifera and for his guidance and support throughout my MSc.

I would also like to acknowledge the funding I received from the Durham University Geography department through the 'Research Masters bursary' for which I am particularly grateful.

I would like to thank the Durham lab technicians, in particular Neil Tunstall for his help with the Geotek Multi-Sensor Core Logger.

Radiocarbon dates in this thesis were provided through the UK NERC research grant 'Britice-Chrono' (PI, Professor Chris Clark, University of Sheffield)

Thank you also to the staff of the X-Ray Department at Newcastle RVI, especially Brian Hobson for granting me permission to use his x-ray machines for my research and Suzanne Doney for taking time out of her busy day to x-ray my cores.

My gratitude goes out to James Scourse for being so patient and understanding in the completion of my MSc thesis.

In addition, thank you to Prof Jaap van der Meer who helped me with my first dissertation on LGM ice sheet limits and whose enthusiasm for teaching and fieldwork has had a lasting effect.

Finally, thank you to Mum and Dad for their endless support throughout and for encouraging me to pursue my interests. I would also like to thank my fellow geography postgraduate students and friends at Grey College for such an enjoyable year, it all went too fast.

Introduction

1.1 Introduction

The extent and dynamics of the British-Irish Ice Sheet (BIIS) have been the focus of scientific research for over a century with particular emphasis on understanding and reconstructing the extent of the ice sheet during the Last Glacial Maximum (LGM) and its subsequent retreat (e.g., Hull, 1891; Charlesworth, 1924; Stephens and Synge, 1965; Bowen et al. 2002; Ballantyne et al. 2007; Scourse et al. 2009; C. Clark et al. 2012; Chiverrell et al. 2013). However in some areas, such as offshore of northwest Ireland (Fig. 1), LGM ice sheet limits remain poorly constrained and therefore controversial. The majority of the research surrounding the LGM limit of the last BIIS has been based on terrestrial data (e.g., Bowen et al. 2002; McCabe et al. 2007; Greenwood & Clark 2009). In NW Ireland there have been many attempts within the literature to constrain the glacial events of Donegal, however chronological data remain sparse (Benetti et al. 2010; Ballantyne et al. 2007). This underscores the need to establish a well constrained chronology for the BIIS in the Donegal region.

The BIIS had an extensive marine margin which has been confirmed by the large suites of moraines that have been identified on the continental shelf surrounding Britain and Ireland (Bradwell et al. 2008; Benetti et al. 2010; Dunlop et al., 2010; Ó Cofaigh et al. 2012). With developments in marine geophysics (e.g., the now routine application of multibeam swath bathymetry to map landforms on continental shelves) the imaging and interpretation of seafloor geomorphology has been significantly advanced (e.g. Dowdeswell & Ó Cofaigh 2002). Access to marine geophysical data has formerly been limited or fragmentary (Ó Cofaigh et al. 2012). However, due to projects such as the Irish National Sea Bed survey, high quality marine geophysical data has been collected from much of Ireland's coastal waters and this data is now publically accessible. By examining the multibeam swath bathymetry data collected through the Irish National Sea Bed survey, we now have direct evidence that ice extended onto the continental shelf offshore of NW Ireland and developed a large moraine complex (Ó Cofaigh et al. 2012; Fig. 2). However, this moraine complex is undated and it is important that such geomorphological interpretations are ground truthed using sedimentological data and that such data are then dated to constrain ice sheet history temporally.

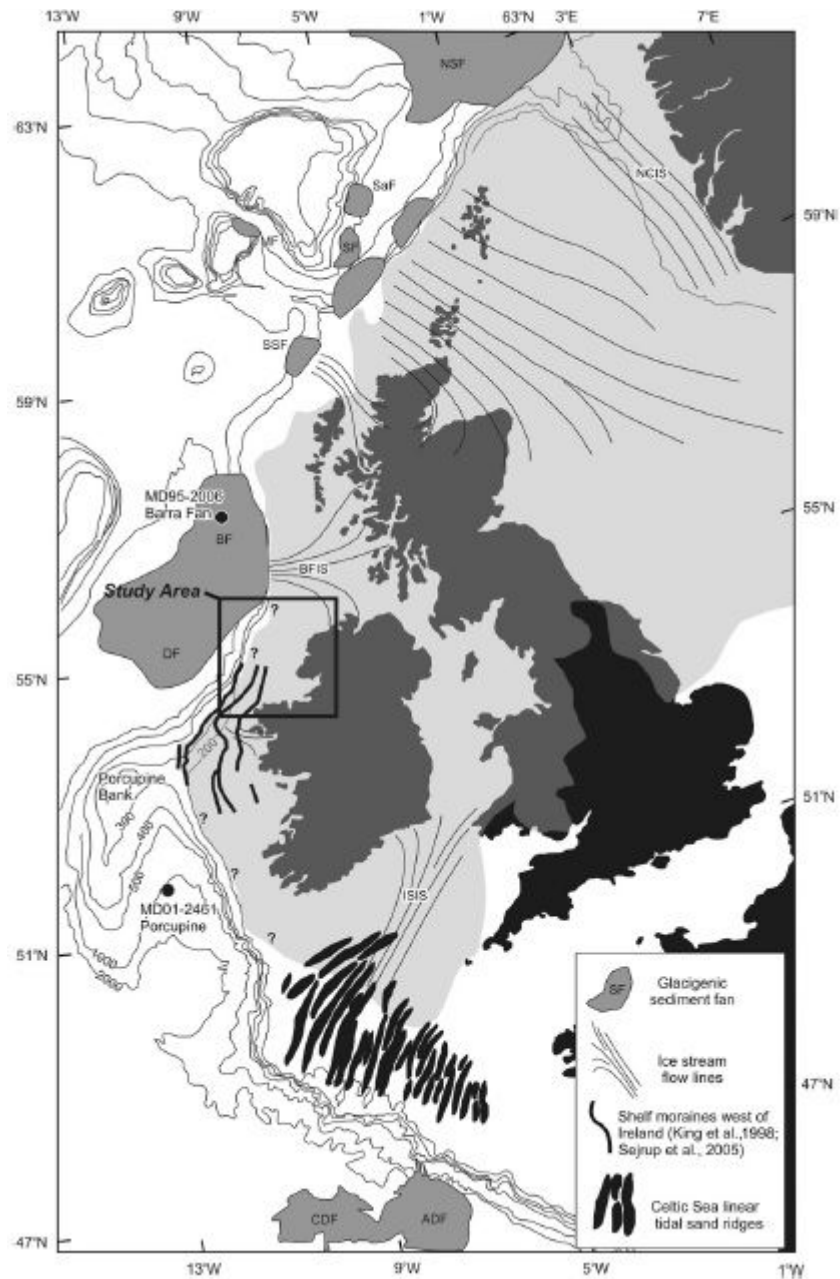


Fig. 1. Location map showing the study area (From Ó Cofaigh *et al.*, 2012).

This research aims to provide dating control in order to resolve conflicting reconstructions of the ice sheet at the LGM on the NW Irish shelf. It is essential to have well defined, well-dated limits for the BIIS at the LGM for the development of accurate ice sheet models (Chiverrell & Thomas 2010). In addition to this, establishing the nature of the BIIS and the dynamics of its NW margin will enable the study to further our understanding of the ice sheets possible impact(s) on the thermohaline circulation due to its North Atlantic location (Ó Cofaigh *et al.* 2012).

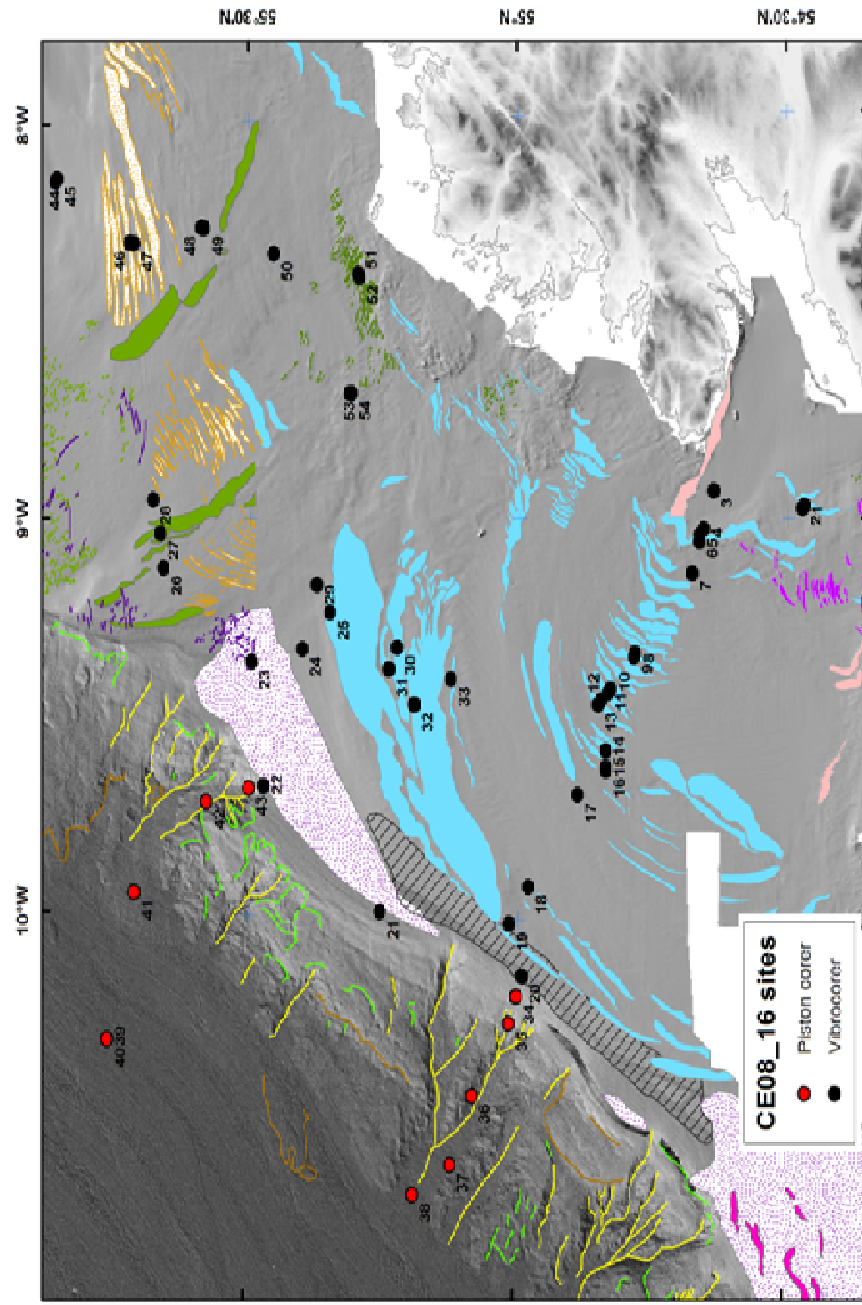


Fig. 2. Location map of the study area of the continental shelf off NW Ireland showing large-scale geomorphology, including a suite of moraines (blue, green, purple shading) and slope gullies (yellow lines). The locations of cores on the shelf (black dots) and slope (red dots) are also shown. The 13 vibrocores analysed in this thesis are numbers 3, 4, 5, 8, 9, 10, 11, 15, 17, 18, 25, 31 and 33. (Ó Cofaigh *et al.* 2012)

1.2 Aim and research questions

The aim of this thesis is to reconstruct the timing, extent and nature of the last advance and retreat of the British-Irish Ice Sheet (BIIS) on the continental shelf offshore of NW Ireland from marine sediment cores (Fig. 2).

Research questions

1. What was the extent of the ice sheet offshore of NW Ireland at the LGM?
2. What is the nature of the sedimentary record of ice sheet advance and retreat across the shelf?
3. What was the timing and rate of deglaciation across the continental shelf?
4. Are there linkages between the response of the last ice sheet off NW Ireland and wider North Atlantic climate and oceanographic forcing during the last cold stage, in particular during deglaciation?

1.3 Study area

This research is focussed on the NW Ireland continental shelf and encompasses an area of 30,000 km² (between 55° 40' and 54° 18' N, and 7° 50' and 11° 4' W) (Fig. 1 and Fig. 2). This area was formerly under the NW sector of the BIIS and was drained by the Donegal Bay Ice Stream at the LGM (Sacchetti et al. 2012b). The local terrestrial topography is dominated by uplands reaching over 500 m.a.s.l which are northeast-southwest trending, and characteristically composed of Dalradian pelites, psammites and schists, whereas, the lowlands are dominated by Carboniferous limestones and shales (Fig. 3; George & Oswald 1957; Ballantyne et al. 2007).

The geomorphology of the study area has been heavily influenced by Late Quaternary glaciation which has shaped the landscape and accounts for the superficial deposits around the area (McCabe 1993). At the LGM ice was centred on the Donegal highlands and would have fed the ice streams that extended on to the continental shelf (Knight & McCabe 1997). From the mouth of Donegal Bay the continental shelf extends 80 km to the shelf edge (Fig. 2) with the shelf break at 120 m water depth.

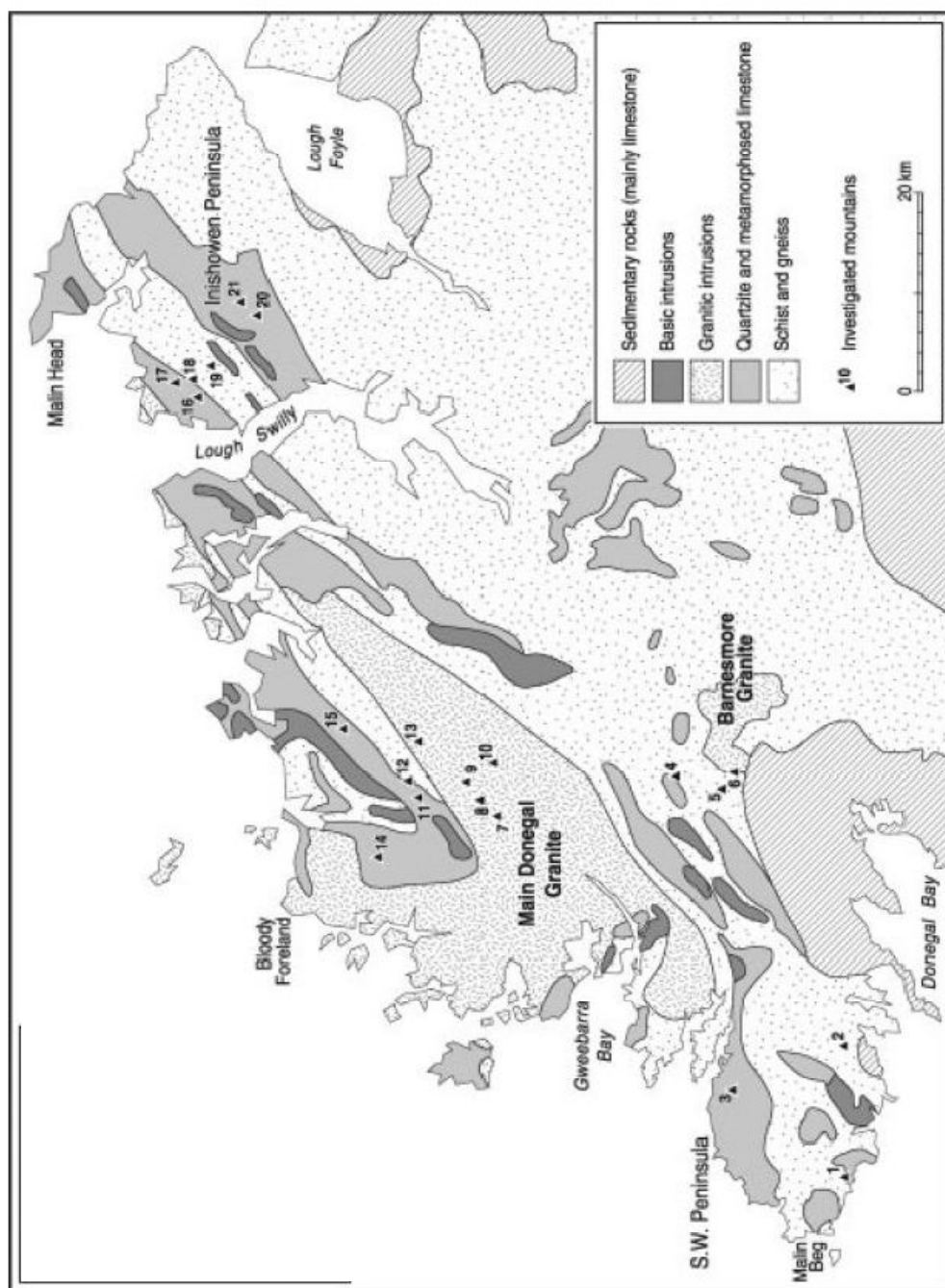


Fig.3. Map showing onshore geology of Donegal (From Ballantyne et al. 2007).

Chapter Two

Synopsis of the conflicting views on the BIIS extent during the LGM in NW Ireland.

2.1 Introduction

Defining the limits of the BIIS has been a focus of scientific research for over a century (e.g. Hull, 1891; Charlesworth, 1924; Stephens and Synge, 1965; Bowen et al. 2002; Ballantyne et al. 2007). NW Ireland is one particular region over which there has been considerable debate, particularly with respect to the extent of the last glaciation. It has recently been established that the BIIS was a very dynamic ice sheet with numerous ice-margin fluctuations (Ballantyne et al. 2007; McCabe et al. 2007). This differs to the traditional reconstructions which favoured a monotonic ice sheet recession (Mitchell et al. 1973). However, there remains a fundamental question as to the extent of the ice sheet in NW Ireland at the LGM. Numerous theories have been proposed over the years, with some authors supporting a land-terminating ice sheet (Synge and Stephens 1965), whereas others have supported an offshore LGM ice sheet extent with either an extensive continental shelf edge position (Ó Cofaigh et al. 2012) or a more restricted inner shelf position (McCabe et al. 2007).

Establishing the precise timing of the LGM is fundamental when discussing the extent of the BIIS during the LGM. The LGM is defined here as the last global glacial maximum when eustatic sea level was at a minimum. However, various dates have been proposed for this such as Mix et al. (2001) 23-19kyr BP, whereas more recently Clark et al. (2009) propose a period of 26.5-19kyr BP based on relative sea level data from various sites. The Clark et al. (2009) chronology for the LGM (26.5-19kyr BP) is adopted here.

2.2 Early studies prior to 1980

The majority of the early research literature (1860-1930) of the Irish sector of the BIIS at the LGM, supported a land terminating ice sheet margin. For example Hull (1891) regarded Bloody Foreland as the northern limit of ice sheet advance (Fig. 4). This theory was adopted and revised by Synge and Stephens (1965) who proposed that the ice sheet terminated between Lough Foyle-Bloody Foreland (LF-BF line) (Fig. 4). This line runs along the northwest coast of Ireland and was identified by the presence of drumlins, 'kame moraines' and kettle holes. This ice limit has been incorporated into subsequent reconstructions of the BIIS (e.g. Bowen et al. 1986; Boulton *et al.*, 1991). Conversely, Charlesworth (1924) suggested that the BIIS extended offshore onto the continental shelf during the LGM. He also proposed that the retreat from

the shelf was slow and was punctuated by the construction of moraines with no subsequent re-advance. After analysing areal patterns of glacial erosion Synge (1978) revised previous interpretations in support of an ice advance onto the continental shelf during the LGM. Charlesworth (1973) suggested that instead of the LF-BF line representing the LGM ice limit it could alternatively represent a post-LGM re-advance limit. This interpretation has been supported by subsequent studies such as that of Warren (1992).

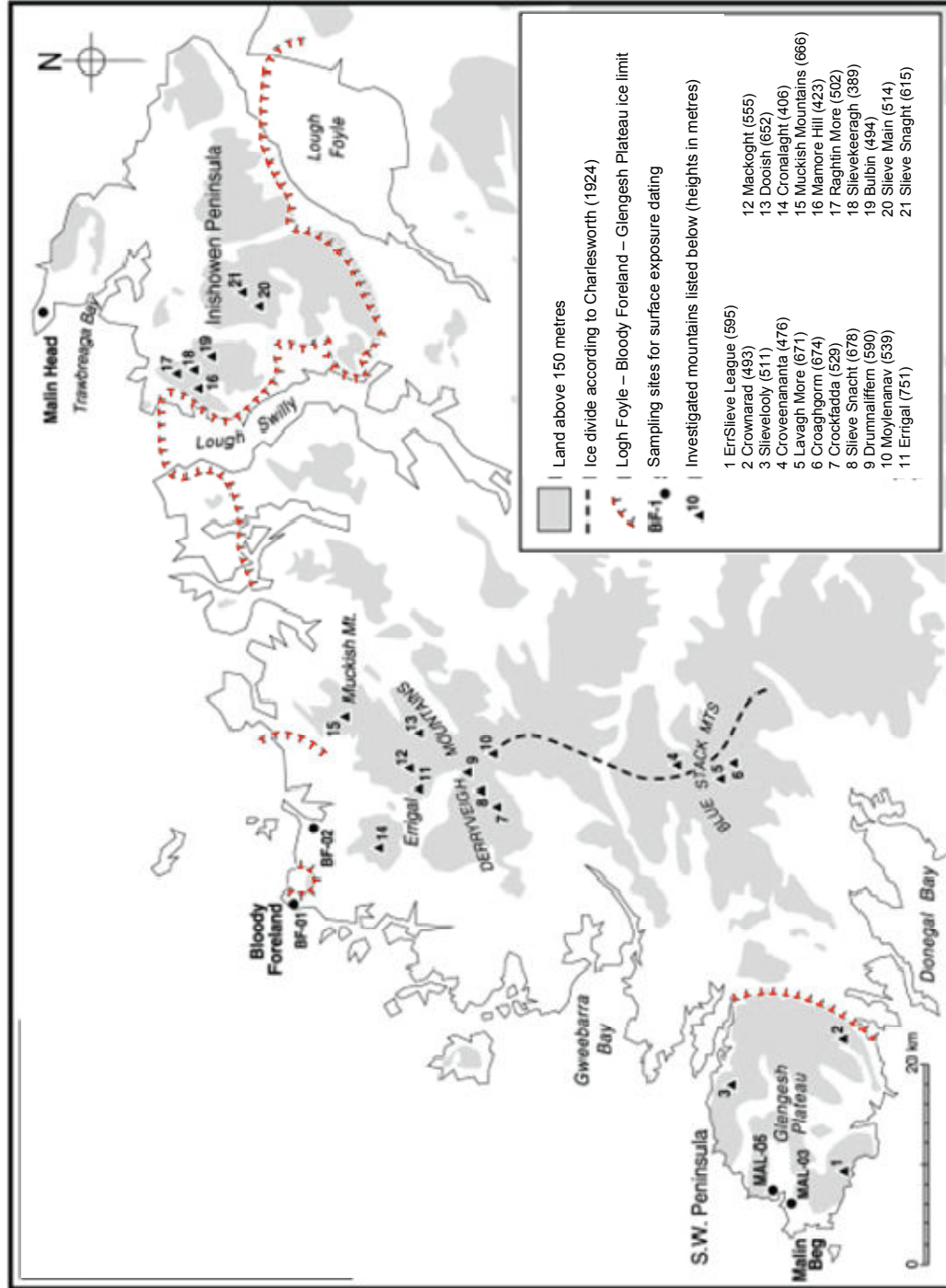


Fig. 4. Map of Northwest Ireland, showing the Lough Foyle-Bloody Foreland ice limit proposed by Stephens and Synge (1965). The map also shows the location of Malin Head. (Modified from Ballantyne, 2007).

2.3 Terrestrial investigations from 1980

Many studies have incorporated the Stephens and Synge (1965) or Synge (1969) mapped ice limits into their reconstructions. Bowen et al. (1986) proposed a predominantly land-terminating ice sheet at the LGM, with the northward limit defined by the LF-BF line. McCabe et al. (1998) also incorporated the original ice sheet limit proposed by Stephens and Synge (1965) as the ice limit during the Killard Point Stadial (ca 15.6 kyr BP). The Killard Point Stadial correlates with Heinrich event 1 (ca. 14 ^{14}C kyr BP or 16.5 cal kyr BP) and has been suggested to be associated with an extensive ice sheet re-advance in Ireland and Britain at that time (McCabe et al. 1998). On the basis of a compilation of cosmogenic surface exposure dates, amino acid geochronology and AMS ^{14}C dates, Bowen et al. (2002) proposed that the NW sector of the BIIS was most extensive prior to the LGM, reaching a maximum extent on the NW shelf at ca 37 ^{36}Cl kyr BP, and was subsequently more restricted during the LGM. They suggested that during the LGM the BIIS was positioned between the 'Donegal Bay' moraine (the prominent ridge at the mouth of Donegal Bay, as referred to by Ó Cofaigh et al. 2012) and the outer shelf (Fig. 5). This interpretation has been supported by McCabe et al. (2007) who propose that the NW sector of the BIIS was extensive ~20 kyrs prior to the LGM, but that the ice sheet was actually less extensive during the LGM itself being confined to Donegal Bay until at least 19 cal kyr BP.

A number of subsequent studies have supported a shelf edge position pre-LGM such as (J. Clark et al. 2012). These authors have proposed that the NW sector of the BIIS extended to the shelf edge between 27-28 cal kyr BP (Fig. 6), i.e., prior to the global LGM and held a shelf edge position until ~24 kyr BP (C. Clark et al. 2012; J. Clark et al. 2012).

Ballantyne et al. (2007) reconstructed the Donegal ice dome during the LGM based on cosmogenic surface exposure dating and trimline mapping. On the basis of four cosmogenic ^{10}Be exposure ages (18.6 ± 1.4 to 15.9 ± 1.0 k yr) from 3 glacially transported boulders and ice moulded bedrock, they proposed that the BIIS extended at least 20 km offshore during the LGM. Based on glacial geomorphological mapping Greenwood & Clark (2009) also propose an extensive ice sheet that extended through Donegal Bay out onto the continental shelf during the LGM.

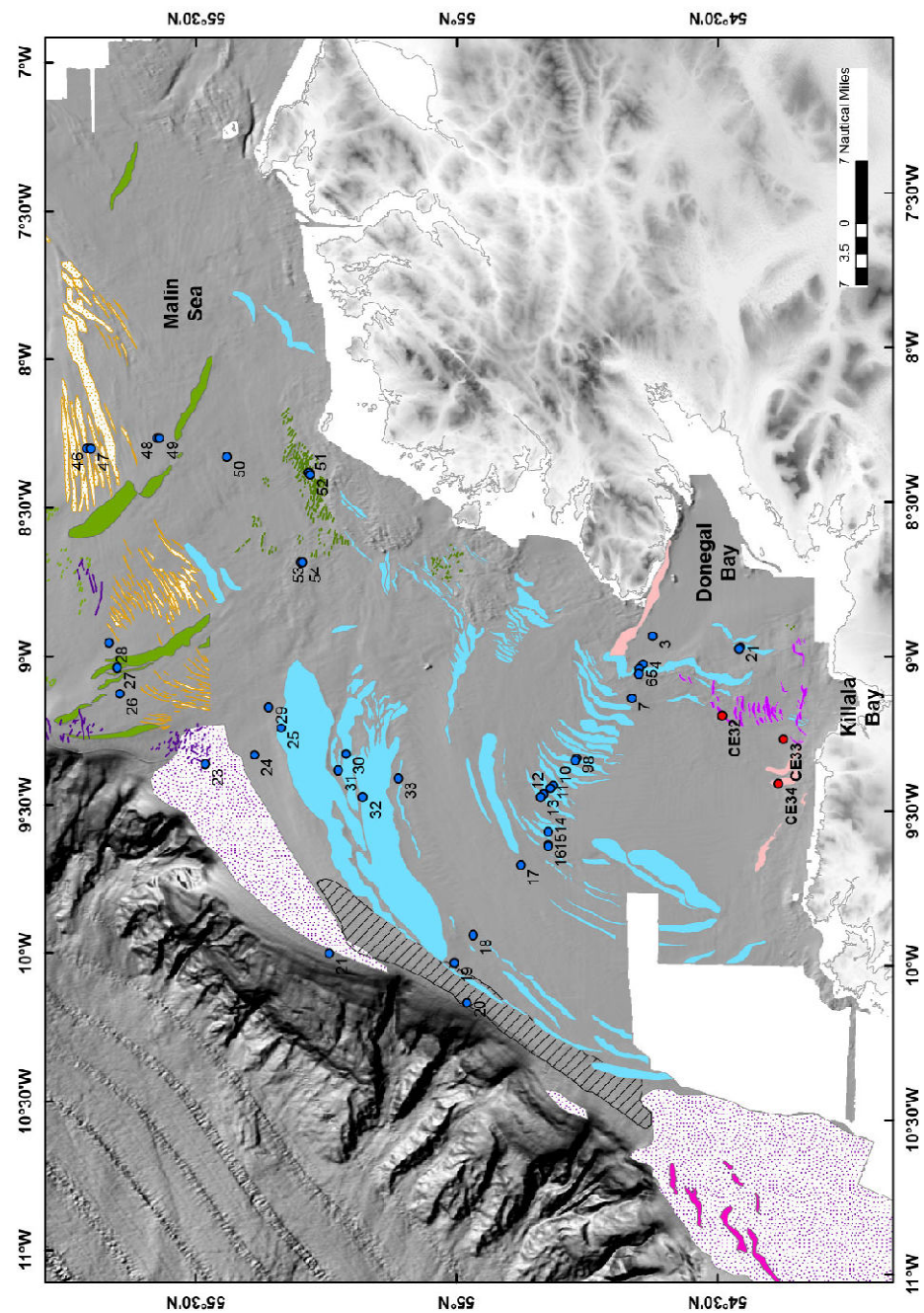


Fig. 5. Bathymetric map of NW Ireland shelf showing positions of cores collected and also interpreted moraines. The Donegal Bay moraine runs between cores 4 and 5 (Ó Cofaigh *et al.*, (2012)

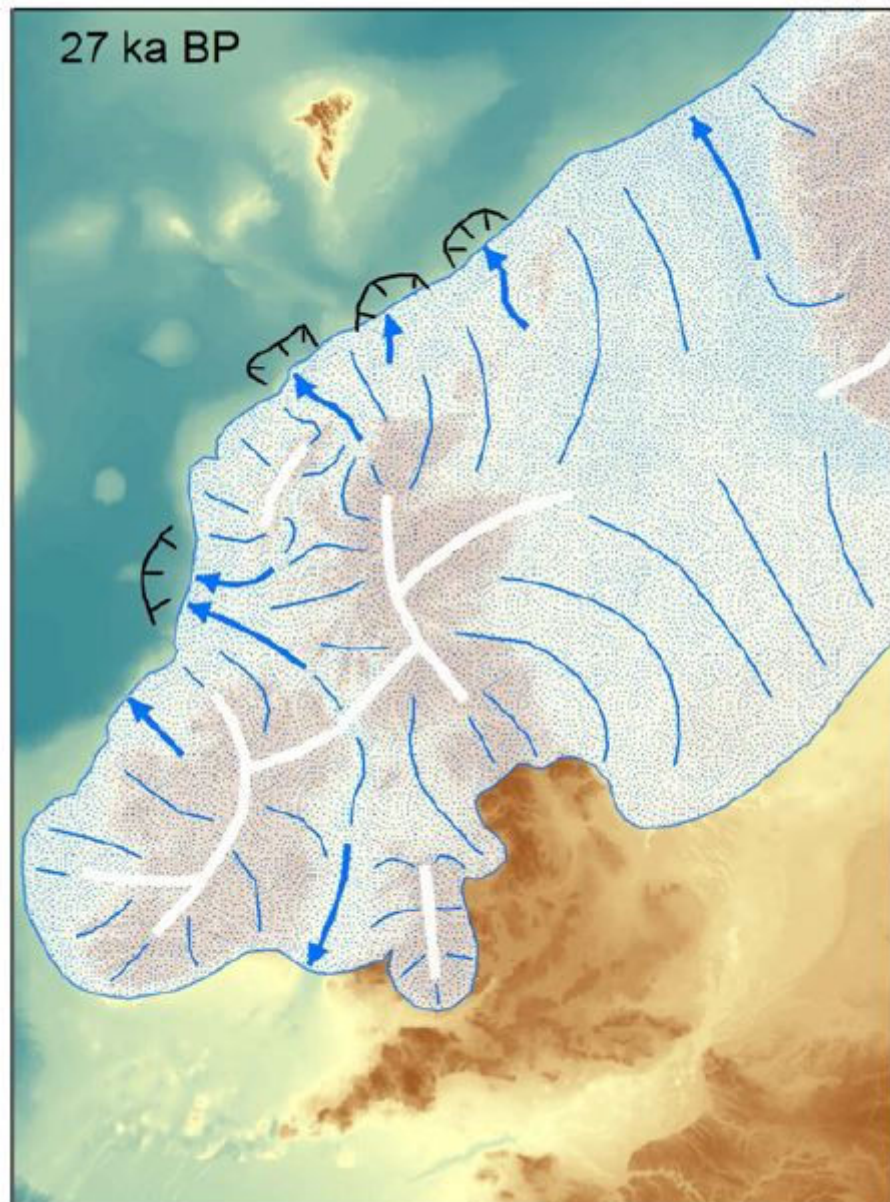
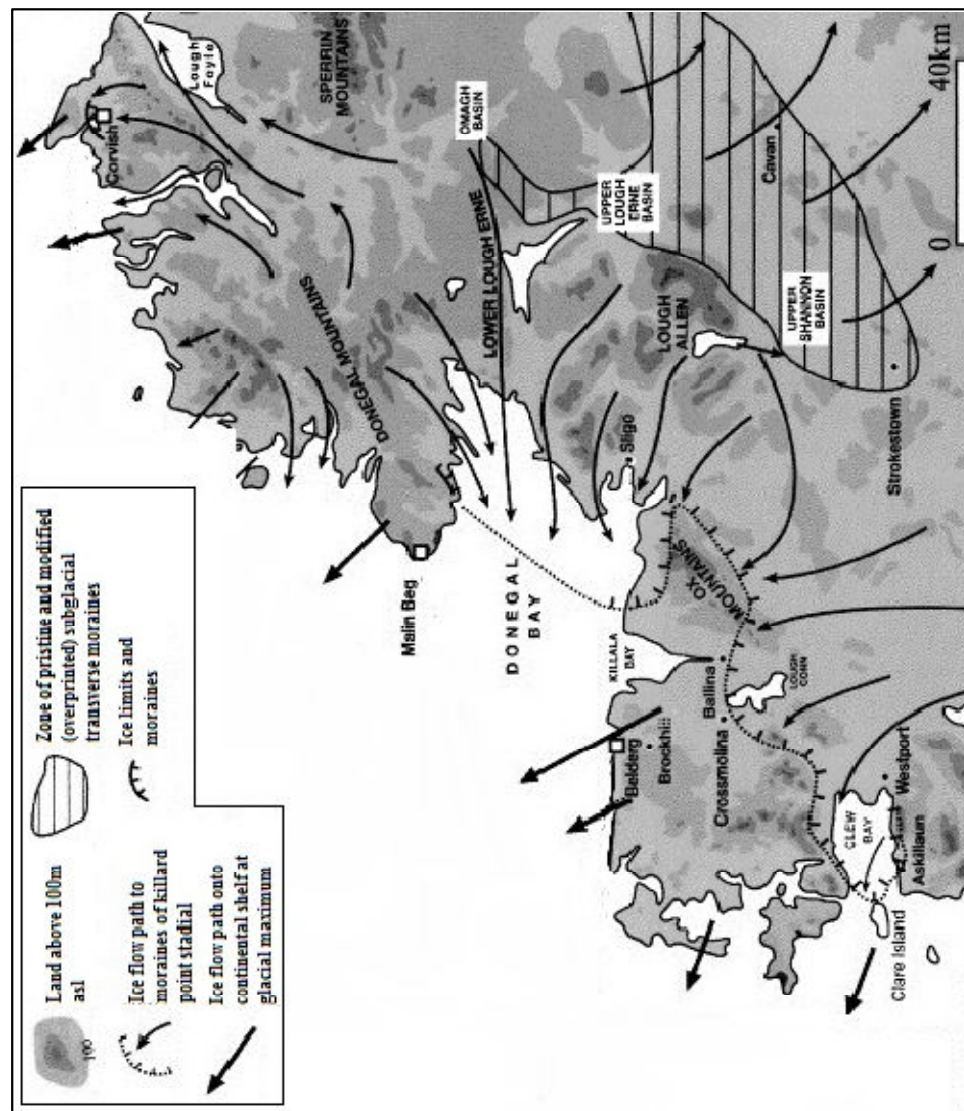


Fig. 6. Map of the proposed ice sheet limits pre-LGM ~27 kyr (From C. Clark et al. 2012).

2.4 Timing of ice sheet retreat

There are numerous studies that propose a range of dates for the retreat of the BIIS offshore of NW Ireland. Dates such as 26 kyr BP (C. Clark et al. 2012), 25 kyr BP (Bowen et al. 2002) and 23 kyr BP (J. Clark et al. 2012) have been suggested for initial retreat from the ice sheet's shelf edge position. Subsequent retreat to the inner shelf was slow, as confirmed by the suite of moraines that are present on the inner shelf. McCabe (1986) and McCabe & Clark (2003) propose glacimarine deposition occurred between ~16.0 kyr BP and ~15.0 kyr BP on the inner shelf and that North Donegal (Corvish, Fig. 7) was deglaciated before Donegal Bay (Belderg, Fig. 7). They state that after retreat the margin remained within inner Donegal Bay as a tidewater ice margin before undergoing a re-advance during the Killard Point Stadial (15 -14 kyr BP) (McCabe & Clark 2003), whereas C. Clark et al. (2012) suggest that the ice sheet did not undergo a subsequent re-advance but remained close to the present coastline (17 kyr BP). It has been stipulated that a rise in sea level triggered the destabilisation of the ice sheet (C. Clark et al. 2012). McCabe & Clark (2003) suggest that the deglaciation of the Irish Sea Basin due to the warming of the North Atlantic Ocean would have raised sea levels and destabilised the marine terminating ice margin offshore of Donegal.

Fig. 7. Map displaying the location of Belderg and Corvish (Edited from McCabe *et al.* 2005).



2.5 Recent marine geophysical investigations 2002-2012

The majority of these previous studies were based on terrestrial sampling and, as a result, provide relatively little direct information for ice sheet advance and retreat on the NW continental shelf. This clearly illustrates the importance of incorporating offshore data from marine geology and geophysics in the reconstruction of marine-terminating ice sheet margins. Marine sediment cores from both continental shelf and continental slope positions have been very useful in constraining the presence of ice sheets on continental shelves. Wilson & Austin (2002) studied marine sediment cores extracted from the Barra Fan. The cores identified an increase in sediment delivery to the Barra Fan shortly after 30 kyr, indicating that the BIIS had extended to the shelf edge. This supports the analysis of deep sea sediment cores by Scourse et al. (2009) who studied IRD on the NE Atlantic continental slope. They record ice sheet growth after 29 cal kyr BP and as a consequence they concluded that the BIIS must have had a marine calving margin near the shelf edge for IRD to be present in the sediment cores. This suggests the BIIS reached its maximum extent *before* the globally defined LGM.

Essential to the reconstruction of ice sheet limits on the continental shelf is the analysis of marine geophysical data. The Irish Government implemented an extensive campaign to survey Ireland's territorial waters from 1999. Since then, the Geological Survey of Ireland and the Irish Marine Institute have coordinated the Irish National Seabed Survey (INSS) and the Integrated Mapping for the Sustainable Development of Ireland's Marine Resource (INFOMAR) programmes. These programmes have involved the acquisition of multibeam swath bathymetry, backscatter and sub-bottom acoustic profiler data. This data is freely available to the science community and consequently offers an unrivalled opportunity to study the offshore ice limits.

A number of recent publications have used this resource to interpret the continental shelf geomorphology and thus infer ice sheet dynamics of the BIIS (e.g. Dunlop et al. 2010; Benetti et al. 2010; Ó Cofaigh et al. 2012; Sacchetti et al. 2012a; Sacchetti et al. 2012b). These publications have investigated the Malin Shelf, the continental shelf offshore of NW Ireland and also the deep water geomorphology of the Rockall Bank, Rockall Trough and the continental slope (Fig. 8) with the aim to gain a more comprehensive understanding of the BIIS and provide an offshore context to the terrestrial studies that have dominated the literature in this region.

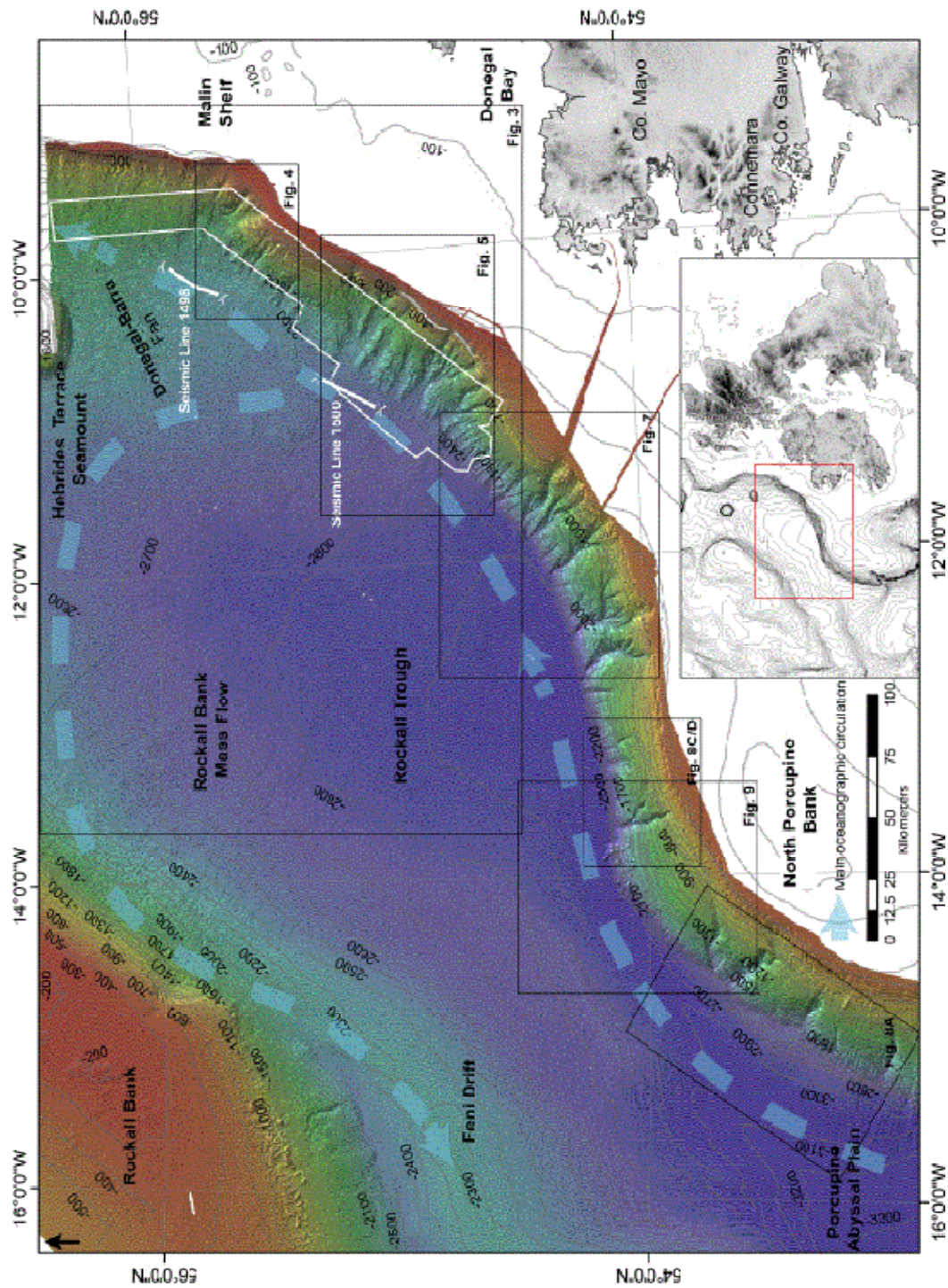


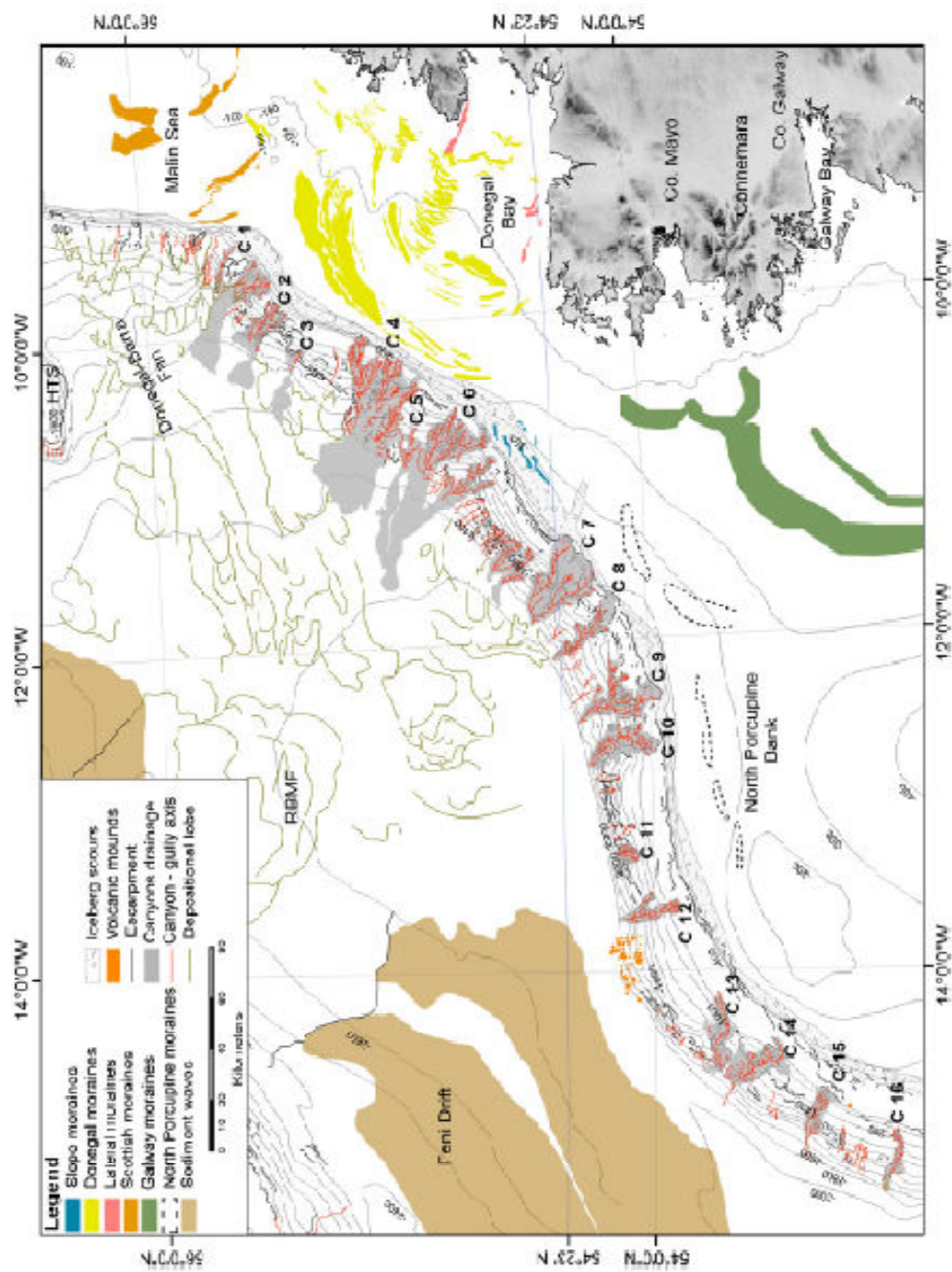
Fig. 8. Location map of the Rockall Trough, Rockall Bank, the continental slope and the Malin shelf. These sites have been the focus of extensive geophysical investigations. (From Sacchetti *et al.*, 2012b)

Benetti et al. (2010) mapped a series of end and recessional moraines on the continental shelf offshore of NW Ireland. Drumlins are located on the north eastern sector of the study area and record a north westerly flow of ice. Benetti et al. (2010) also interpret a series of iceberg scours distal to the outermost shelf moraine. These scours have an east to west orientation in the northern part of the study area, whereas the iceberg scours located in the southern part of the study area have a northeast to southwest orientation, which has been attributed to a change in the direction of the palaeocurrent. Other notable glacial geomorphological features identified within the study area include the gully and canyon systems located on the upper continental slope. In accordance with Sacchetti et al. (2012b) the authors also propose that the location of these features correlate with the BIIS presence at the shelf edge or nearby on the outermost shelf. This study provides evidence that confirms the presence of the BIIS on the continental shelf.

Ó Cofaigh et al. (2012) used marine geophysical data to investigate the glacial features on the continental shelf off the northwest coast of Ireland. The research identified arcuate moraines on the shelf documenting former ice margin positions (Fig. 5). These moraines provide evidence for a grounded ice sheet that extended over 80km from the mouth of Donegal Bay. Although Ó Cofaigh et al. (2012) did not report any dating, they did use dated marine stratigraphic records from other regional studies on the north west margin (Scourse et al. 2009) to propose a provisional chronology for ice sheet advance and retreat from the shelf edge. They suggested that the ice sheet extended to the shelf edge between 29-27 cal kyr BP and remained at the shelf edge until about 24 cal kyr BP after which it then underwent recession. Ó Cofaigh et al. (2012) infer that the retreat of the BIIS from the continental shelf was slow and episodic as illustrated by the closely spaced nested arcuate moraines present on the continental shelf (Donegal moraines). Iceberg scour marks are identified distal to the outermost moraines, indicating initial retreat was linked to a large calving event (which could have been driven by a rise in sea level). The study also discusses the interpretation of the Donegal Bay moraine. J. Clark et al. (2012) suggested that the Donegal Bay moraine represents the ice sheet limit during the Killard Pont Stadial, whereas Ó Cofaigh et al. (2012) propose an alternative explanation that the moraine could be recessional, formed as the BIIS retreated from its outer shelf position. Ó Cofaigh et al. (2012) provide unequivocal evidence for extensive glaciation on the continental shelf offshore of northwest Ireland. The study demonstrates that the NW sector of the BIIS held an extensive shelf edge position pre-LGM, which is in agreement with numerous publications (e.g. Bowen et al. 2002; Wilson & Austin 2002; McCabe et al. 2007; Scourse et al. 2009; C. Clark et al. 2012; J. Clark et

al. 2012) . The authors also suggest that initial retreat of the ice sheet from the shelf edge commenced after 24 kyr BP, which is similar to the ~23 kyr BP retreat from the Barra fan proposed by J. Clark et al. (2012). The chronology of ice sheet advance and retreat on the continental shelf, however, is still poorly constrained and requires further chronological controls.

Sacchetti et al. (2012a) and (2012b) investigated the deep water geomorphology of Rockall bank, Rockall Trough and the continental slope utilising multibeam bathymetric and backscatter data (Fig. 8). The authors identify iceberg scours located on the eastern part of Rockall Bank and identify them as icebergs that were calved from the Irish sector of the BIIS. Sacchetti et al. (2012a) claims that these icebergs were calved after ~46 kyr BP from the grounded ice sheet near the shelf edge offshore of Donegal. Sacchetti et al. (2012b) also identify well developed canyon systems located in front of the large arcuate moraines identified near the shelf edge offshore of Donegal (Fig. 9). The canyon systems distal to the Donegal Bay moraines are very mature and illustrate a high level of complexity. The maturity exhibited by these canyon systems suggest that the BIIS was in close proximity to the shelf edge and held this marginal position for a considerable period of time during the LGM.



2.6 Summary

As illustrated by the review above, there are conflicting interpretations of the timing and extent of the last BIIS in NW Ireland at, and following, the LGM. Central to this uncertainty has been the complete absence of any direct sedimentological and chronological data from the adjacent continental shelf. Although there is direct geomorphological evidence for a grounded ice sheet on the shelf offshore of NW Ireland (Benetti et al. 2010; Dunlop et al. 2010; Ó Cofaigh et al. 2012) this evidence is undated. This project is therefore fundamental to resolving the debate that surrounds the LGM limit(s) of the BIIS offshore of Northwest Ireland. Dating of the marine sediment cores will contribute to providing a chronology of ice sheet advance and retreat on the continental shelf, which will assist in determining the extent of the BIIS offshore of NW Ireland during the LGM. Analysis of the sediment cores will provide essential data for understanding the pattern of ice sheet advance and retreat across the shelf. It has been stated that the BIIS was a very dynamic ice sheet (McCabe et al. 2007) and retreat was episodic with many still stands and minor re-advances (Ó Cofaigh et al. 2012). These interpretations will be tested through the description, interpretation and dating of the various lithofacies identified throughout the cores that are the subject of this thesis from the NW shelf offshore of Donegal Bay. It has also been suggested that initial ice sheet retreat was triggered by rising sea level, and it has been proposed that ice sheet break-up coincided with Heinrich Event 2 (~24 cal kyr BP) (Bradwell et al. 2008; Ó Cofaigh et al. 2012). This proposal will be examined through the analysis of the benthic foraminifera within the sediment cores, thus identifying the impact of the North Atlantic climate and oceanographic forcing on the break-up of the BIIS.

Chapter 3-Methods

3.1 Introduction

This chapter details the methods used to address the research questions discussed in Chapter 1. Here I describe core site selection, the methods used to investigate core sedimentology, the proxies used to reconstruct ice sheet dynamics and the dating methods employed to develop a chronology for the retreat of the BIIS from the NW continental shelf.

The marine sediment cores were collected from the continental shelf offshore of NW Ireland on the RV Celtic Explorer in July 2008. The aim of the cruise was to reconstruct the behaviour of the British Irish Ice Sheet during the last glaciation. Long and short sediment cores were collected by using a gravity corer and a vibrocorer.

3.2 Core site selection

The cores were extracted across the continental shelf offshore NW Ireland from the mouth of the Donegal Bay to the shelf edge. The cores form a transect across a series of arcuate moraines on the continental shelf identified from marine geophysical data (Ó Cofaigh et al. 2012). These moraines mark the extent of the former lobate margin of the BIIS on the shelf. Cores were extracted from the moraine crest and within the inter-moraine troughs in order to constrain the timing of deglaciation (Fig. 10) and to determine their associated core lithostratigraphy and sedimentology. Following collection, the cores were stored horizontally +3°C at Durham University and the University of Ulster, Coleraine.

Thirteen cores from the transect were examined for the purpose of this study (Fig. 10 and Table 1). Physical analysis of the cores comprised a multi-proxy approach to characterise the sediment facies, and thus establish the depositional environment as well as to identify the suitable horizons and material within the cores for dating.

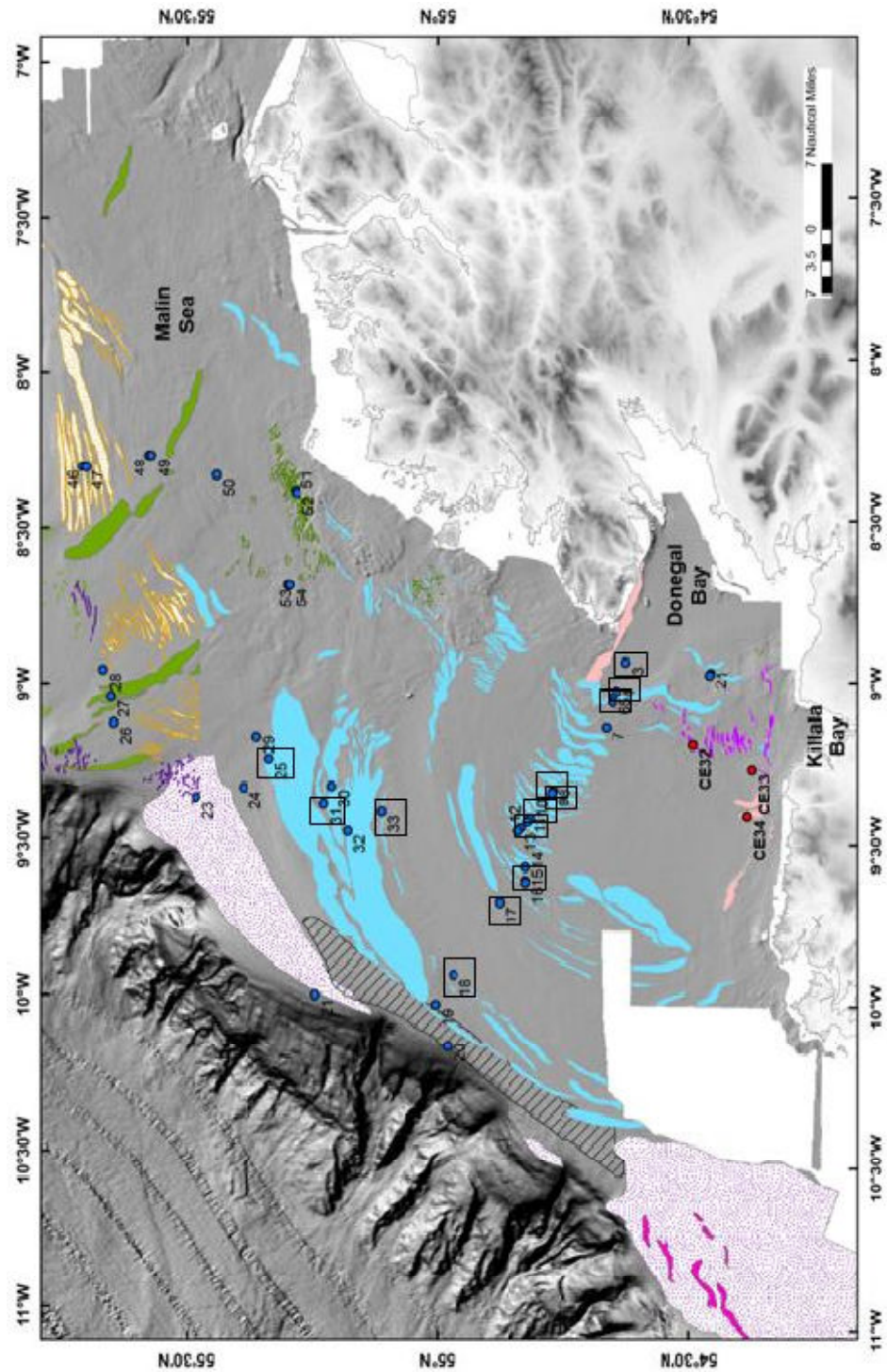


Fig. 10. Location map showing cores collected in cruise CE-08 of the Celtic Explorer from the NW Irish continental shelf. The cores that are the focus of this study are indicated by boxes.

Table 1. Details of the investigated cores.

Core name	LOCATION		Water depth (m)	Recovery (m)
	Latitude (°N)	Longitude (°W)		
CE_08-003	54.6415	-8.9324	88 m	5.12
CE_08-004	54.6601	-9.0260	82 m	2.75
CE_08-005	54.6679	-9.0414	67.2m	6.9
CE_08-008	54.7869	-9.3348	90m	3.22
CE_08-009	54.7891	-9.3428	90m	0.74
CE_08-010	54.8316	-9.4233	97 m	5.78
CE_08-011	54.8370	-9.4332	95m	1.39
CE_08-015	54.8403	-9.6179	99 m	2.78
CE_08-017	54.8926	-9.6872	122 m	1.3
CE_08-018	54.9822	-9.9172	122.3m	1
CE_08-025	55.3532	-9.2366	100.3m	0.58
CE_08-031	55.2436	-9.3785	113m	137.5
CE_08-033	55.1288	-9.4019	110m	268.7

3.3 Core sedimentology

The 13 cores were split and logged from core sections and x-rays in order to characterise the stratigraphy and lithofacies. Lithofacies were logged using a modified version of Eyles et al. (1983) lithofacies coding (See Table 2). Information was recorded on sediment texture, lithology, colour, grain size, sedimentary structures, sorting and bed contacts in order to assign lithofacies which were subsequently used in determining their genesis and associated depositional environment (i.e subglacial, ice proximal, ice distal or postglacial) (Evans and Benn 2004; Ó Cofaigh et al. 2005; Hogan et al. 2010a; Kilfeather et al. 2011; Ó Cofaigh et al. 2013).

Table 2. Lithofacies identified in cores from the continental shelf offshore of northwest Ireland (after Evans and Benn, 2004).

Lithofacies	Description
Dmm	Diamict, matrix supported and massive
Gms	Gravel, matrix supported and massive
Gm	Gravel, clast supported and massive
Gfu	Gravel, upward fining (normal grading)
Sm	Sand, massive
Sh	Sand, very fine to very coarse, with laminae
Suf	Sand, upward fining
Fm	Mud, massive
Fl	Mud, fine lamination often with minor fine sand

Grain size and sedimentary structures are important for both the classification and interpretation of lithofacies. The presence of massive diamictons within the cores could indicate a subglacial till, a debris flow deposit, iceberg rafted sediment or iceberg turbate (Dowdeswell & Elverhöi 2002; Dowdeswell et al. 2004; Ó Cofaigh et al. 2005; Kilfeather et al. 2011) whereas massive mud can be attributed to the vertical accretion of suspended sediments in a distal glacimarine environment (Hogan et al. 2010a). A deglacial sequence in a shelf core will be recognised by a sequence of till overlain by a glacimarine deposit which can be identified due their laminated nature such as those discussed by Ó Cofaigh & Dowdeswell (2001). Identifying the facies that indicate full glacial conditions overlain by deglacial sediments will be important to constrain the timing of deglaciation.

Identifying unconformities or breaks in a sequence will help interpret the stratigraphic record. The absence of certain lithofacies or an ‘overstep’ in the record will reveal information about the nature of deglaciation. An overstep is produced when a section of an older sequence is removed by erosion from a younger series, and therefore produces a discordance or ‘break’ within the sequence (Park, 1997). The absence of deglacial

sediments within the cores could indicate a rapid retreat of the margin (Ó Cofaigh et al. 1999; Ó Cofaigh and Evans, 2007) or the removal of the deglacial sequence by current reworking (Anderson et al. 1984; Evans et al. 2005)

The internal structure, sorting of grain sizes, lithofacies bed contacts and the presence or absence of ice rafted debris (IRD) in the cores can also be used to investigate the depositional environment. The internal structure of the lithofacies could be matrix or clast-supported. The presence of a clast supported gravel within a core could indicate the winnowing of fine grained sediments by bottom currents (Anderson et al. 1984), conversely, a matrix supported normal graded gravel could indicate a mass flow deposit (Dowdeswell et al. 1994). Sorting is an important parameter when trying to determine how to classify the sediment and therefore infer its depositional environment. Well sorted sediment implies that the deposition of the lithofacies was associated with water, whereas a poorly sorted sediment implies the chaotic deposition of sediment (i.e. a diamicton is a poorly sorted sediment; Evans and Benn, 2004).

The bed contacts between lithofacies characterise the transition between various depositional environments such as erosional, gradational, conformable, deformed or faulted (Eyles et al. 1983; Evans and Benn, 2004). An erosional bed contact can indicate an abrupt change or a hiatus in the depositional environment (Evans and Benn, 2004). Gradational or conformable bed contacts are classified as non-erosive contacts usually associated with a passive process such as suspension settling (Ó Cofaigh & Dowdeswell 2001). In contrast, deformed or faulted bed contacts usually result from deformation post deposition (Evans and Benn, 2004).

The presence of IRD within sediment cores reveals information about the nature of ice sheet retreat. IRD can be identified within a core through a multitude of techniques such as wet sieving (Haapaniemi et al. 2010) or using x-rays (cf. Grobe 1987). This study used x-rays, shear strength data and bed contacts to determine IRD. IRD grains can be identified within cores by counting grains >2 mm in x-rays (cf. Grobe 1987). IRD diamict can be differentiated from glacial till because of its lower shear strength and the presence of gravel or coarse sand lenses which result from the overturning of an iceberg (Dowdeswell et al. 1994). Analysis of the bed contacts, sorting and IRD in this study will determine the nature of retreat and whether initial retreat was associated with a large calving event at the shelf edge as proposed by Benetti et al. (2010) and Ó Cofaigh et al. (2012).

3.4 Shear strength

Shear strength tests have been used in many studies to help identify and distinguish between subglacial sediments and glacimarine deposits (Kilfeather et al. 2011). For the purpose of this study, shear strength will be used to aid classification of the lithofacies and to support interpretations established through other sediment characteristics. Shear strength measurements using a torvane were taken for cores CE-08-008, CE-08-010, CE-08-011 and CE-08-033 at 10cm intervals. Where the core lithofacies were more complex, smaller intervals were used to ensure characterisation of the shear strength of all of the lithofacies. Shear strength can be a very useful tool for identifying and classifying till. High shear strength values associated with a diamict lithofacies are likely to reflect the loading and compaction of grounded glacier ice (Evans & Pudsey 2002; Evans et al. 2005), whereas lower shear strength values can be associated with softer till which display lower shear strength values because of its higher porosity (Ó Cofaigh et al. 2007).

3.5 Magnetic susceptibility and gamma density

Magnetic susceptibility and gamma density are useful parameters that are often used to aid stratigraphic correlation between cores and for the detection of ice-rafted debris (Kilfeather et al. 2011). Magnetic susceptibility and gamma density have also been used by some authors as a mechanism to identify subglacial till (Heroy & Anderson 2007).

Nine of the thirteen cores were analysed using a Geotek multi-sensor core logger (MSCL). These cores were chosen because they displayed glacial and deglacial sediments and were a suitable length (more than 1 metre). The split cores were cleaned using a microscope slide and covered with cling film in order to reduce the effect of surface roughness which will affect how the probe rests on the core and therefore effects the measurements obtained. Attenuated gamma counts (Gamma density) and magnetic susceptibility were measured. Magnetic susceptibility was measured using a Bartington MS2E point sensor with a down core resolution of 0.5cm.

3.6 ¹⁴C dating

Radiocarbon dating is the most common type of dating technique used in marine sediment cores on continental shelves. Dates are determined by accelerator mass spectrometry (AMS), this project will use foraminifera and marine shells to obtain ¹⁴C dates. These samples are vital in order to constrain the timing of ice sheet retreat from the continental shelf. The sedimentological and physical properties of the cores will

be utilised to identify the most appropriate locations to obtain ^{14}C dates in order to determine the timing of deglaciation. The optimum location for constraining the timing of ice sheet retreat would be to date the material that occupies the transition from a subglacial to an ice proximal glacialmarine environment (McCabe & Clark 2003).

A total of nine samples (shell and foraminifera) were sampled for radiocarbon dating; four samples from core CE_03-003, two samples from core CE-08-004, and one sample from cores CE-08-010, CE-08-015 and CE-08-018. Samples were extracted from the lowermost part of the deglacial facies which had sufficient quantities of foraminifera or where shells were present. Sampling for foraminifera involved obtaining on average 50 ml of sediment (extraction avoiding the core edges). The sediment was subsequently wet sieved and the coarser fraction $>63\mu\text{m}$ was analysed for foraminifera. The samples were processed and dated at the NERC radiocarbon facility (East Kilbride) and the Keck C Cycle AMS Lab at the University of California, Irvine. Radiocarbon ages were calibrated to calendar years using CALIB v7.0 software in conjunction with MARINE 13 calibration data set. The samples were corrected for a 400 yr reservoir age (Reimer, 2013) with a ΔR value of 53. Radiocarbon dating is a widely used dating technique however uncertainties arise from variation in the marine reservoir effect 'MRE'. A marine reservoir effect of 400 is used because North Atlantic ^{14}C ages are ~400 years older than atmospheric carbon. However, recent research has shown that during periods of reduced AMOC the MRE would have been altered due to changes in ocean circulation (Austin et al. 1995). To reduce associated uncertainties marine samples are routinely corrected (Reimer, 2013).

3.7 Biological analysis

3.7.1 Foraminifera abundances

Micropalaeontological analysis is a powerful tool in the study of Quaternary stratigraphy, palaeoceanography and palaeoclimatic reconstruction (Peck et al. 2006; Kilfeather et al. 2011; Jennings et al. 2014). Micropalaeontological analysis can comprise analysing ostracods, chironomidae and foraminifera. Foraminifera are used for palaeo reconstructions particularly palaeoceanography because their present day distribution is closely related to sea-surface temperatures, and therefore analysis of their fossil assemblages, allows the reconstruction of past sea surface temperature (Peck et al. 2006). As a consequence, foraminiferal analysis has been used to investigate deglacial chronologies on high-latitude continental

shelves and oceanographic evolution (e.g. Lloyd et al. 2005; Jennings et al. 2006; Pudsey et al. 2006; Peck et al. 2007; Kilfeather et al. 2011; Jennings et al. 2014). Foraminiferal studies can analyse both benthic and planktonic species, however this project will focus on the analysis of benthic foraminifera due to their abundance on the continental shelf offshore of northwest Ireland.

The study of benthic foraminifera assemblages in the marine sediment cores will allow inferences to be made about the changes in water mass properties through time (e.g. temperature and salinity through time). This will enable the project to investigate whether there are linkages between the response of the BIIS to the wider North Atlantic climate and oceanographic forcing particularly during deglaciation (research question 4). The examination of the foraminifera identified within the cores will also assist with the classification of the facies whether they are ice proximal or ice distal and therefore help determine the pattern of retreat across the shelf.

3.7.2 Sampling

Foraminifera samples were prepared by extracting a 6ml of sediment at 16cm intervals for CE-08_003 and CE-08_010. The samples were soaked overnight to disaggregate and subsequently sieved at 500 μm and 63 μm , with residues being placed in the oven to dry overnight. The samples were picked dry from the coarser fraction $>63\mu\text{m}$ using a microscope, with a target of 300 foraminifera (where abundance were sufficient). Foraminifera identification followed (Feyling-Hanssen, 1972) and Olausson (1982). Once identified the foraminifera were then converted to a percentage and represented on a foraminiferal assemblage chart using C2 software for later analysis (Lloyd 2006).

Chapter 4- Results and Interpretation

4.1 Introduction

This chapter presents the results of the core analysis outlined in Chapter 3. The chapter has five aims: 1) to highlight the dates obtained from the radiocarbon analysis; 2) to describe the sedimentological characteristics of each core and identify the lithofacies based on sediment logging from core section and x-rays, as well as measurements of shear strength, gamma density, and magnetic susceptibility; 3) to identify the lithofacies associations (LFAs) across the transect of cores investigated; 4) to investigate the benthic foraminiferal assemblages from selected sections of two cores; and 5) to interpret the LFAs based on the data presented in order to understand their genesis and depositional environment(s).

4.2 Chronology

Six AMS radiocarbon dates were obtained on samples of shells and foraminifera from cores CE-08-003, CE-08-004, CE-08-010, CE-08-015 and CE-08-018. The calibrated and raw radiocarbon ages are displayed in Table 3. These radiocarbon dates have been corrected for isotopic fractionation and the marine reservoir effect. A marine reservoir effect of 400 years has been used (Reimer 2013) with a delta R value of 53, which correlates to the date of the local living shells at 347 years (<http://calib.qub.ac.uk/marine>). Dates were calibrated using CALIB v7.0 software. These calibrated radiocarbon dates have been plotted alongside the cores in which they were derived from in Fig. 11.

Table 3. NW Ireland continental shelf radiocarbon dates. Specific dates are discussed below within the section on sediment description

Core name	Sample depth (cm)	Publication code	Sample material	Radiocarbon age (^{14}C yr BP $\pm 1\sigma$)	Lower calibrated age (cal. yr BP)	Upper calibrated age (cal. yr BP)	Mean calibrated age (cal. yr BP)
CE-08-003	390-387	SUERC-47514	Marine shell fragments	10772 \pm 40	11946	12393	2170
CE-08-003	466	SUERC-47515	Macoma Calcareo-Single bivalve	11060 \pm 40	12468	12661	12565
CE-08-003	477	SUERC-47516	Macoma Calcareo-Single bivalve	11187 \pm 40	12564	12734	12649
CE-08-003	499-493	UCIAMS-133550	Benthic foraminifera	11345 \pm 30	12654	12871	12763
CE-08-004	217	SUERC-47517	Marine shell fragment	11522 \pm 41	12780	13086	12933
CE-08-004	273-264	SUERC-47522	Benthic foraminifera	15072 \pm 50	17622	17971	17797
CE-08-010	478-471	UCIAMS-133551	Benthic foraminifera	13205 \pm 35	15060	15320	15190
CE-08-015	275-272	SUERC-47518	Marine shell fragments	12457 \pm 43	13748	14027	13888
CE-08-018	Core catcher	UCIAMS-133552	Benthic foraminifera	20170 \pm 90	23471	24012	23742

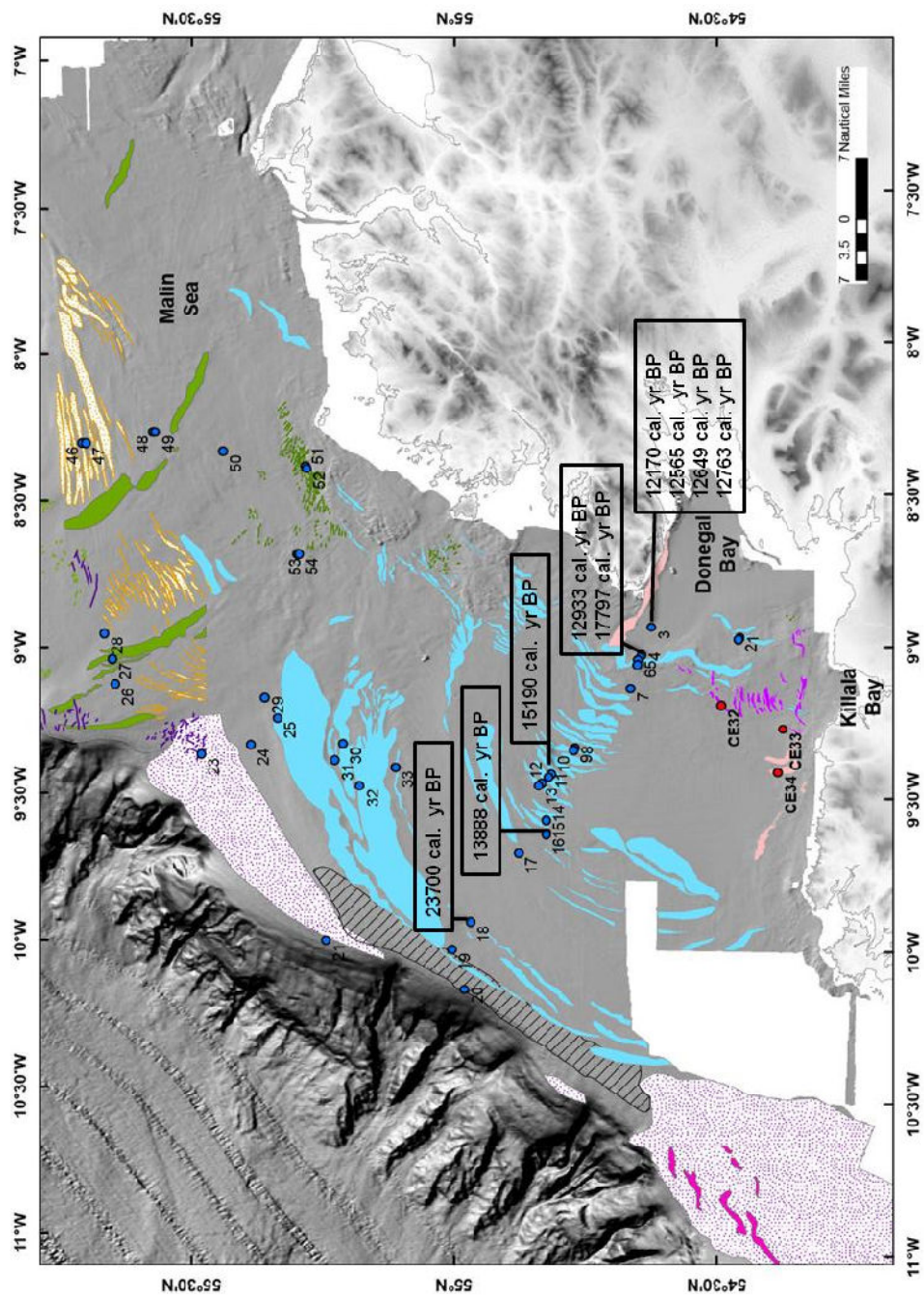


Fig. 11. Map showing the radiocarbon dates obtained from the continental shelf and the location of cores they were obtained from.

4.3 Core Sedimentology - Description

The cores are described along a transect starting with core CE-08-003 nearest the coast, working out towards the shelf edge (Fig.11). Based on sediment characteristics of all thirteen cores studied a total of nine lithofacies have been identified (Table 2). Figures 12 and 13 display x-ray images of these lithofacies.

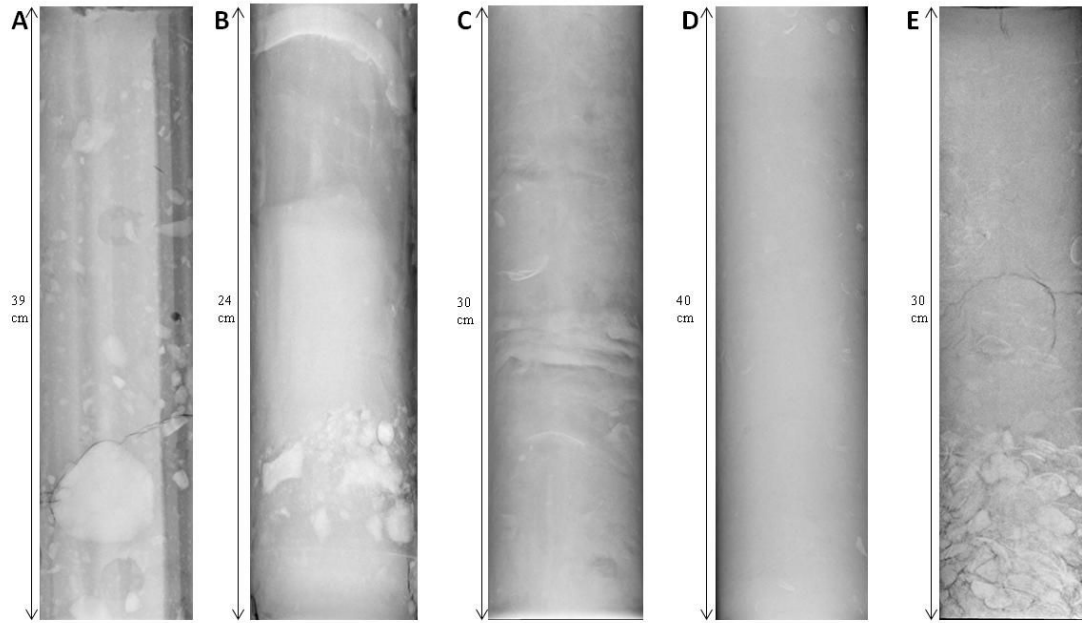


Fig. 12. X-rays of various lithofacies. A) Dmm with a few large clasts dispersed throughout (CE-08-011; 39-78 cm) B) Dmm with a clast rich layer (CE-08-010; 455-479 cm) C) Fl and Fm lithofacies and a few shells (CE-08-003; 442-472 cm) D) Fm lithofacies (CE-08-003; 150-190 cm) E) Suf and Sm lithofacies with a high abundance of shelly material (CE-08-033; 0-30 cm).

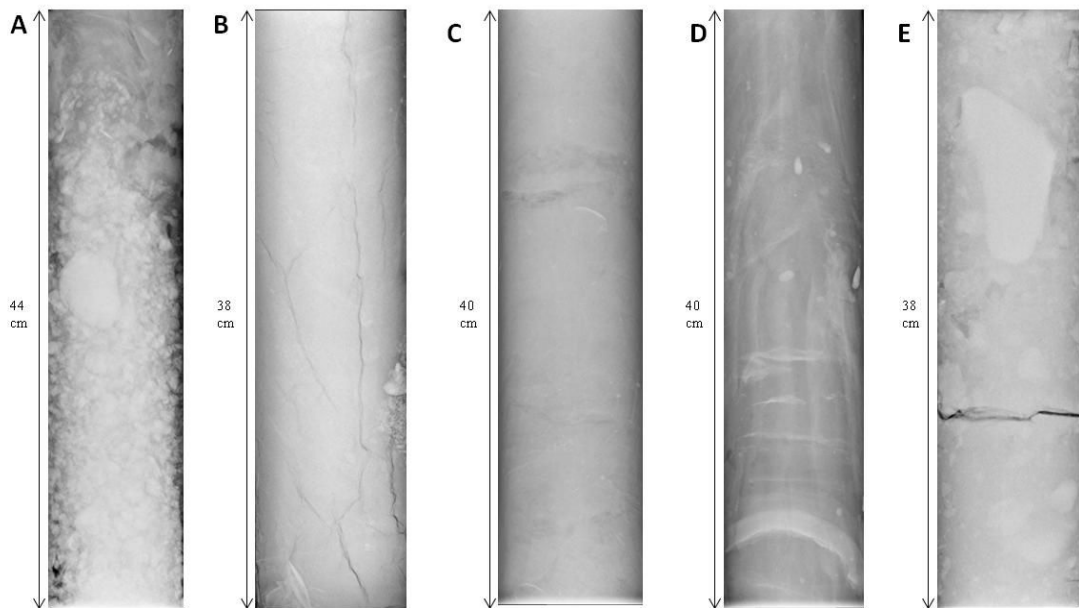


Fig. 13. X-rays of various lithofacies. A) Gms with a few large clasts (CE-08-010; 278-322 cm) B) Sm and a few shells (CE-08-015; 240-278 cm) C) Sh ,Sm lithofacies and a shell (CE-08-003; 353-393 cm) D) Fl and bioturbated Fm with a few scattered pebbles (CE-08-010; 415-455 cm) E) Dmm with numerous clasts dispersed throughout but one particular large outsized clast (CE-08-008; 226-264 cm).

4.3.1 Core CE-08-003

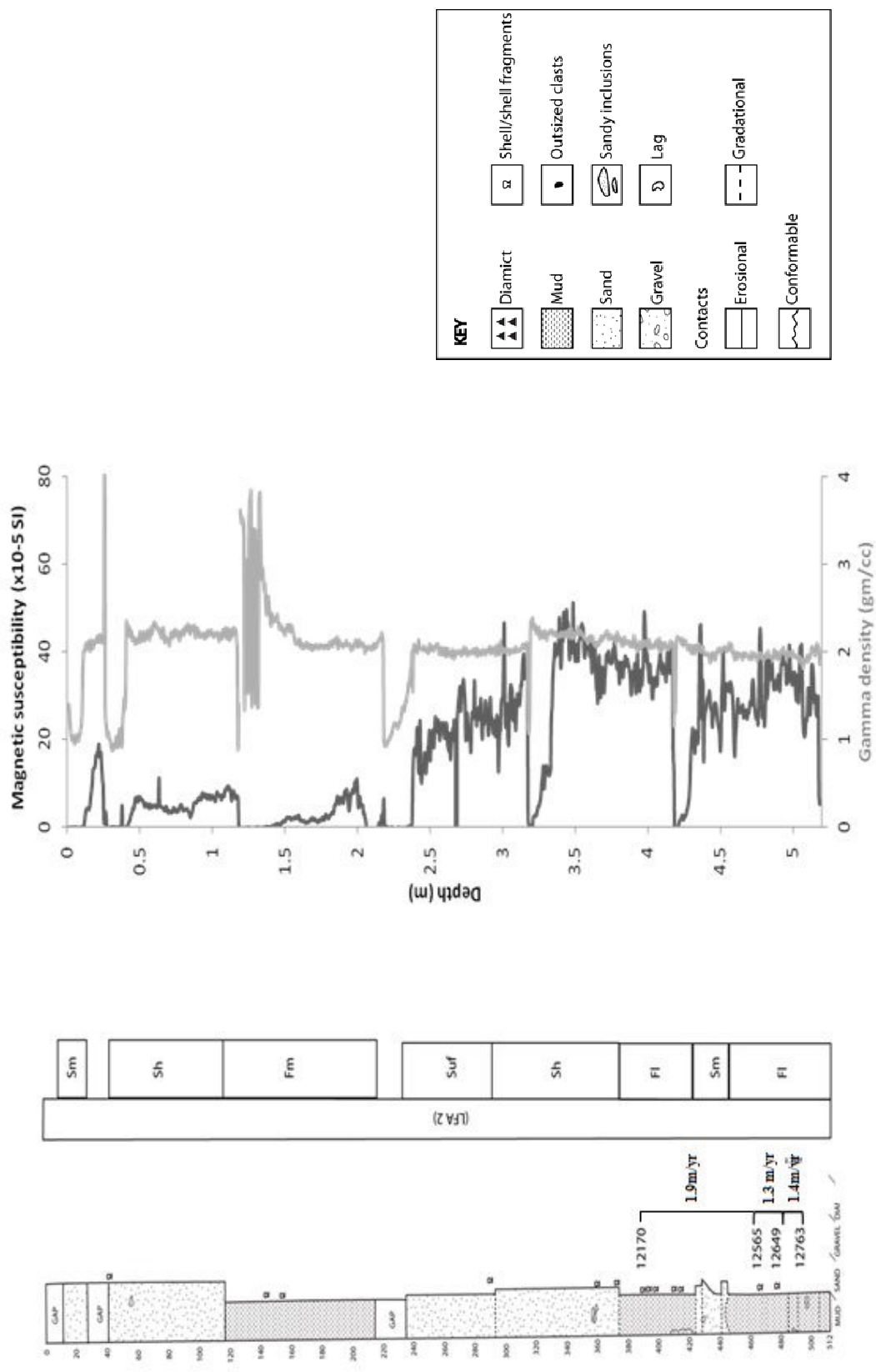
This core was extracted from layered sediment inshore of a moraine (Fig.11). The core consists of eight mud and sand lithofacies (Fig. 14). The base of the core (512-443.5 cm) is dominated by laminated mud (Lithofacies Fl, Table 2) comprising grey soft mud with faint laminae and numerous inclusions of sand. These sandy inclusions increase in abundance up-core and contain whole single shell valves and fragments. Two single shell valves were sampled from this lithofacies (at 477 and 466 cm) for radiocarbon dating (see section 4:2). The two single shell valves sampled yielded dates of 12649 cal yr. BP and 12565 cal yr. BP respectively (Table 3, SUERC-47516 and SUERC-47515). The laminated muds also contain foraminifera (described in section 4:4) a sample of which were collected from 499-493 cm for the purpose of radiocarbon dating, yielding a date of 12763 cal yr. BP (Table 3, UCIAMS-133550). There is a gradational upwards transition to the overlying lithofacies of massive sand (Sm, Table 2) (443.5-425 cm). The massive sand ranges in texture from a medium grained (443.5-441 cm), to more muddy (441-436 cm), before increasing in coarseness again from 436-430 cm and then becoming fine-sand in its upper 5 cm (430-425 cm). The massive sand is overlain gradationally by laminated mud (Fl, 425-374 cm). This lithofacies consists of grey, fairly stiff, silty clay mud, with inclusions of sand. Laminae are fine-grained and horizontal and overall the lithofacies has a mottled appearance. A cluster of shell fragments were sampled for the purpose of radiocarbon dating at 390-387 cm depth, and dated 12170 cal yr. BP (Table 3, SUERC-47514). The contact between the laminated mud and the overlying laminated sand (374-293 cm) is gradational. The laminated sand (Sh, Table 2) is fine grained and contains a high proportion of shell fragments. The laminated sand is in turn overlain gradationally by normally graded sand (293-234 cm) (Suf, Table 2). The upwards fining of this lithofacies is accompanied by a lightening in the colour of the sand (lighter brown).

The upper 211 cm of the core consists of three distinct lithofacies. From 211-116 cm the core comprises a grey massive mud (Fm, Table 2). The mud is fairly stiff and contains small shell fragments throughout. There is a sharp transition to the overlying laminated sand (Sh) (116-40 cm). This sand is fine grained, displays some crude bedding, and shell fragments are common from 116-102 cm depth. The upper lithofacies (27-0 cm) is a massive, fine grained and well sorted sand (Sm).

This core displays a general upwards decrease in magnetic susceptibility values (Fig. 14). At the base of the core average values are $\sim 40 \times 10^{-5}$ SI, whereas from 320-230 cm average values decrease to $\sim 30 \times 10^{-5}$ SI and subsequently at the top of the core values average below 10×10^{-5} SI. Gamma density, however, is fairly

uniform with average values ~ 2 gm/cc. There is a gradual increase in gamma density from the base of the core to the top. Spurious values and fluctuations can result from uneven core surface. A few dips in gamma density values correspond to gaps in the core (Fig. 14). Shear strength was not tested because of the absence of diamict in the core. Foraminifera samples were also collected for the purpose of abundance analysis, 1 cm samples were collected every 16 cm from 510 cm to 425 cm, with an additional two samples at 179 cm and 102 cm. This analysis will be outlined in section 4:4 (see below).

Fig. 14. Sedimentology, magnetic susceptibility and gamma density of core CE-08-003. Core log, calibrated 14C dates and associated sedimentation rates and LFAAs are shown on the left.



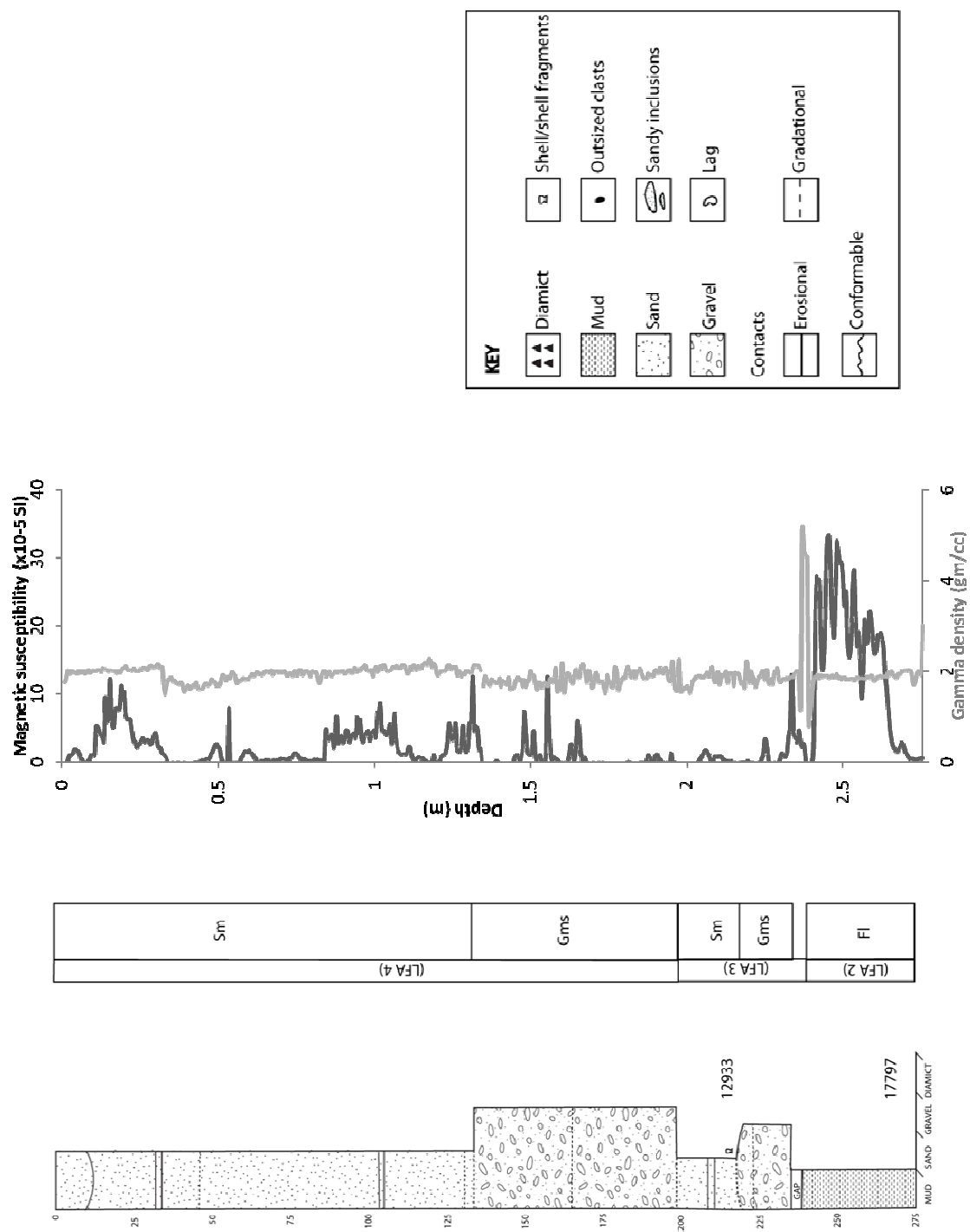
4.3.2 Core CE-08-004

This core was extracted from inshore of a moraine (Fig. 11). It contains five lithofacies (Fig. 15). The base of the core (275-239 cm) consists of laminated and consolidated clayey silty mud (Fl) with sandy inclusions. There is dark mottling throughout, and the mud displays some crude bedding. Foraminifera were sampled from 273-264 cm depth from the laminated mud for the purpose of radiocarbon dating and yielded a date of 17797 cal yr. BP (Table 3, SUERC-47522). The basal laminated mud is overlain by a massive, matrix-supported, granule gravel from 236-218 cm (Gms, Table 2). The gravel has a sandy matrix and the matrix is particularly common from 223-218 cm. The contact with the overlying massive sand (Sm, 218-199 cm) is sharp. The sand is dark grey, fine grained and very well sorted. There is a band of lighter coloured sand at 211-209 cm depth. A shell fragment was sampled from 217 cm depth in the massive sand for radiocarbon dating and yielded a date of 12933 cal yr. BP (Table 3, SUERC-47517). The massive sand is in turn overlain sharply by a poorly-sorted, matrix-supported pebble gravel with a sandy matrix (Gms, 199-134 cm). The lower half of the lithofacies is darker than the upper half and there is a gradational change to the overlying massive sand which caps the core (Sm, 134-0 cm). This capping sand is well sorted and fairly coarse-grained. There are distinct variations in the colour of the massive sand throughout; in general it becomes gradually darker up core. The sand contains two bands of clasts each 2-3 cm thick with ~1cm clasts at 134-131 cm and 105-103 cm respectively. From 131-105 cm it is light brown, becoming brown at 103-33 cm and changing to dark brown from 32-12cm. There is a band of fairly coarse grained orange sand from 33-32 cm and this reappears at 12-0 cm.

The core shows a general decrease upwards in magnetic susceptibility (Fig. 15). The base of the core is characterised by relatively high values, $20-30 \times 10^{-5}$ SI from 275-238 cm which coincides with the laminated mud. However, values are reduced to significantly lower levels (below 15×10^{-5} SI) from 238 cm upwards which correlates with the presence of gravel and sand lithofacies. The gamma density data can be split into five phases. The base of the core (Phase 1 275-239 cm) is characterised by fairly uniform gamma density values with little variation. Phase 2 (239-236 cm) shows significant fluctuations in gamma density however this corresponds to the gap in the core. Phase 3 (236-134 cm) displays more variation within the values (1.5-2.2 gm/cc) which corresponds to the presence of gravel within the core, however this variation becomes less pronounced up core and there is a general decrease in gamma density. Within phase 4 (134-33 cm) values do not display too much variation however there is a general decrease. Phase 5 (33-0 cm) is

marked by a pronounced increase in gamma density to values ~ 2.0 gm/cc. (Fig. 15). Shear strength was not tested in this core because diamict is absent.

Fig. 15. Sedimentology, magnetic susceptibility and gamma density for core CE-08-004. Core log, calibrated ¹⁴C dates and LFAs are shown on the right.



4.3.3 Core CE-08-005

This core was extracted from a moraine crest (Fig. 11). It contains four lithofacies (Fig. 16). The lowermost lithofacies (67.5-58 cm) is a massive, clast-supported cobble gravel (Gm, Table 2). It has a gradational transition into the overlying normally-graded clast supported gravel with sub-angular to sub-rounded clasts (Gfu, 58-14cm). The normally graded gravel has a gradational transition in turn into structureless, clast supported granule gravel with a gradational upper bed contact (Gm, 14-8 cm). The core is capped by 8 cm of poorly sorted, massive sand (Sm, 8-0 cm) containing small granules. Magnetic susceptibility and gamma density data was not obtained for this core, because the majority of the core consisted of gravel (59.5 cm), and thus magnetic susceptibility and gamma density data would not provide useful data. Shear strength was not measured because of the absence of diamict.

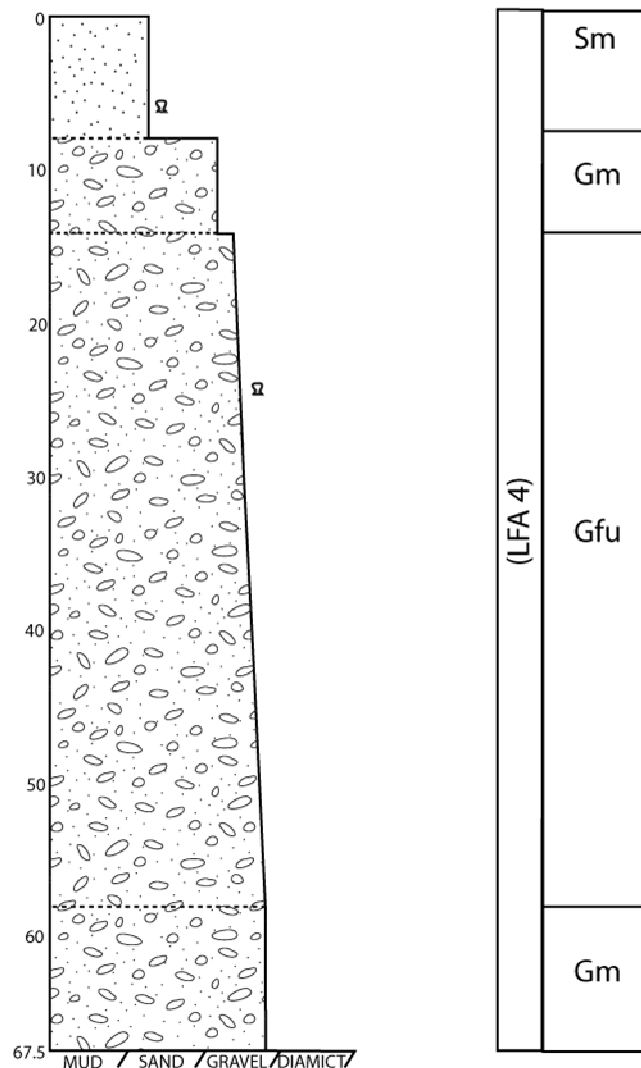


Fig. 16. Sedimentology of core CE-08-005, with the core log and associated LFAs.

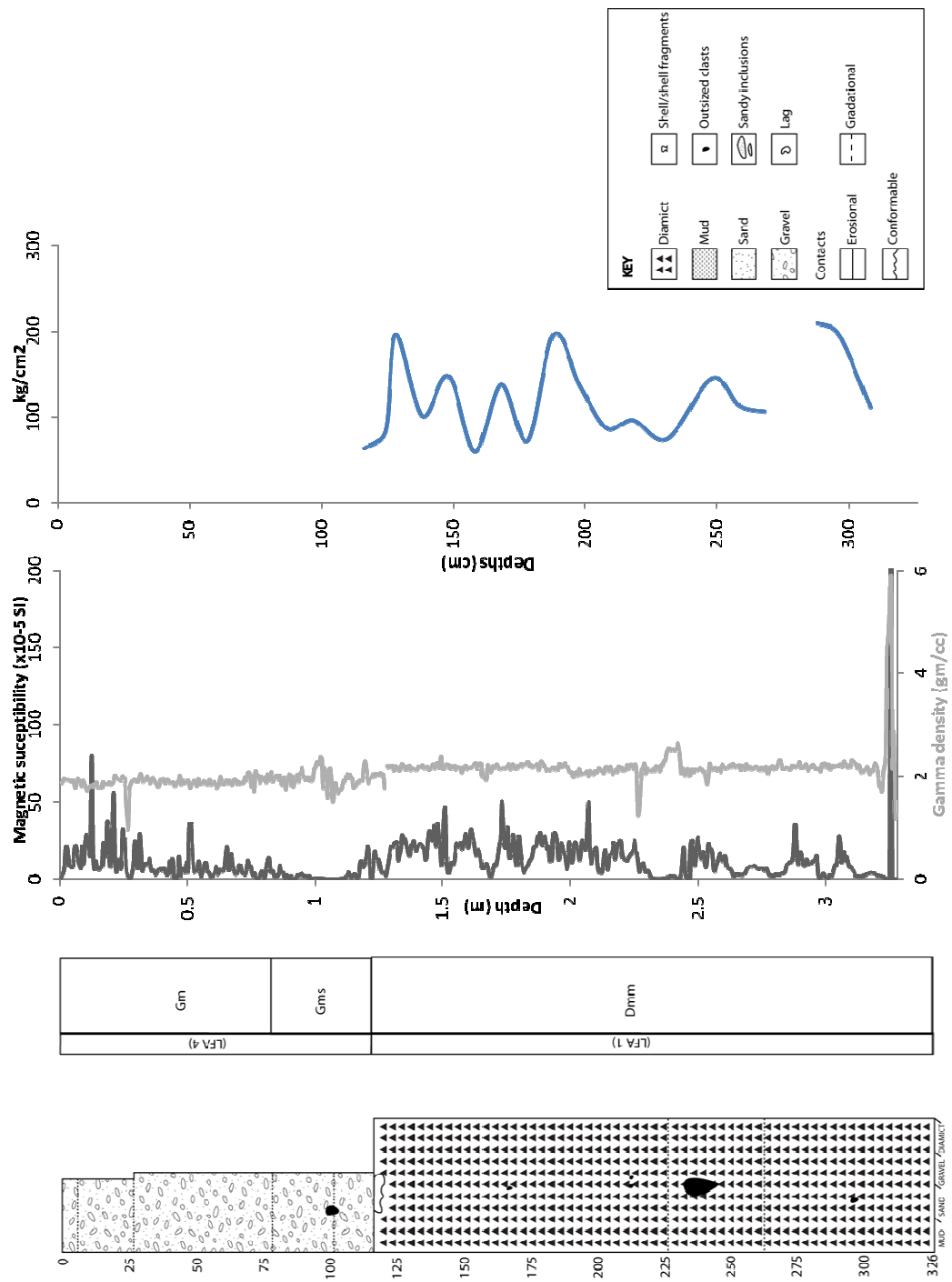
4.3.4 Core CE-08-008

This core was extracted from inshore of a moraine (Fig. 11). The core consists of a series of diamict and gravel lithofacies (Fig. 17). The lowermost lithofacies (326-116 cm) is a brown, massive diamict (Dmm, Table 2) there is a lag at the base of this lithofacies. From 326-253 cm depth the diamict is very stiff (shear strength values from 110.3 kg/cm² to values exceeding 200 kg/cm²) but above this, from 253-226 cm, it is markedly less consolidated (shear strength values ranging from 73 kg/cm² to 144 kg/cm²). This transition is gradual. The diamict contains numerous large clasts throughout, up to (an exceptionally large clast) a maximum of 11 cm in length. From 226-116 cm depth the diamict is fairly stiff, although it is not as consolidated as the lowermost diamict lithofacies within the core. This is confirmed by the shear strength measurements from the diamict which range from 196 kg/cm² to 58 kg/cm².

The diamict is overlain by matrix-supported, poorly sorted, pebbly gravel (Gms, 116-78 cm). The contact between the diamict and the gravel is sharp and it is marked by a downward intrusion of small clasts from the gravel into the diamict (120-116 cm). The gravel has a clayey mud matrix. There is a gradational transition to the overlying clast-supported pebble gravel (Gm, 78-0 cm). From 26-0 cm the gravel is a well sorted granule gravel and contains some shell fragments. However, from 6-0 cm it has a fine matrix of sand.

At the base of the core there is a lag in the diamict lithofacies which resulted in high magnetic susceptibility and gamma density values. For the purpose of analysing trends these values will be excluded. The base of the core to 116 cm, the magnetic susceptibility values are highly variable (ranging from 0.8 to 49.8x10⁻⁵ SI) which coincides with the diamict lithofacies. There is a drop in values from 240-234 cm which correlates to the large clast identified in the core which would have disrupted the magnetic susceptibility probe from taking a measurement. From 116-0 cm the magnetic susceptibility is very variable (ranging from 1 to 49 x10⁻⁵ SI) and shows a general increase up core. (Fig. 17). Gamma density values average ~2 gm/cc from the base of the core to 129 cm, however from 240-234 cm there is a rise in values which corresponds to the large clast within the core. Fluctuations in gamma density (1.4-2.3 gm/cc) from 129-70 cm corresponds to the Gms lithofacies. The gamma density values from 70-0 cm become less variable ~1.9 gm/cc (Fig. 17).

Fig. 17. Sedimentology, magnetic susceptibility, gamma density and shear strength values for core CE-08-008.



4.3.5 Core CE-08-009

This core was extracted from a moraine crest (Fig. 11). The core consists of three gravel lithofacies (Fig. 18). The lowermost is a matrix-supported, pebble gravel (Gms). The gravel is massive, poorly sorted, and has a muddy matrix. The matrix-supported gravel is overlain by an upward fining pebble gravel from 66-56 cm depth (Gfu, Table 2). Clasts within this normally graded gravel are coated in mud. The uppermost lithofacies in the core (56-0 cm) is a shell 'hash' (a loose accumulation of shells both whole and broken, (CMECS, 2014)) and granule gravel that is clast supported and structureless. This core was not analysed for magnetic susceptibility and gamma density data because the majority of the core consisted solely of gravel and thus magnetic susceptibility and gamma density data would not provide useful data. Shear strength was also not tested in this core because diamict is absent.

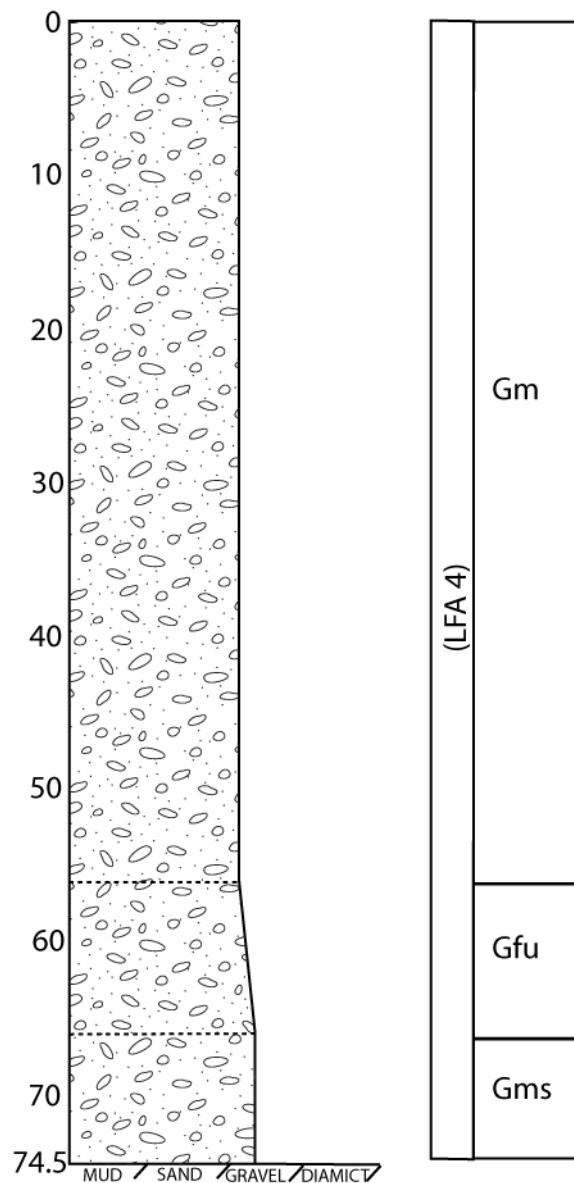


Fig. 18. Sedimentology for core CE-08-009, with the core log and associated LFAs.

4.3.6 Core CE-08-010

This core was extracted from a trough between moraine ridges (Fig. 11). It consists of a range of diamict, mud, sand and gravel lithofacies (Fig. 19). The lowermost lithofacies is a massive, matrix-supported, stiff brown diamict (Dmm, 578-505 cm). The diamict displays shear strength values of 76-48 kg/cm² from 572-534 cm (Fig. 19), whereas above 534 cm depth, the diamict is softer with shear strength values ranging from 48-31 kg/cm² (Fig. 19). Although the diamict is predominantly massive, there is a curved band of massive sand and silt with shell fragments from 546-541 cm. This could, however, be due to deformation from the coring process. From 521-505 cm the diamict is also noticeably sandier.

Overlying the diamict from 505-492.5 cm depth is an olive grey, soft massive mud with shear strength ranging from 24 kg/cm² to 17 kg/cm² (Fig. 19) which is overlain sharply in turn by a brown diamict (492.5-461 cm). This diamict is massive and fairly stiff. It is markedly sandy at its base but sand content appears to decrease upwards. There is a band of clasts, sand and shell fragments at 472-468.5 cm. Shear strength ranges from 24-36 kg/cm² (Fig. 19). The diamict is overlain by a massive mud (461-452 cm). The mud is a structureless, soft olive grey clayey silty mud. The massive mud is overlain by laminated mud (450-373 cm) and the two lithofacies are separated by a sharp 2 cm thick band of fine grained sand with a few 2mm clasts (452-450 cm). The laminated mud consists of soft clayey silty mud and it contains sandy inclusions which increase up core in abundance as well as laminae of coarse sand. The sandy inclusions dominate the left hand side of the core and are massive in structure. From 452cm to 278cm shear strength values are very low which corresponds to the mud, sand and gravel lithofacies (<5 kg/cm²); values do increase briefly between 278 and 230cm (ranging from 1.9 kg/cm² to 15 kg/cm²) however, towards the top of the core values do not exceed 0.5 kg/cm² (Fig. 19).

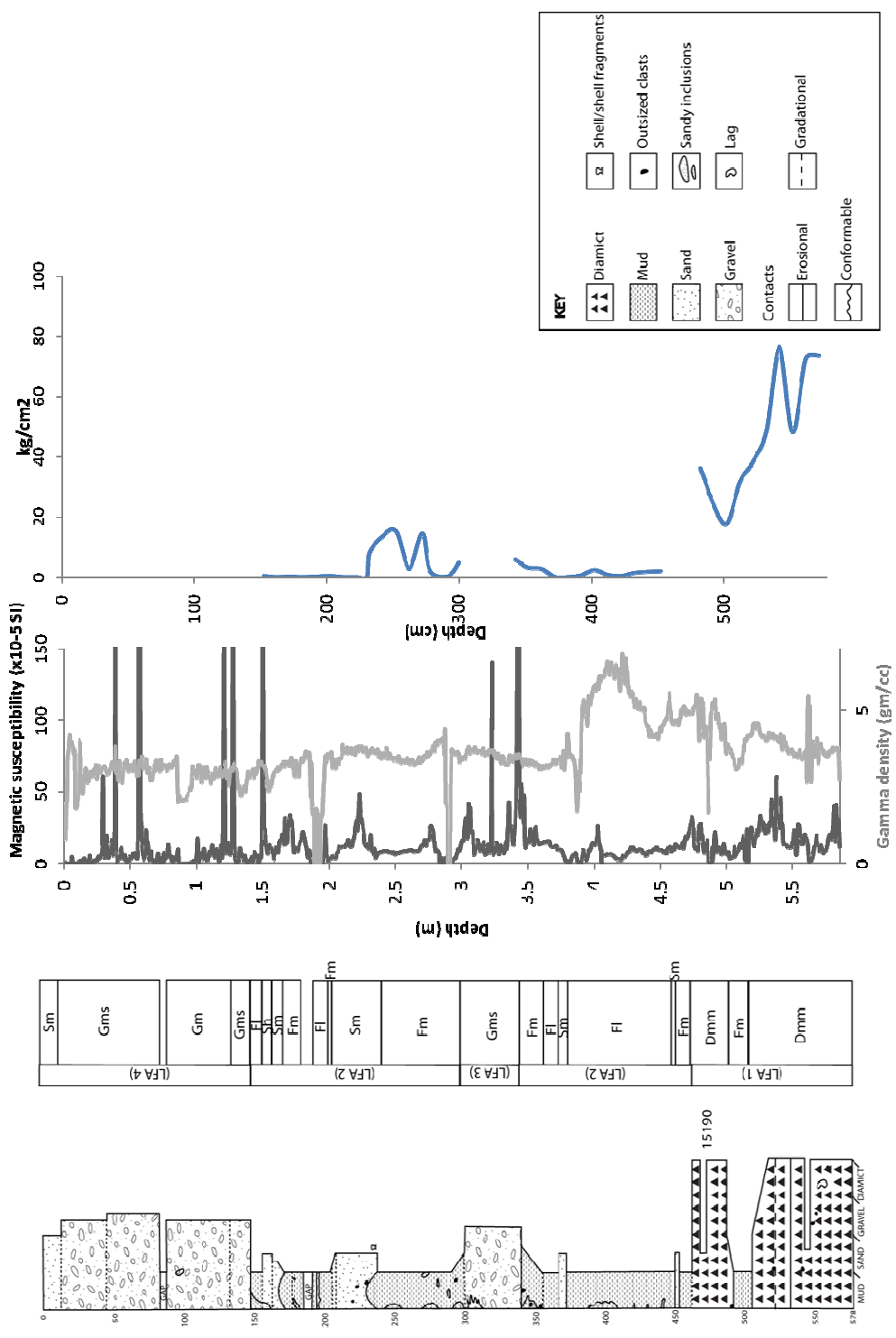
From 373-340 cm the core changes from a massive, fairly well-sorted sand (Sm), to a soft laminated mud (Fl) with a few 1 mm clasts to a massive mud (Fm) which displays an upward increase in sand. The massive mud is overlain by 40 cm of matrix-supported gravel (Gms, 340-300 cm). The gravel has a muddy matrix and contains numerous shell fragments. It also contains sandy inclusions from 312-300 cm which dominate the left hand side of the core and are massive in structure. From 300-229 cm depth the core consists of olive grey, soft massive mud (Fm) with numerous sandy inclusions particularly towards the base. There is a sharp concave transition into overlying massive sand (Sm, 229-208 cm). The sand is well sorted and contains numerous 3 mm clasts and shell fragments; it is overlain by a massive mud (Fm, 208-205 cm). The lower

boundary of this mud is mixed with coarse sand. From 205-191 cm the massive mud transitions to laminated mud (Fl). From 191-183 cm depth there is a gap in the core material. However, the next lithofacies is a massive mud (Fm) from 183-167 cm. This massive mud is sandy in its lower part from 183-176 cm. It has a sharp, concave, upper bed contact which could have resulted from the coring process. It is overlain in turn by massive sand (Sm, 167-164 cm), and fine-grained laminated sand (Sh, 164-155 cm). The laminated mud (Fl, 155-149 cm) is olive grey and displays laminae of darker sand. It is overlain sharply by poorly-sorted, massive matrix-supported pebble gravel (Gms, 149-134 cm) with a muddy matrix. This grades upwards into a clast-supported pebble gravel (Gm, 134-87 cm) and then matrix-supported granule gravel (Gms, 45-14 cm). The latter is intermixed with granular sand and there are some shell fragments present. The core is capped by 14 cm of granular sand (Sm).

The magnetic susceptibility data displays many peaks and troughs although the majority of the core has magnetic susceptibility values below 50×10^{-5} SI (Fig. 19). From 578-464 cm (Dmm and mud units) the results show considerable variability with values reaching 60×10^{-5} SI, although the average magnetic susceptibility is 13.3×10^{-5} SI. From 464-358 cm the magnetic susceptibility values are lower and show less variability which corresponds to the mud and sand lithofacies. From 358-298 cm magnetic susceptibility is very variable with a few peaks in these data; this variability corresponds to the Gms lithofacies. From 298-151 cm the mud and sand lithofacies have an average magnetic susceptibility of 8.4×10^{-5} SI. Magnetic susceptibility data for the top of the core is characterised by high variability corresponding to the gravel lithofacies excluding the top 14 cm which shows a steady decline in values in relation to the massive sand. Gamma density results for the core display numerous peaks and troughs (Fig. 19). The gamma density data shows a general decline in gamma density up core. The base of the core displays a steady increase in gamma density with values reaching 6.8 gm/cc. There is a drop in values from an average of 4.5 gm/cc at the base of the core to an average of 3.1 gm/cc for the rest of the core.

This core was also sampled for foraminifera from the Dmm lithofacies at 478-471 cm for the purpose of radiocarbon dating. The sample yielded a date of 15190 cal yr. BP (Table 3, UCIAMS-133551). Foraminifera were also sampled for abundance analysis from 516-259 cm which encompasses the diamict and various mud and sand lithofacies. The foraminifera data are discussed below in section 4:4.

Fig. 19. Sedimentology, magnetic susceptibility, gamma density and shear strength values for core CE-08-010, with calibrated 14C date.

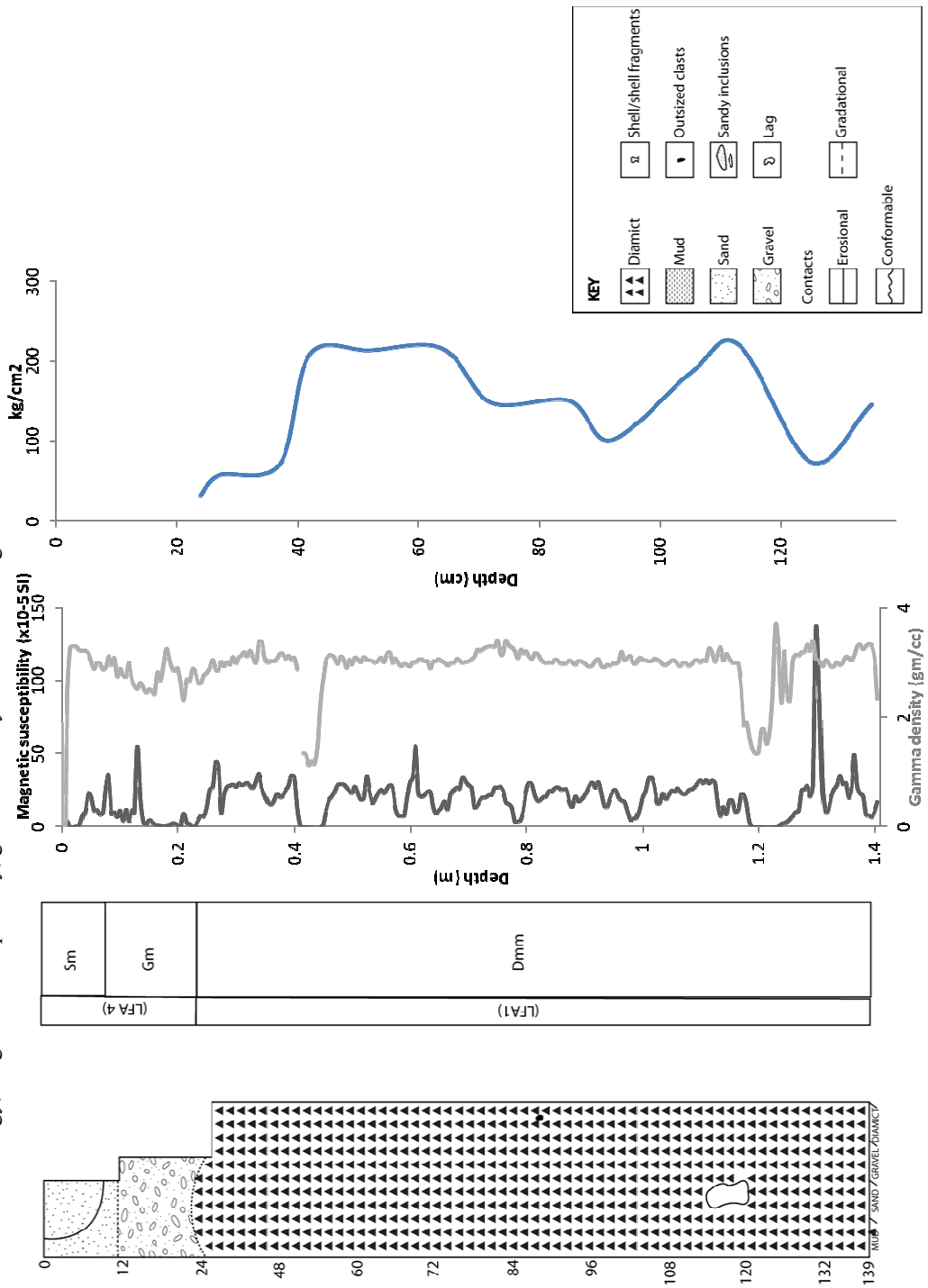


4.3.7 Core CE-08-011

This core was extracted from the crest of a moraine (Fig. 11). It consists of a vertical sequence of diamict, gravel and sand although the majority of the core is diamict (Fig. 20). From 139-22 cm depth the core is composed of a very stiff brown diamict (Dmm). From the base of the core to 42cm the majority of shear strength values exceed 100 kg/cm^2 and on four occasions values exceed 200 kg/cm^2 . There is a decrease in the shear strength from 42cm to the top of the core with values falling to 31 kg/cm^2 (Fig. 20). The diamict contains patches of clayey silty mud. There is a gradational boundary between the diamict and the overlying pebble gravel (Gm, 22-11 cm) which is a poorly sorted, clast-supported and contains numerous shell fragments. The uppermost lithofacies (11-0 cm) is well sorted, massive sand (Sm) that ranges in texture from granular to fine grained.

The magnetic susceptibility results for the core are quite variable and display numerous peaks and troughs. The majority of values range from $0\text{-}30 \times 10^{-5}$ SI. The Dmm lithofacies (139-24 cm) has an average magnetic susceptibility of 20×10^{-5} SI, whereas from 24-0 cm the core has an average of 7.3×10^{-5} SI (sand and gravel lithofacies). The average gamma density value for the Dmm lithofacies (139-24 cm) is 2.9 gm/cc . There is a trough in the dataset from 126-116 cm this could be explained by the lag in core and an additional trough at 43 cm which correlates to the end of the core section. The average gamma density for the sand and gravel lithofacies from 24-0 cm is 2.7 gm/cc . There is more variability in gamma density in the sand and gravel lithofacies.

Fig. 20. Sedimentology, magnetic susceptibility, gamma density and shear strength values for core CE-08-011.

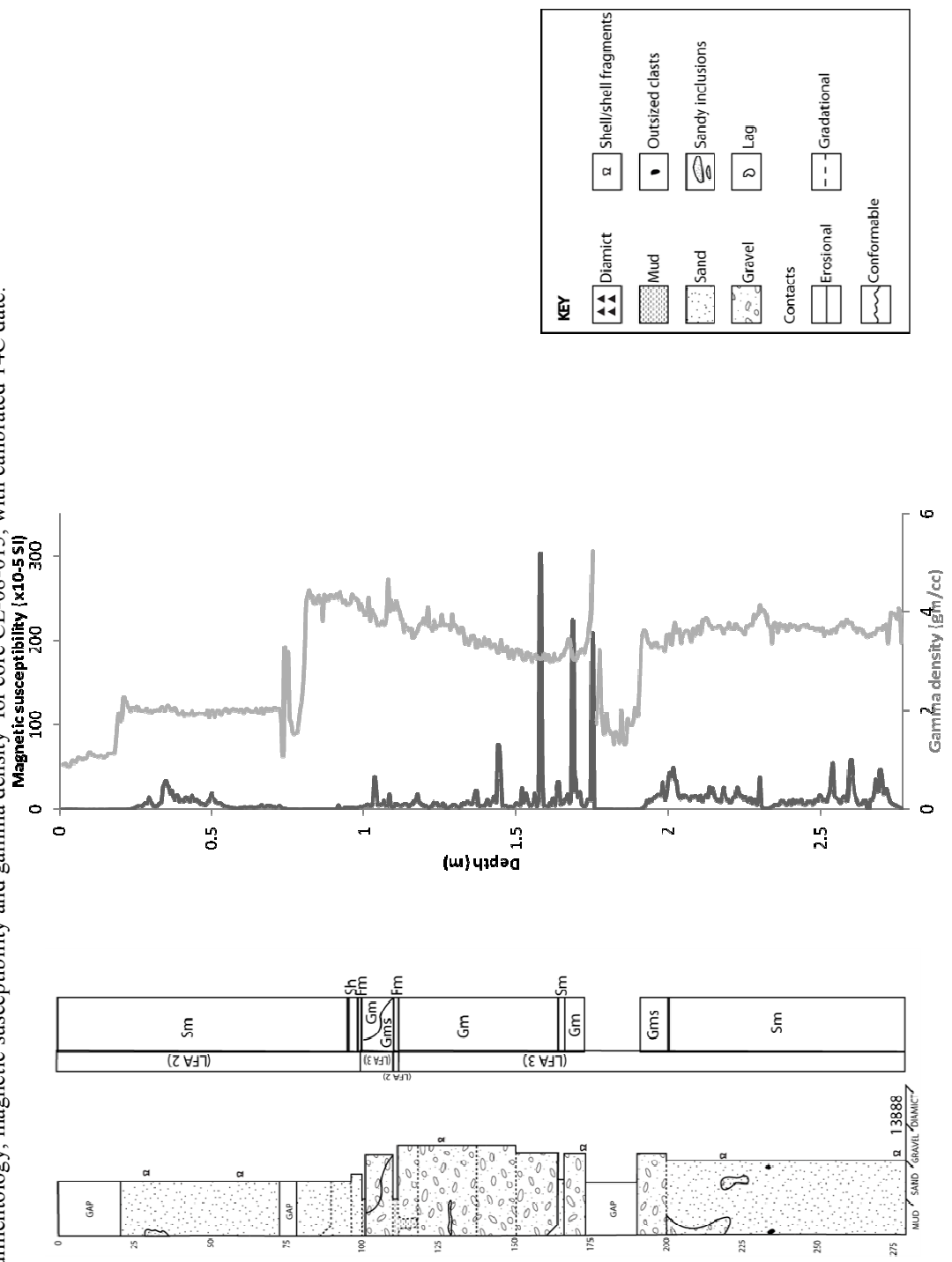


4.3.8 Core CE-08-015

This core was extracted from an inter-moraine trough (Fig. 11). It consists of a variety of sand, gravel and mud lithofacies (Fig. 21). The lowermost lithofacies is massive sand (Sm, 278-200 cm). The sand is well sorted, fairly coarse grained and contains numerous shells and inclusions of darker sand. From 218-200 cm there is an intrusion of ~2 mm black pebbly massive gravel along the left hand side of the core. The intrusion has a gradational bounding contact. A cluster of shells from 275-272 cm were sampled for radiocarbon dating and provided a date of 13888 cal yr. BP (Table 3, SUERC-47518). There is a gradational transition upwards into an overlying 10 cm thick bed of matrix-supported granule gravel (Gms). This gravel is poorly sorted and there is a high occurrence of ~2mm black clasts. The next lithofacies is a clast supported, well sorted granule gravel (Gm, 173.5-167 cm) that is overlain sharply in turn by well sorted, massive sand (Sm, 167-165 cm). The overlying lithofacies is a clast supported gravel (Gm, 165-112 cm). From 165-148 cm a well sorted, clast supported granule gravel dominates, which is preceded by a clast supported pebble gravel from 148-112 cm. This clast supported pebble gravel contains numerous shells from 148-137.5 cm and from 137.5-119 and a few of the clasts are surrounded by a sandy matrix. This sandy matrix becomes more noticeable from 119-112 cm. The overlying lithofacies is a massive silty clay mud (Fm, 112-110 cm) which is overlain by a matrix-supported gravel (Gms, 110-102 cm) with a sandy matrix. The subsequent lithofacies is a clast supported, poorly sorted, granule gravel (Gm, 110-102 cm) which is overlain sharply by olive green, massive sandy mud (Fm, 102-101 cm). This sandy mud grades up core into 4 cm thick lithofacies of laminated sand (Sh). The uppermost lithofacies in this core is a massive sand (Sm, 97-20 cm). From 97-90 cm the sand is brown, fine grained and very well sorted. The sand grades into a well sorted light brown massive sand from 90-79.5 cm. There is a gap in the core between 79.5-72.5 cm. From 72.5-20 cm the massive sand is brown and fairly coarse grained. It also displays some inclusions of darker brown coarse grained sand. There is also a gap in the core from 20-0 cm. From the base of the core to 191 cm the magnetic susceptibility is quite variable reaching values of 57×10^{-5} SI. Data between 191-175 cm is below zero and therefore omitted from analysis, these data points coincide with the gap in the core. From 175 cm upwards, magnetic susceptibility rarely exceeds 40×10^{-5} SI excluding a few erroneous data points where values exceed 200×10^{-5} SI. There is a general decrease in magnetic susceptibility from 175-91 cm with values descending below zero from 91-72.5 cm (there is gap in the core from 79.5-72.5 cm). This core displays an overall decrease in gamma density up core (Fig. 21). From 276 cm to 191 cm gamma density values average ~3.6 gm/cc. There is a drop in values from 192-177 cm which

corresponds to the gap in the core. From 177-82 cm there is a general increase in gamma density, with another significant drop in values from 79-72 cm (due to a gap in the core). There is minimal variability in gamma density from 72- 20 cm with average values ~ 2 gm/cc. Shear strength was not tested in this core because of the absence of diamict.

Fig. 21. Sedimentology, magnetic susceptibility and gamma density for core CE-08-015, with calibrated 14C date.



4.3.9 Core CE-08-017

This core was extracted from the crest of a moraine (Fig. 11). It consists of a range of gravel and sand lithofacies (Fig. 22). The lowermost lithofacies (130-89 cm) is a clast-supported, massive gravel (Gm). From 130-109 cm the gravel is a structureless cobble gravel with numerous rounded clasts. It grades upwards into clast-supported, poorly-sorted pebble gravel from 109-89 cm depth. Clasts are sub-rounded to sub-angular and numerous shell fragments are present. It is overlain in turn by normally graded, well-sorted, clast-support pebble gravel (Gfu, 89-30 cm). The upward fining coincides with an increase in sand within the gravel. The normally graded gravel is overlain gradationally by 6 cm of matrix-supported pebble gravel (Gms) with numerous shell fragments. The core is capped by 24 cm of massive sand (Sm), which is poorly sorted, fairly coarse which becomes progressively lighter in colour up core. The sand contains a 1 cm band of darker, coarser sand with some granule gravel. This core was not analysed for magnetic susceptibility and gamma density data because the majority of the core was gravel lithofacies and thus magnetic susceptibility and gamma density data would not provide useful data. Shear strength was not tested in this core because of the absence of diamict.

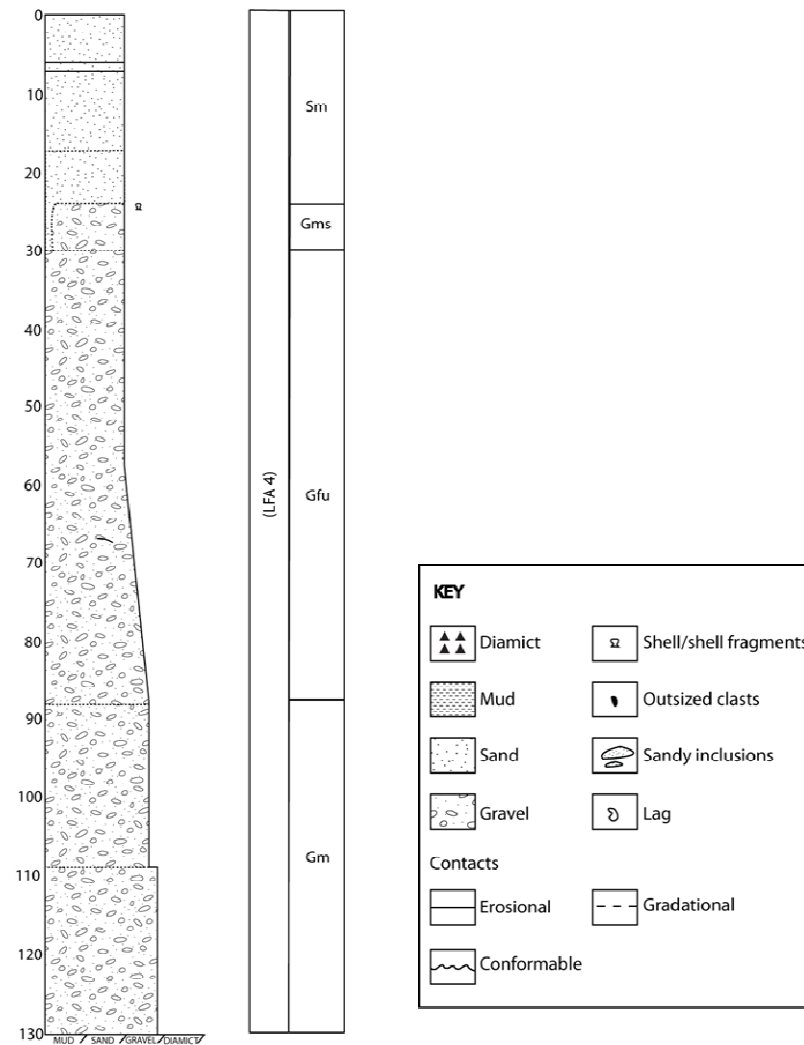


Fig. 22. Sedimentology of core CE-08-017 and associated LFAs.

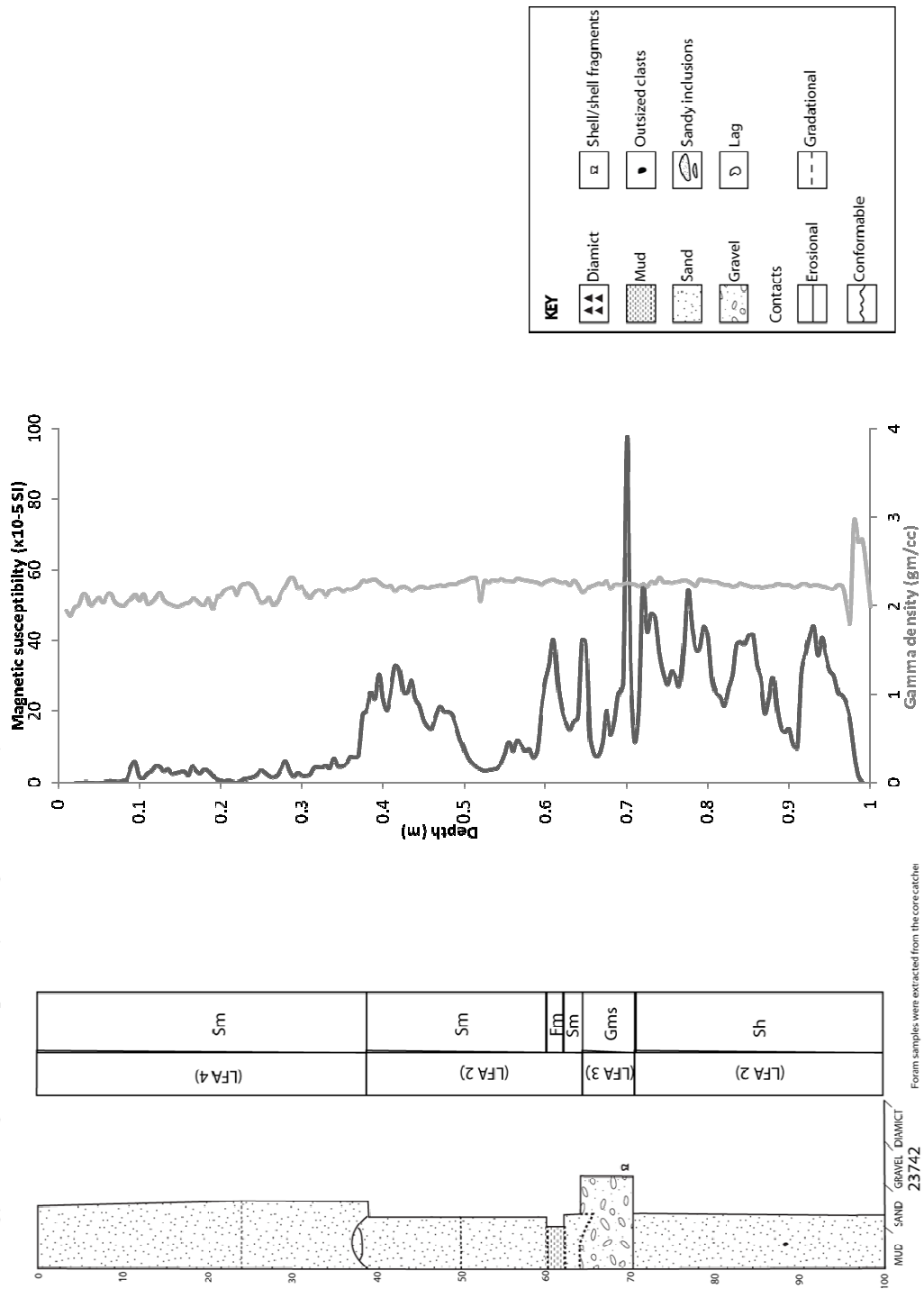
4.3.10 Core CE-08-018

This core was extracted from directly inbound of the shelf edge moraine (Fig. 11). It consists of sand, gravel and mud (Fig. 23). The lowermost lithofacies is a fine-grained, well sorted and faintly laminated sand (Sh, 100-70 cm). There is dark mottling at the base of the sand. Overlying the sand there is a sharp transition to a matrix-supported, well sorted gravel (Gms, 70-64 cm) with occasional single shell valves and shell fragments. The core is capped (64-0 cm) by massive sand (Sm), which contains an interbed of massive mud (Fm, 62-60 cm). The massive mud is very soft and has a gradational upper and lower bed contact. The massive sand is initially fine grained (64-62 cm), but from 60-50 cm the sand contains small pebbles and shell fragments. The sand is variable in colour; from 50-37 cm the sand is orange and contains a high prominence of clay-silty mud. There is a sharp transition to poorly sorted granular sand, with numerous

shells (37-0 cm). From 37-24 cm the granular sand is dark brown, however, from 24-0 cm the sand becomes much lighter in colour (sandy beige) than the underlying dark brown massive sand.

This core displays variable magnetic susceptibility values. From the base of the core to 37 cm the values average 23×10^{-5} SI, with fluctuations between 10 and 55×10^{-5} SI (Fig. 23). From 37 cm there is a drop in values $\sim 2 \times 10^{-5}$ SI, There is a notable spike in the data at 70 cm (97.6×10^{-5} SI), this data point coincides with a shift to the Gms lithofacies, however it is classified as a spurious data point. Gamma density values average 2.2 gm/cc throughout the core. There is little variation in the values except from above 31 cm where there is a little more variation but only by 0.3 gm/cc (Fig. 11). Shear strength was not tested in this core because of the absence of diamict. Foraminifera were sampled from the core catcher (which bottomed out in laminated sand) for radiocarbon dating and provided a date of 23742 cal yr. BP (Table 3, UCIAMS-133552).

Fig. 23. Sedimentology and magnetic susceptibility and gamma density for core CE-08-018, with calibrated 14C date.



4.3.11 Core CE-08-025

This core was extracted from the crest of the outermost (shelf edge) moraine (Fig. 11). It consists of gravel and sand (Fig. 24). The lowermost lithofacies is inversely graded, clast-supported pebble gravel (Gm, 65-49 cm). From 65-60 cm the gravel is fairly sorted, although clasts are coated in mud and average clast size is ~5 mm. From 60-55 cm the gravel is fairly sorted, although clasts are coated in mud and average clast size is ~5 mm. From 60-55 cm the clasts are well sorted, sub-angular to sub-rounded and larger than the underlying gravel (~15mm), whereas the clasts from 55-49 cm are significantly larger (~4.5cm) than the other massive clast- supported gravel units. The overlying lithofacies is an upwards fining gravel (Guf, 49-24 cm). This lithofacies consists of a pebble gravel that fines upwards gradationally into a granule gravel. Between 38-27 cm depth the gravel is markedly sandy. The core is capped by 24 cm of massive, fine grained and well sorted sand (Sm) with occasional granules in the upper 13 cm. From 22-13 cm along the right hand side of the core there is an incursion of matrix-supported, granule gravel (Gms) with a sharp bounding contact. This may have occurred as a result of the coring process.

This core was not analysed for magnetic susceptibility and gamma density values because the majority of the core was composed of gravel and thus magnetic susceptibility and gamma density data would not provide useful data. Due to the absence of diamict shear strength measurements were not carried out.

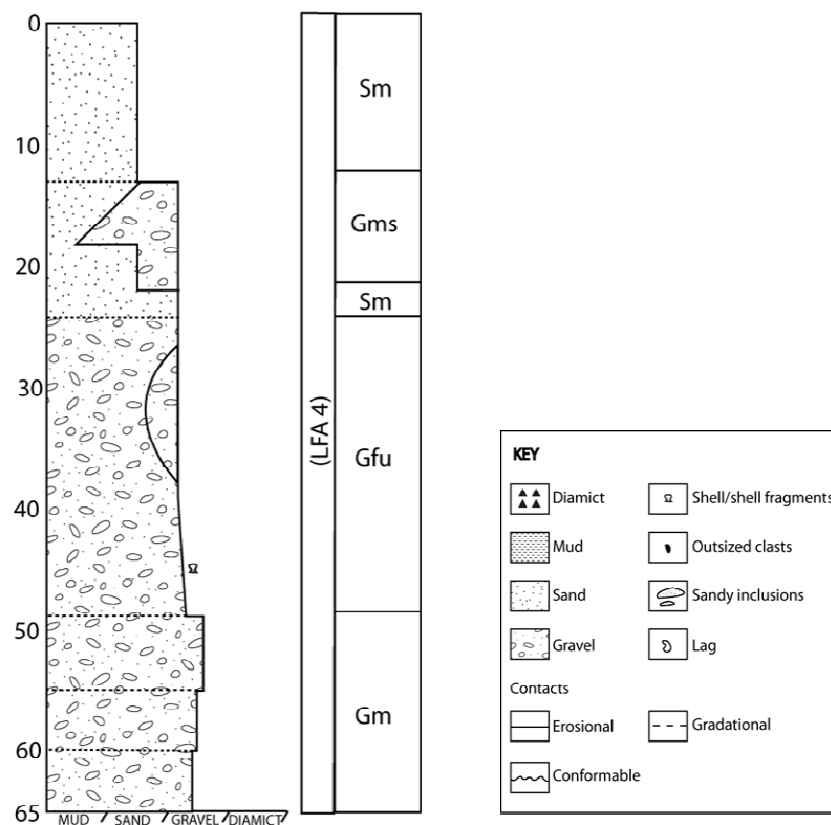
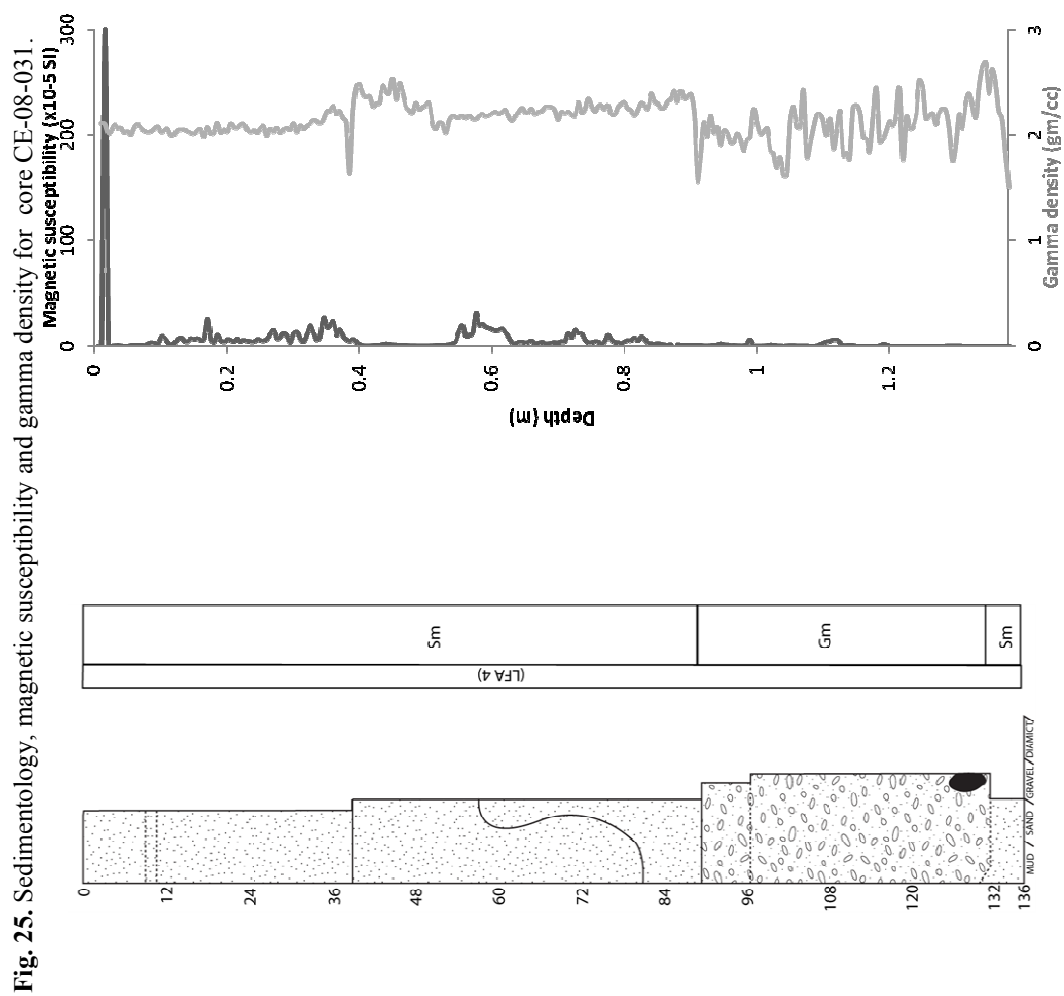


Fig. 24. Sedimentology of core CE-08-025 and associated LFAs.

4.3.12 Core CE-08-031

This core was extracted from the bathymetric low area behind the outermost moraine (Fig. 11). It consists of a range of gravel and sand lithofacies (Fig. 25) the lowermost of which is a sandy mix of shell hash and small pebbles (Sm, 136-131 cm). It is overlain gradationally by a normally graded pebble gravel (Gm, 131-89 cm) which is clast supported and poorly sorted. The gravel contains occasional shells (single valves) and shell fragments and has an average clast size of ~40mm, although from 97-89 cm there is less shelly material present and clast sizes are smaller (~12 mm). The gravel is overlain by a thick bed of massive sand (Sm) from 89-0 cm depth. The base of this massive sand is characterised by a coarse textured dark beige sand (89-57 cm). There is a convoluted but sharp contact separating this darker unit from the overlying massive sand which is markedly lighter in colour. This sand consists of a mixture of coarse sand and shell hash (81-39 cm). From 39-0 cm the massive sand is light brown in colour, very well sorted, fine grained and contains a prominent lamination of lighter sand at 8-7 cm depth.

This core displays very low magnetic susceptibility values (Fig. 25). From the base of the core to 82.5 cm the results display readings below $\sim 1 \times 10^{-5}$ SI. The values become more amplified from 84-0 cm with values reaching $\sim 30 \times 10^{-5}$ SI, however values do become very low between 52-40 cm. Gamma density values are also variable ranging from 1.5 to 2.6 gm/cc (Fig. 25). From 136-91 cm the gamma density is very variable and fluctuates from 1.6-2.6 gm/cc, this corresponds to the clast supported gravel. Gamma density values from 91-39 cm remain relatively high (~ 2.2 gm/cc), although from 39-0 cm values drop to ~ 2.0 gm/cc. . Shear strength was not measured in this core because of the absence of diamict.

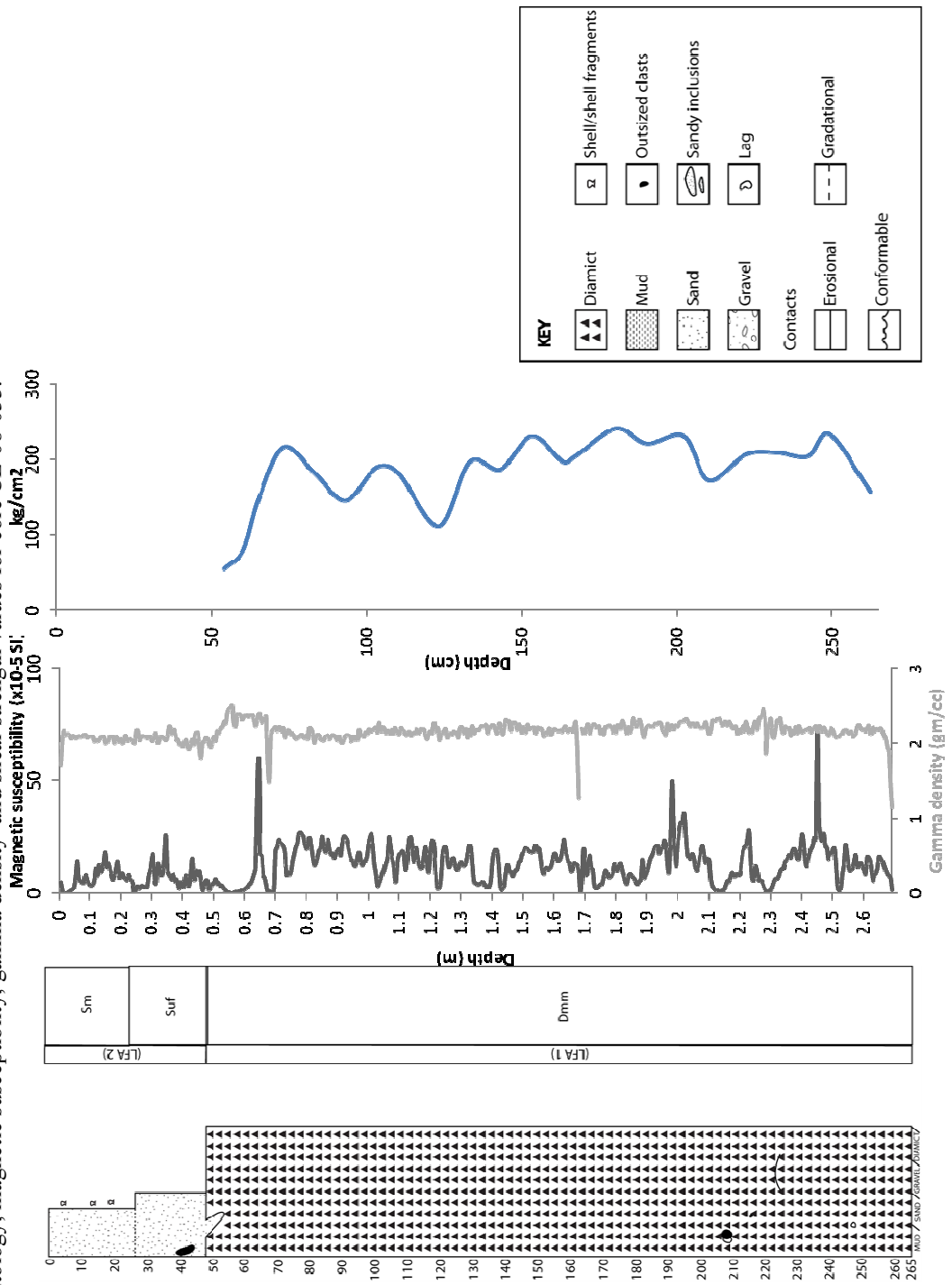


4.3.13 Core CE-08-033

This core was extracted from ~9 km inshore of the outermost moraine (Fig. 11). It consists of three lithofacies (Fig. 26). The lowermost lithofacies is a brown, very stiff massive diamict (Dmm, 265-48 cm). It is characterised by shear strength values that typically exceed 150 kg/cm^2 , and occasionally exceed 200 kg/cm^2 (Fig. 26). The upper 12 cm of the diamict is less consolidated as shown by a dramatic decrease in shear strength ranging from 78 kg/cm^2 to 53 kg/cm^2 . The diamict is overlain by normally graded, granular sand (Suf) from 48-26 cm depth. This Suf is a poorly sorted granular sand with a few large clasts and numerous single shell valves and fragments. The top 26 cm of the core is a massive, very well sorted, fine-grained sand.

This core shows considerable variability in its magnetic susceptibility measurements, however, the majority of the values are below $30 \times 10^{-5} \text{ SI}$ (Fig. 26). From 265-58 cm the core shows oscillating magnetic susceptibility values which coincides with the diamict lithofacies. This diamict lithofacies has an average magnetic susceptibility $\sim 13 \times 10^{-5} \text{ SI}$. From 58-0 cm the amplitude of these oscillations decreases. The sandy lithofacies (Sm and Suf) have an average magnetic susceptibility of $6.6 \times 10^{-5} \text{ SI}$. Gamma density measurements throughout the core remain consistent around 2.2 gm/cc , with only minor fluctuations (Fig. 26). However the graph does illustrate a peak between 68-49 cm.

Fig. 26. Sedimentology, magnetic susceptibility, gamma density and shear strength values for core CE-08-033.

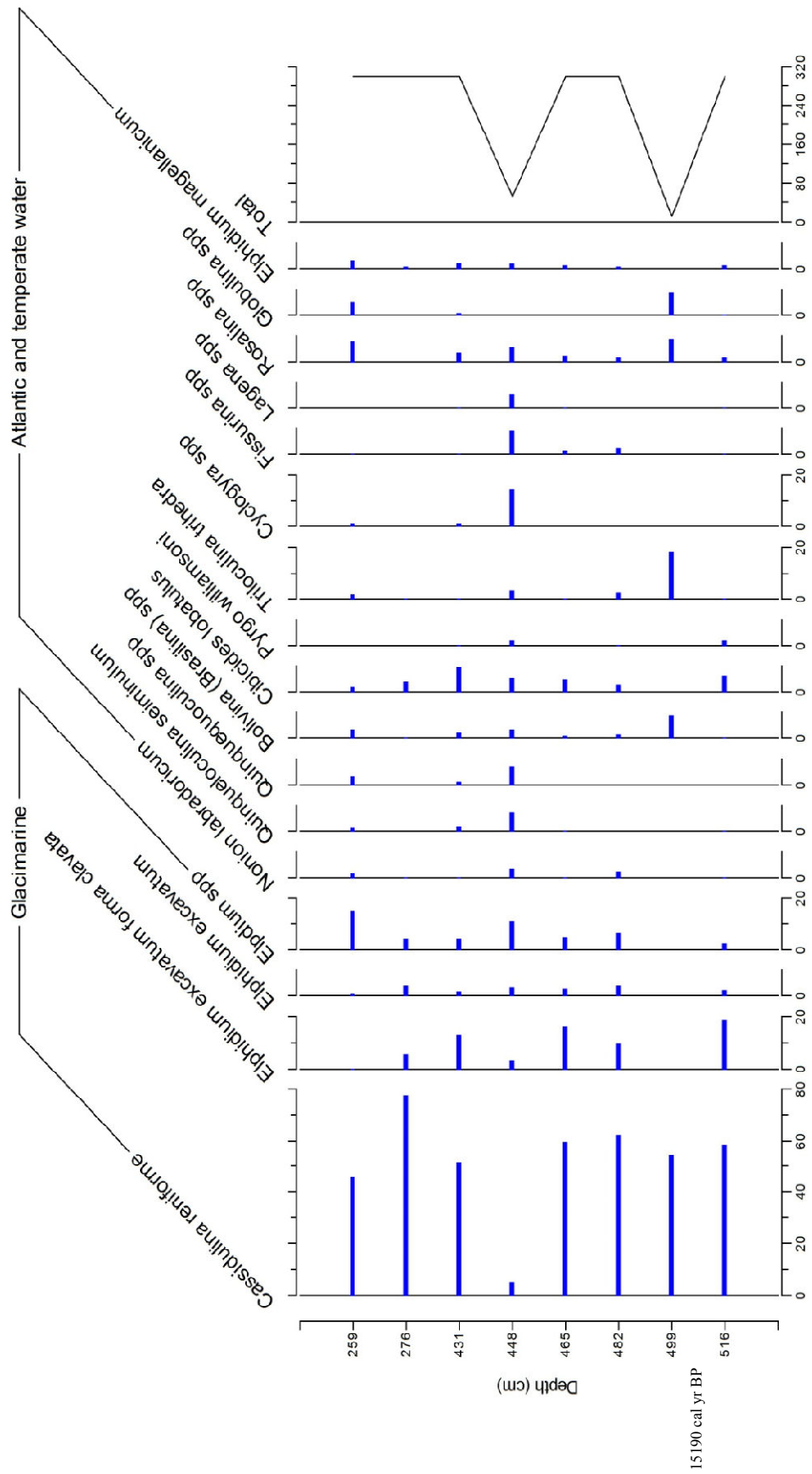


4.4 Foraminifera abundance analysis

Cores CE-08-003 and CE-08-010 were both analysed to identify the foraminiferal assemblages present. Core CE-08-003 (Fig. 27) displays glacimarine indicator species at all depths sampled such as *Cassidulina reneforme*, *Elphidium excavatum forma clavata*, *Elphidium excavatum* and *elphidium spp.* *C. reneforme*, was a very common species located throughout all depths but particularly between 510-425 cm where their abundance exceeded 41%. The remaining glacimarine species also display significant abundance between 510-425 cm in comparison to the Atlantic and temperate species (Fig. 27). The percentage of Atlantic and temperate species are very low from depths of 510-459 cm, although *Elphidium magellanicum*, *Rosalina spp* and *Cibicides lobatulus* do have percentages ranging up to 5%. There is a marked difference from 442-425 cm where Atlantic and temperate species increase in abundance such as *Pyrgo williamsoni*, *Rosalina spp*, *Triloculina trihedral*, *Cyclogyra spp* and *E. magellanicum*. Glacimarine species decrease dramatically to less than 10% between 180-163 cm depth, whereas all Atlantic and temperate species show an increase in abundance excluding *P. williamsoni*, *T. trihedral*, *Cyclogyra spp* and *Nonion obiculare*. The foraminiferal abundance chart also displays data relating to the abundance of molluscs. Although this was not within the original aim of the research, molluscs occurred in such a high percentage in the upper two samples (180 and 163 cm) that they are included.

Foraminifera abundance data for Core CE-08-010 (Fig. 28) shows glacimarine indicator species at all depths such as *C. reneforme*, *E. excavatum forma clavata*, *E. excavatum* and *Elphidium spp.* *C. reneforme* was a very common species with a high abundance, exceeding 46% at all depths excluding the 448 cm sample. Atlantic and temperate water species abundance is low in comparison to the glacimarine indicators. However, at depths of 499 and 448 cm the percentage of Atlantic and temperate water species do increase. At 499 cm the percentage of *Bolvina spp*, *T. trihedral*, *Rosalina spp* and *Globulina spp* all increase. Additionally at 448 cm the majority of Atlantic and temperate water species also increase in abundance (excluding *Globulina spp*), whereas the *C. reneforme* decreases to 5%. However, it must be noted that at both 499 and 448 cm the overall sample size is much smaller due to lack of foraminifera at these depths. Abundance of all Atlantic and temperate water species is very low at 276 cm (excluding *C. lobatulus*).

Fig. 28. Foraminiferal assemblage from core CE-08-010, classified into two faunal assemblage zones, the 14C date obtained this core is also shown.



4.5 Lithofacies Associations

Nine lithofacies have been identified from the cores analysed (Table 2). These lithofacies were grouped into four lithofacies associations (LFAs) based on their physical similarities, physical properties, foraminifera assemblages and the contacts between the individual lithofacies (Fig. 29)

4.5.1 LFA 1: Brown diamict and mud association

LFA 1 was observed in cores CE-08-008, CE-08-010, CE-08-011 and CE-08-033. LFA 1 comprises a brown, massive, matrix-supported, over-consolidated diamict (Dmm) which is the basal unit within all four cores. It is characterised by very high shear strength values ($>200 \text{ kg/cm}^2$) which decrease upwards. In core CE-08-010 this stiff diamict is overlain by a softer diamict. The softer diamict contains inclusions of sand which increase vertically upwards. LFA1 was sampled for foraminifera for the purpose of radiocarbon dating (15190 cal yr BP (UCIAMS-133551)) and abundance analysis (Fig. 28). Samples from the diamict at 516, 482 and 465 cm, are associated with the softer Dmm and a high percentage of glacimarine indicator species and low percentages of Atlantic and temperate water species (as discussed in section 4.4). The magnetic susceptibility of this LFA is highly variable possibly as a result from the variable grain sizes and differing grain provenance. The gamma density for this LFA is $\sim 2.8 \text{ gm/cc}$ but also displays some variability especially within core CE-08-010.

4.5.2 LFA 2: Mud and sand association

LFA 2 (Fm, Fl, Sm, Sh, Suf) was observed cores CE-08-003, CE-08-004, CE-08-010, CE-08-015, CE-08-018 and CE-08-033. LFA 2 comprises massive sand, massive mud, laminated sand, laminated mud and normally graded sand. Although LFA 2 is dominated by laminated lithofacies, the massive mud lithofacies that are present in the majority of the cores are quite thick, ranging from 30-99 cm. LFA 2 was also sampled for foraminifera in cores CE-08-003 and CE-08-010 for the purpose of abundance analysis (Figs. 27 and 28). The foraminifera associated with this LFA are dominated by glacimarine indicator species as illustrated by Fig. 27 and 28. In core CE-08-010 this LFA is characterised by low foraminifera counts (excluding samples from 431-459 cm) and a subtle increase in Atlantic and temperate water species. The upper sample depths of 179 and 102 cm from core CE-08-003 are also dominated by Atlantic and temperate water species and additionally *Pteropods*. This LFA was heavily sampled for the purpose of radiocarbon dating from core CE-08-003, CE-08-004 and CE-08-018. The core catcher from the outer shelf (CE-08-018) was dated to

23742 cal yr. BP (UCIAMS-133552), the laminated mud in core CE-08-004 was dated to 17797 cal yr. BP (SUERC-47522) and the dates obtained for core CE-08-003 provide a minima for ice sheet retreat (12763 to 12170 cal yr. BP). This LFA is also associated with high sedimentation rates (ranging from 1.3 m – 1.9 m kyr⁻¹) which were calculated using the radiocarbon dates and presented in Fig. 14.

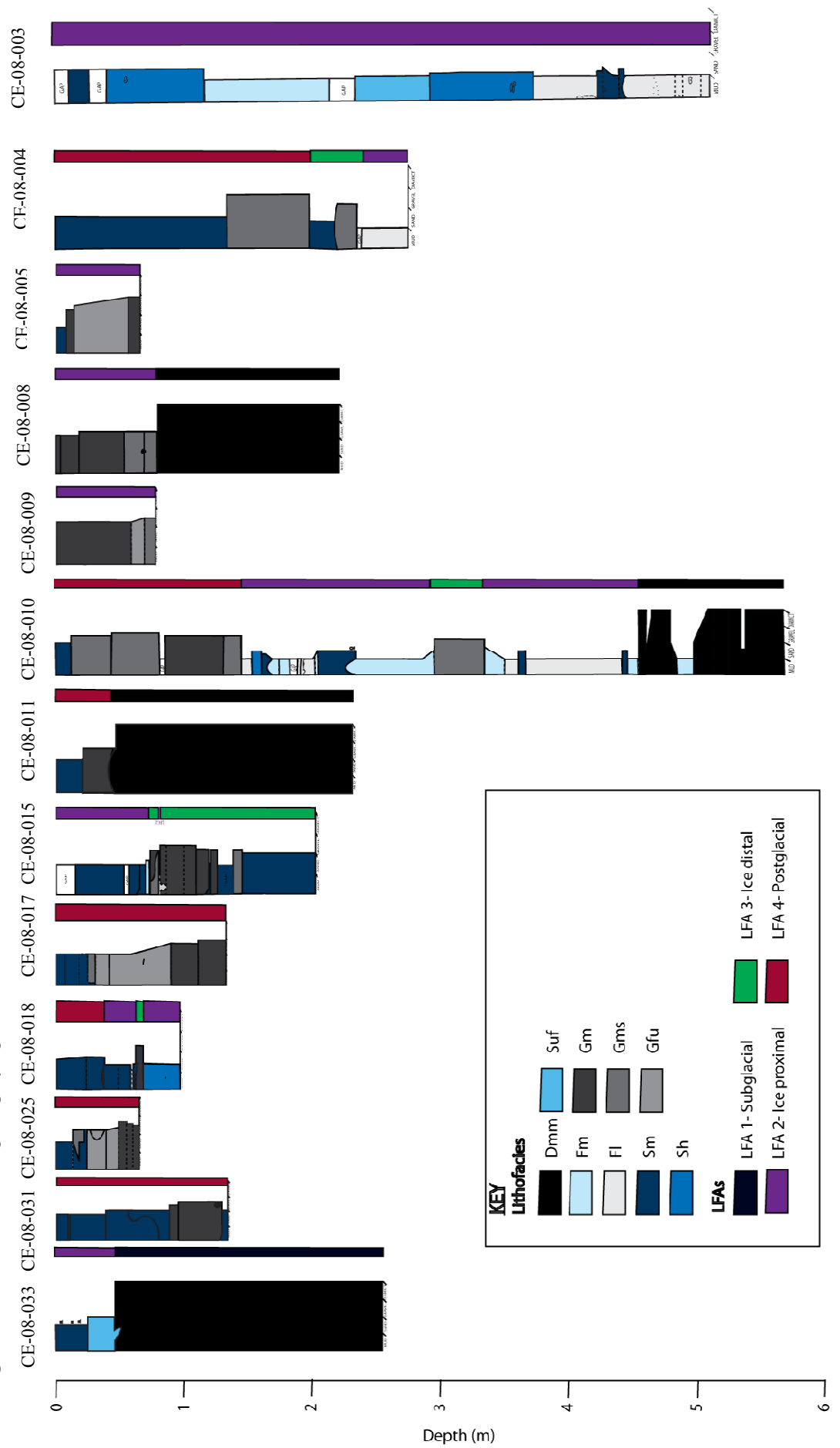
4.5.3 LFA 3: Sand and gravel association

LFA 3 (Sm, Gm and Gms) was observed in cores CE-08-004, CE-08-010, CE-08-015 and CE-08-018. LFA 3 is characterised by poorly-sorted, massive units of sand as well as matrix-supported and clast-supported gravels. These lithofacies have been grouped together because they are usually small units that are underlain and overlain by interbeds of massive mud. The transitions between the lithofacies are gradational and they are not as coarse grained as the overlying LFA4. No foraminifera were sampled from this LFA. Core CE-08-004 and CE-08-015 were sampled for the purpose of radiocarbon dating. LFA 3 in core CE-08-004 was dated to 12933 cal yr. BP (SUERC-47517) and in core CE-08-015 the LFA was dated to 13888 cal yr. BP (SUERC-47518).

4.5.4 LFA 4: Sand and gravel association

LFA 4 (Sm, Gm, Gms and Gfu) was observed in all cores except from core CE-08-003, CE-08-015 and CE-08-033. LFA 4 consists of massive gravel and sand lithofacies with occasional normally graded gravel (Gfu). The massive sand has been placed into this association because it is more coarse grained than the other massive sands that are associated with LFA2 and LFA 3. No foraminifera were sampled from this LFA.

Fig. 29. Colour coded core logs displaying lithofacies and associated LFAs.



4.6 Core Sedimentology - Interpretation

4.6.1 LFA 1: Brown diamict and mud association

LFA 1 was observed at the base of cores CE-08-008, CE-08-010, CE-08-011 and CE-08-033. The brown diamict of this LFA is characterised by a massive structure, abundant matrix and typically very high shear strength values. This is interpreted as supporting a subglacial origin for the diamict (J.M. van der Meer 1993; Ó Cofaigh et al. 2005; Evans et al. 2006; Pudsey et al. 2006; Ó Cofaigh et al. 2007; Hogan et al. 2010b). In addition, the absence of lenses of gravel or coarse sand within the diamict does not support an ice rafted debris origin, and the lack of bedding and grading suggests that it is not a mass flow deposit (Dowdeswell et al. 1994). The high shear strengths that characterise the diamict are likely related to the loading and compaction by grounded glacier ice (Evans & Pudsey 2002; Evans et al. 2005). This LFA is therefore interpreted as a subglacial traction till (hybrid till) produced by an array of processes in the traction zone (Evans et al. 2006). However, the overlying softer diamict in core CE-08-010 is interpreted as deglacial sediment due to the high sand content which increases up core, lower shear strength and high abundance of glaci-marine foraminifera (e.g. *C. reneformis*) (Figs. 19 & 28). This interpretation is also supported by the massive mud (LFA 2) that separates the diamict lithofacies (Polyak & Solheim 1994; Ó Cofaigh et al. 2005). The presence of such massive marine muds can indicate ice proximal glaci-marine conditions with high sedimentation rates from sediment-rich meltwater plumes, or alternatively, deposition in an ice distal setting by sediment settling through the water column (Boulton 1990; Cowan et al. 1999; Evans et al. 2005). As a consequence, the softer diamict within core CE-08-010 is interpreted here as an ice rafted diamict due to its massive nature, gradational contacts, poor sorting and large number of clasts which lack a common orientation (at least based on visual assessment from the x-radiographs) and sandy lenses (Domack and Lawson, 1985; Dowdeswell et al. 1994; Cowan et al. 1997; Ó Cofaigh et al. 2001). This deglacial sediment was dated from core CE-08-010 (15190 cal yr. BP) and provides a date that constrains the timing of deglaciation. From 534 to 505 cm (within core CE-08-010) this softer diamict consists of stacked beds and has an erosive basal contact with a graded zone at the top suggesting that subsequent to its emplacement the ice rafted diamict was remobilised and resedimented by mass flow processes (Kurtz & Anderson 1979; Ó Cofaigh et al. 2001). The mass flow most likely can be attributed to an intermediate strength cohesive debris flow because it is encased in mud and is less than 1 metre in thickness (Talling 2013).

The foraminifera abundance analysis focused on the transition between the diamict, the massive mud interbed and the overlying diamict (Fig. 28). The foraminifera that dominated this transition were glacialmarine species (e.g *C. reniforme* and *E. excavatum forma clavata*) as discussed in section 4.4. The abundance of *C. reniforme* is high within the diamict and the massive mud interbed (LFA 2) which indicates a proximal glacialmarine setting. However, the massive mud interbed also displays an increase in the percentage of Atlantic water and temperate species. This influx of warmer temperature foraminifera species could indicate that warm water was driving ice sheet retreat. However, the foraminifera counts were very low in this mud interbed, which could be a result of high meltwater and sediment flux as a result of a retreating ice margin and as a consequence this could bias the assemblage identified (Lloyd 2006; Kilfeather et al. 2011).

4.6.2 LFA 2: Mud and sand association

This LFA comprises Fm, Fl, Sm, Sh and Suf lithofacies but is dominated by laminated sediments. LFA 2 is dominated by glacialmarine foraminifera species such as *C. reniforme* and *E. excavatum forma clavata*. Within core CE-08-003 there is a progressive decrease in glacialmarine species up core and a corresponding increase in Atlantic and temperate water species (such as *Rosalina spp* and *C. lobatulus*). The large proportion of *Pteropods* within samples from 180-163 cm indicates an open marine environment. Core CE-08-010 (Fig. 28) does not display such a clear transition from glacialmarine to more temperate species. In this core the glacialmarine taxa dominate the samples up to a depth of 258cm, which indicates that the ice sheet was still in fairly close proximity (Lloyd 2006). The majority of foraminifera samples were extracted from the laminated sediments that dominate this LFA. Laminated sediments can be formed as a result of suspension settling from turbid meltwater plumes (Cowan et al. 1999), deposition from turbidity currents (Gilbert et al. 1998), or from contour current activity (Howe and Pudsey, 1999). Ó Cofaigh & Dowdeswell (2001) distinguish the genesis of laminated sediments through the identification of sedimentary structures, thickness, texture and sorting, contacts, fauna and stratigraphic relationships. The laminated sediments of LFA2 are interpreted as having formed from a combination of turbidity currents and suspension settling from meltwater plumes. This interpretation is supported by their graded nature, their variability in texture and thickness, their sharp lower boundaries, and their grain (Anderson et al. 1984; Cowan et al. 1999). The homogeneous mud that occurs above these laminated sediments could have been deposited at the end of a turbidity current flow (Cowan et al. 1999). This evidence, in conjunction with the high sediment rates

supports an ice proximal interpretation for this LFA which has also been established through the foraminifera analysis. LFA 2 also contains massive mud and sand lithofacies which can indicate a waning of the meltwater influx to the core sites, high rates of sedimentation or high rates of bioturbation (Elverhøi et al. 1989; Evans et al. 2005). As a consequence this LFA has been interpreted as an ice proximal glacial-marine deposit and thus the dates obtained from LFA 2 can be used to infer the timing of deglaciation across the shelf.

4.6.3 LFA 3: Sand and gravel association

LFA 3 is a transitional lithofacies association. It demonstrates a shift from laminated to massive sediments and more gravelly lithofacies (Sm, Gm and Gms). The presence of massive and poorly sorted sediments points to the decreasing influence of meltwater and an increasingly ice distal environment (Stevens 1990). The poor sorting, overall lack of grading and lamination suggests a hemipelagic environment (Hillenbrand et al. 2005). The muddy gravels identified are interpreted as ice rafted debris due to their gradational contacts and lack of bedding or normal grading that would indicate deposition from mass flow (Dowdeswell et al. 1994), whereas the clast supported gravels are interpreted as a product of debris flows, due to their inversely graded nature (cf, Shanmugam 2000). The material that comprises these debris flows most likely originated from the base of the ice sheet during a standstill whilst undergoing overall retreat (Ottesen & Dowdeswell 2006). These mass flows could have been triggered through the movement of the ice sheet to an increasingly distal position, which would have destabilised the material (Salvi et al. 2006). The radiocarbon dates from this LFA were obtained from the mid shelf (core CE-08-015) and the inner shelf (core CE-08-004). The dates indicate that the ice sheet had significantly retreated from the mid shelf before 13888 cal yr. BP and from the inner shelf before 12933 cal yr. BP.

4.6.4 LFA 4: Sand and gravel association

LFA 4 comprises a series of typically poorly-sorted, sandy and gravelly facies that are predominantly massive but also include some graded sediments (Sm, Gm, Gms and Gfu). Stratigraphically LFA 4 forms the uppermost LFA in the cores and because of this a first order interpretation it represents deposition after ice sheet retreat. Massive and graded gravels can result from a number of different processes in the marine environment including sediment gravity flows or bottom current activity (Anderson et al. 1984). In the case of LFA4, the gravels are inferred to originate from a combination of both processes due to their normal grading (indicative of sediment gravity flows) and the dominance of clast supported gravel within the LFA

indicates the winnowing of finer grained material from bottom currents (Anderson et al. 1984; Evans et al. 2005). The high occurrence of shelly, coarse grained sand and gravel can be attributed to a lag deposit from current activity (Dowdeswell et al. 1998; Howe et al. 2001; Howe et al. 2006). LFA 4 directly overlies LFA1 with an erosional contact in three of the cores (cores CE-08-008, CE-08-011 and CE-08-033), and implies that the intervening deglacial sediments have been removed by bottom current activity which reworked the shelf sediments (Ó Cofaigh et al. 2001; Hogan et al. 2010b).

4.7 Summary

This chapter has presented the results obtained from the analyses performed on thirteen marine sediment cores from the northwest Irish shelf. Four lithofacies associations (LFAs) are identified within the cores; LFA1 (Brown diamict and mud association); LFA 2 (Mud and sand association); LFA 3 (Sand and gravel association) and LFA 4 (Sand and gravel association). These LFAs have been interpreted as representing a subglacial (LFA 1), ice proximal (LFA 2), ice distal (LFA 3) and postglacial (LFA 4) depositional environment based on the cores sedimentology, physical properties and foraminifera assemblages. The presence of subglacial till in one of the outer shelf cores (CE-08-033) confirms that the BIIS had an extensive continental shelf position with initial retreat underway by ~23800 cal kyr BP (14C dates from core CE-08-018), ice proximal glacialmarine deposits located on the mid shelf could verify a slow ice sheet retreat across the mid shelf accompanied by the suite of nested moraines. Radiocarbon dates from inner shelf core (CE-08-003 and CE-08-004) indicate deglaciation of the inner shelf commenced before c. 17,800 cal. yr BP. The implications of these results for the nature and extent of the BIIS on the continental shelf offshore of northwest Ireland are discussed in chapter 5.

Chapter 5 - Discussion

5.1 The sedimentary record of ice sheet advance and retreat on the NW continental shelf

Analysis of the marine sediment cores from Donegal Bay and the adjoining shelf offshore of NW Ireland has identified lithofacies associated with both ice sheet advance (e.g. subglacial till) and retreat (e.g. glacimarine sediments) across the continental shelf. Four LFAs have been identified and interpreted; LFA 1) subglacial; LFA 2) ice proximal; LFA 3) ice distal and LFA 4) postglacial (see Chapter 4 above).

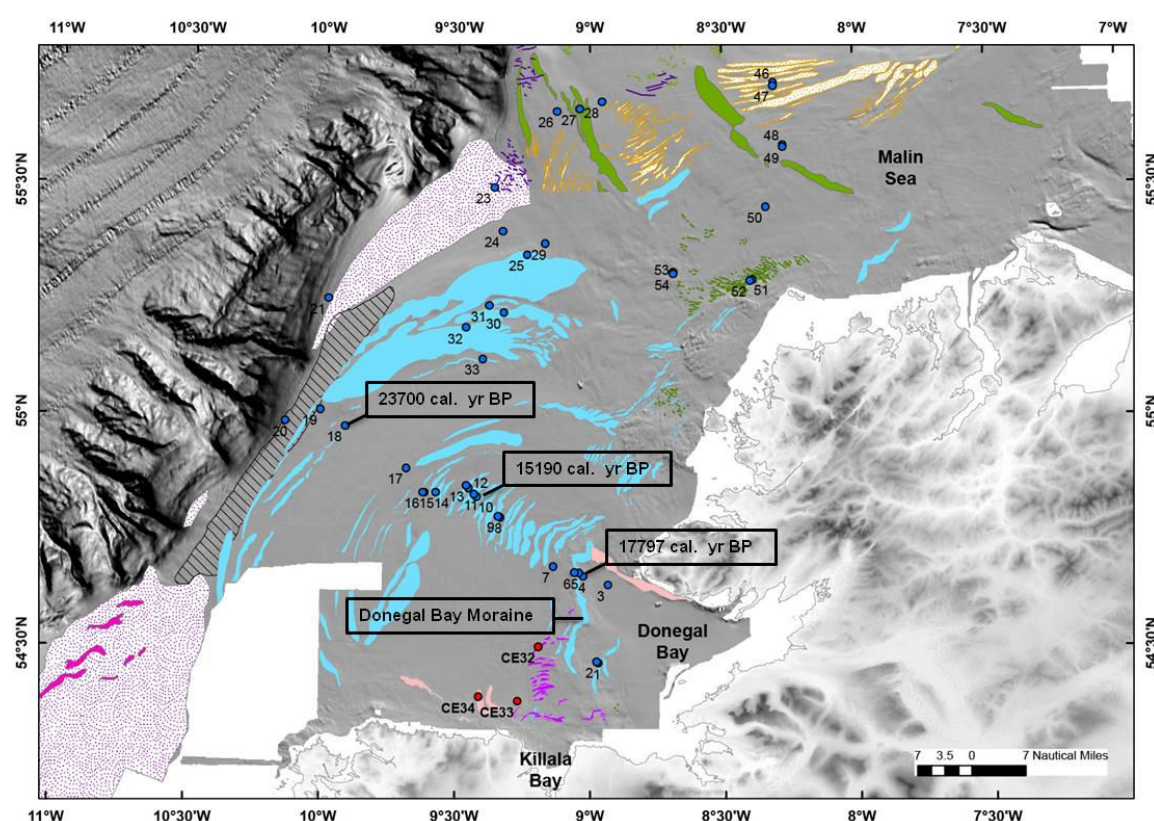


Fig. 30. Location map showing cores collected during cruise CE-08 of the Celtic Explorer from the NW Irish continental shelf, the prominent arcuate moraines (blue shading) including the Donegal Bay moraine and three of the obtained from radiocarbon dating in this study.

The continental shelf offshore of NW Ireland is characterised by a large moraine complex (Fig. 30) with iceberg ploughmarks distal to the shelf edge moraine (Ó Cofaigh et al. 2012). It has been proposed that these moraines record the extension of the ice sheet to the shelf edge pre-LGM and its subsequent slow and punctuated retreat (Ó Cofaigh et al. 2012). The presence of subglacial till in core CE-08-033 (Fig. 26 and 30) confirms the flow of grounded ice to the shelf edge during the LGM. An LGM age for this deposit has been assigned on the basis of the dates from the overlying glacimarine sediments (see section 4:2), in

conjunction with wider evidence in the form of IRD from the Barra Fan that suggest a shelf edge position for the BIIS offshore of NW Ireland during the LGM (Wilson & Austin 2002). The overlying glacimarine sediments identified within the cores, document ice sheet retreat across the shelf. Cores sampled from the outer shelf are dominated by postglacial deposits related to bottom current activity and contain less than 50 cm of ice proximal glacimarine material, where present (cores 18, 25, 31 and 33; Figs. 23, 24, 25 and 26). The absence of ice proximal glacimarine sediments might suggest rapid retreat and an abrupt change to an ice distal environment (Hogan et al. 2010a; Jennings et al. 2014). However, because of the location of these cores from the outer shelf and the typically thick package of postglacial bottom current deposits that overlie the glacimarine sediments, it is possible that at least part of the deglacial sequence has been removed by current reworking (Anderson et al. 1984; Evans et al. 2005). Iceberg ploughmarks are present distal to the shelf edge moraine, which indicates that initial retreat was associated with ice sheet break up by a large calving event (Ó Cofaigh et al. 2012). Therefore initial retreat from the ice sheet's shelf edge position may have been rapid and associated with a calving event.

The nature of ice sheet retreat across the mid shelf contrasts with that of the outer shelf. Sediment cores from the mid-shelf (cores 8, 9, 10, 11, 15 and 17; Figs. 17, 18, 19, 20, 21 and 22) record ice proximal sedimentation (LFA 2) which are overlain by transitional sediments (LFA 3). The glacimarine sediments relate to three main processes: 1) turbidity currents and debris flows; 2) suspension settling from turbid meltwater plumes; and 3) the rainout of IRD. The thick ice proximal glacimarine facies point to slow ice sheet retreat across the mid shelf. This interpretation is supported by the numerous moraines identified on the mid shelf between the locations of cores CE-08-017 to CE-08-008 (Fig. 30). The laminated nature of the glacimarine sediments indicates that meltwater was a significant contributor to sedimentation (Polyak & Solheim 1994; Hogan et al. 2010a; Jennings et al. 2014). Two of the marine sediment cores (CE-08-011 and CE-08-008) consist solely of LFA 1 (subglacial deposits) and LFA 4 (postglacial deposits). In these instances the deglacial sediments are inferred to have been eroded by bottom currents (Anderson et al. 1984; Evans et al. 2005). The presence of ice proximal glacimarine sediments above the LFA 3 transitional lithofacies in Cores CE-08-010 (Fig. 19) and CE-08-015 (Fig. 21) suggests some possible minor oscillations of the ice sheet margin during overall deglaciation, which is confirmed by the strong glacimarine foraminifera signal at 276 cm in core CE-08-010 (Fig. 28) and the moraine sequence on the shelf (cf. Ballantyne et al. 2007; McCabe et al. 2007; Bradwell et al. 2008; C. Clark et al. 2012; Ó Cofaigh et al. 2012).

The sedimentary record of the inner shelf is characterised by the transition from ice proximal (LFA 2) to ice distal (LFA3) glacimarine deposition and subsequent post glacial bottom current activity (LFA 4) (Cores 3, 4 and 5; Figs. 14, 15 and 16). Core CE-08-005 was extracted from the Donegal Bay moraine (Fig. 29) and consists solely of postglacial bottom current deposits. Cores CE-08-003 and CE-08-004 were extracted from inshore of the Donegal Bay moraine (Fig. 30), these cores record ice proximal glacimarine deposition. The thick beds of glacimarine sediments in core CE-08-003 indicate high sedimentation rates which are common in tidewater environments (Kilfeather et al. 2011).

The sediments recovered in cores from the shelf offshore of NW Ireland contain a range of glacimarine lithofacies but importantly they include laminated and massive muds related to meltwater deposition (Polyak & Solheim 1994). This emphasises the role of meltwater delivery and sedimentation during retreat of the last ice sheet across the shelf in this region and contrasts with deglacial sequences of glacimarine sediments described from Antarctica, where glacimarine deposits reflect minimal meltwater derived lithofacies and are largely dominated by coarse grained lithofacies (Evans et al. 2005). The ice sheet on the NW shelf was therefore likely a tidewater margin in which meltwater contributed strongly to both retreat and sedimentation (cf. Mackiewicz et al. 1984; Dowdeswell et al. 1994; 1998).

The sedimentary record indicates that the ice sheet was grounded at the shelf edge offshore of NW Ireland. Initial retreat from the shelf edge was rapid, followed by a slow retreat across the mid shelf. This is in contrast to the reconstruction of C. Clark et al. (2012) who propose a slow rate of ice loss during retreat from the shelf edge.

5.2 Timing and nature of ice sheet retreat

Previous reconstructions of the extent of the BIIS on the continental shelf during the LGM have largely been inferred from terrestrial evidence (e.g., Ballantyne et al. 2007; Greenwood & Clark 2009) or from the analysis of deep sea sediment cores (Wilson & Austin 2002; Scourse et al. 2009). These reconstructions range from an extensive pre-LGM ice sheet at the shelf edge (J. Clark et al. 2012) to a more restricted LGM ice sheet that was confined to a position between the Donegal Bay moraine (Fig. 30) and the shelf edge (McCabe et al. 2007), to an ice sheet that extended through Donegal Bay onto the continental shelf during the LGM (Ballantyne et al. 2007; Greenwood & Clark 2009). The radiocarbon dates obtained in this study

from benthic foraminifera and shells within the cores from the continental shelf (see Chapter 4) are the first to directly constrain the timing of deglaciation from the shelf edge. These dates are used to test the validity of the C. Clark et al. (2012) reconstruction for NW Ireland (Fig. 31).

The analysis of geophysical data by Ó Cofaigh et al. (2012) and the core sedimentological analysis from this study have presented strong evidence that the last ice sheet was grounded to the shelf edge offshore of NW Ireland. However crucial to determining the timing of this advance to the shelf edge and subsequent ice sheet retreat is stratigraphically well-constrained, dated marine sediment cores. The date obtained from core CE-08-018 (which is located directly inboard of the shelf edge moraine, see Fig. 30) indicates that deglaciation from the shelf edge commenced prior to c. 23,700 cal. yr BP. This date is supported by the analysis of IRD records from deep sea cores along this margin, which proposed that the ice sheet remained at the shelf edge until 24 cal kyr BP and then underwent retreat at 23 cal kyr BP (Wilson & Austin 2002; Scourse et al. 2009).

Radiocarbon dates obtained from glaci-marine sediments in cores from the mid shelf indicate that retreat had occurred before 15,190 cal. yr BP (core CE-08-010, Fig. 30). This corresponds to the dates that have previously been suggested by several previous studies such as McCabe (1986) and McCabe & Clark (2003) for retreat from the mid shelf. However these dates are *minima* for ice sheet retreat due to the older dates obtained from glaci-marine sediments in cores from the inner shelf (see below). On this basis, retreat from the mid shelf had occurred before c. 17,800 cal. yr BP and therefore much earlier than proposed by McCabe (1986) and McCabe & Clark (2003).

Radiocarbon dates obtained from cores CE-08-003 and CE-08-004 indicate deglaciation of the inner shelf before c. 17,800 cal. yr BP (Fig. 30). The Donegal Bay moraine (core CE-08-005) has previously been referred to as the marine continuation of the LF-BF line (see chapter 2). The Bloody Foreland moraine was dated in Northern Donegal by Clark et al. (2009) to 19.3 ± 1.2 kyr. This date was obtained by using ^{10}Be surface exposure ages from granitic erratics deposited on the Bloody Foreland moraine. Therefore the Donegal Bay moraine could also be assigned to a similar age. Either way the date from core CE-08-004 (this study) indicates ice sheet retreat from the Donegal Bay moraine by c. 17,800 cal. yr BP. Hence this rules out the possibility of the Donegal Bay moraine being of Killard Point Stadial age (15.6 kyr BP) as proposed by McCabe et al. (2005). The Donegal Bay moraine could be interpreted as either a re-advance or a longer still stand during retreat. The former interpretation is preferred due to the re-appearance of LFA 2

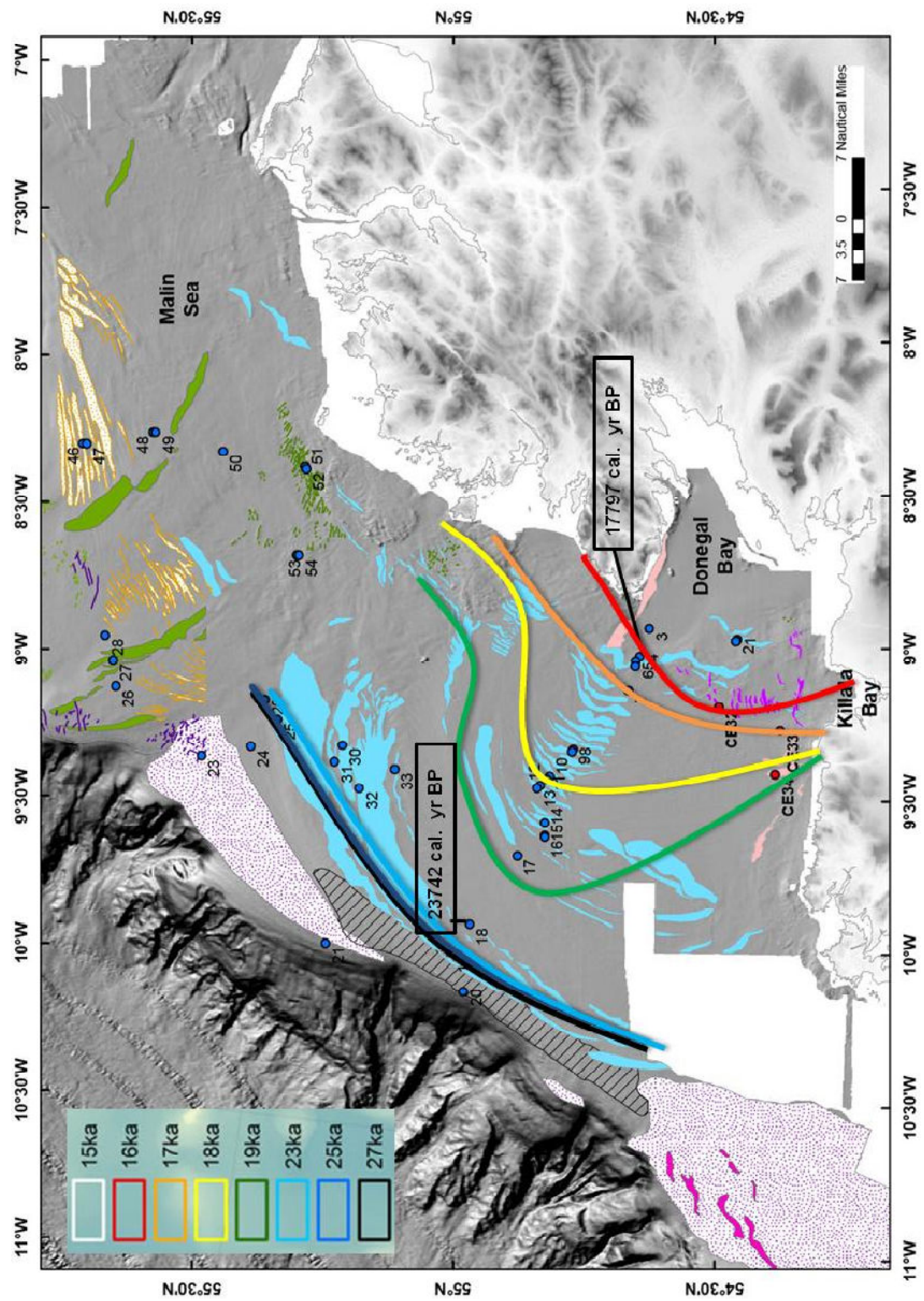
(proximal glacimarine sediments) above LFA 3 (distal glacimarine sediments) in core CE-08-010 which corresponds to an increase in glacimarine foraminifera indicator species (*C. reneforme*) at 276 cm. Evidence for a re-advance between ca. 24 kyr BP and 18 kyr BP has been documented elsewhere on the BIIS margin by Bradwell et al. (2008).

The radiocarbon dates from the marine sediment cores presented in this study are the first direct chronological constraints on the timing of retreat of the BIIS from the shelf edge offshore of NW Ireland. Initial retreat was underway by ~23800 cal kyr BP, this retreat was rapid and associated with a large calving event. This was followed by slow and punctuated retreat across the mid shelf to the inner shelf (Core CE-08-004). The ice sheet experienced a stillstand or re-advance to the Donegal Bay moraine sometime between >17800-19300 kyr BP with final retreat from the moraine to the inner shelf taking place before c. 17,800 cal. yr BP. The dates and associated core stratigraphy provide the first unequivocal evidence that during the LGM the BIIS extended to the shelf edge offshore of NW Ireland. This study has established that the ice sheet had retreated to the inner shelf before c. 17,800 cal. yr BP, consistent with the reconstruction of C. Clark et al. (2012) which proposed that the ice sheet was close to the present coastline ~17 kyr BP.

5.3 Wider implications

Establishing a chronology and retreat pattern for the last ice sheet offshore of NW Ireland has implications for current models and understanding of the dynamics of the BIIS. A comparison of the results of this study with the pattern of retreat proposed by C. Clark et al. (2012) indicates that there are some discrepancies (Fig. 30). Incorporating the dates obtained from this study would require an inward shifting of the isochrones offshore of NW Ireland towards the coast (excluding the 27 and 25 kyr isochrones). Retreat into Donegal Bay had occurred by 17.8 cal kyr BP and thus much earlier although at a slower rate (~12 m/yr) than their reconstruction suggests (17.5 m/yr). This alteration would modify the retreat rates that C. Clark et al. (2012) proposes for this ice stream and consequently highlights the importance of incorporating marine chronologies into ice sheet reconstructions.

Fig. 31. Map showing a selection of radiocarbon dates (from this study) plotted against the isochrones proposed by C. Clark et al. (2012).



The foraminifera fauna identified in this study also provide insights into the reconstruction of ice sheet retreat and associated depositional environments on the continental shelf. The foraminifera identified are mainly glacialmarine species (e.g. *C. reneforme* and *E. excavatum forma clavata*, Fig. 27 and 28). Hence a glaciallacustrine interpretation for the deglacial subaqueous sediments in the cores can be ruled out. The sediments identified on the continental shelf are glacialmarine and are likely associated with retreat of a grounded tidewater margin across the shelf (see above). The glacialmarine foraminifera also indicate that deglaciation occurred in a cold but meltwater dominated environment (Kaplan 1999; Jennings et al. 2014). It has been proposed that an influx of warmer Atlantic water instigated the retreat of the BIIS from the continental shelf offshore of NW Ireland as shown by the rise in SST in a core from Rockall Trough (Knutz et al. 2007). However, the foraminifera from core CE-08-010 from the mid shelf do not show a significant increase in warmer Atlantic taxa (Fig. 28). Glacialmarine foraminifera such as *C. reneforme* and *E. excavatum forma clavata* are present at high percentages across all depths sampled. There is evidence for an influx of warmer water species such as *Rosalina spp* in core CE-08-003 from the inner shelf but this influx occurred after c. 12,600 cal. yr BP as indicated by the date from 466 cm (core CE-08-003) by which time the ice sheet margin may have been terrestrially based according to C. Clark et al. (2012). As a consequence it would appear that warmer Atlantic water did not drive ice sheet retreat across the shelf in this region. However, the meltwater derived lithofacies are common in the cores from the continental shelf, indicating that meltwater was a major contributor to ice wastage. The high volumes of meltwater could have disrupted the influence of the resurgence of warmer Atlantic water (Lloyd et al. 2005).

Sea level rise has been proposed as the main driver for collapse of the BIIS (McCabe & Clark 2003). Abrupt sea level rise associated with Heinrich event 2 (c. 24 kyr BP; Bond & Lotti 1995; Peck et al. 2007) and the collapse of the Laurentide Ice sheet could have destabilised the marine terminating margins of the BIIS ensuing a rapid break up associated with a large calving event (Bradwell et al. 2008; Chiverrell et al. 2013). Based on the results from this study, retreat from the shelf edge offshore of NW Ireland commenced prior to c. 23,700 cal. yr BP. This date corresponds to Heinrich event 2 and the eustatic jumps generated by discharge of the LIS during Heinrich events (Haapaniemi et al. 2010). Thus it is proposed that the BIIS margin offshore of NW Ireland initiated deglaciation as a result of abrupt relative sea level rise. The ploughmarks documented by Ó Cofaigh et al. (2012) distal to the outer shelf moraine, in conjunction with the sedimentary record presented here, provides evidence to suggest initial ice sheet collapse was associated with a large calving event. Ice sheet destabilisation would have resulted in large scale reorganisation of the

ice lobes draining the BIIS which is confirmed by the extensive suite of moraines that span the continental shelf from south west Ireland to the Shetlands (Bradwell et al. 2008; Ó Cofaigh et al. 2012).

The dates and analysis of the marine sediment cores from offshore of NW Ireland has implications for the use of numerical models (Hubbard et al. 2009). Alterations in ice sheet extent and timing of retreat would affect the thickness of the ice sheet, the isostatic loading and the associated sea level history (Chiverrell & Thomas 2010). Well defined and well dated limits are crucial for verifying glaciological models that have been constructed. This study highlights the importance of incorporating constrained ice sheet limits to help improve the accuracy of numerical models reconstructing the dimensions of the BIIS.

Chapter 6-Conclusion

6.1 Introduction

In Chapter 1 the overall aim of this study was defined as:

To reconstruct the timing, extent and nature of the last advance and retreat of the British-Irish Ice Sheet (BIIS) on the continental shelf offshore of NW Ireland from marine sediment cores.

To address this aim a series of research questions were proposed:

1. What was the extent of the ice sheet offshore of NW Ireland at the LGM?
2. What is the nature of the sedimentary record of ice sheet advance and retreat across the shelf?
3. What was the timing and rate of deglaciation across the continental shelf?
4. Are there linkages between the response of the last ice sheet off NW Ireland and wider North Atlantic climate and oceanographic forcing during the last cold stage, in particular during deglaciation?

6.2 Main findings

6.2.1 BIIS extended to the shelf edge during the LGM

A transect of 13 cores from offshore of Donegal Bay NW Ireland provide direct evidence for extensive glaciation of the continental shelf. Sedimentological evidence from the cores indicate the presence of a grounded ice sheet at the shelf edge with subglacial till in one of the outer shelf cores (core CE-08-033). This interpretation is supported by the large moraine identified at the shelf edge by Ó Cofaigh et al. (2012). Chronological evidence from core CE-08-018 indicates that retreat was underway from the shelf edge by 23,700 cal. yr BP. Hence the ice sheet was present at the shelf edge during the LGM.

6.2.2 Initial retreat from the shelf edge was rapid and associated with a large calving event

Cores from the outer shelf do not contain thick sequences of glacimarine material, and this is interpreted as reflecting rapid ice sheet retreat from the shelf edge probably combined with at least the partial removal of such sediments by current reworking. Iceberg ploughmarks distal to the shelf edge moraine indicate that initial retreat from the shelf edge was associated with a large calving event.

6.2.3 Mid shelf and inner shelf cores indicate the slow retreat of a tidewater ice margin

The presence of thick beds of laminated glacial marine sediments produced by meltwater deposition in cores from the mid shelf point to the slow retreat of a grounded tidewater margin. The abundance of glacial marine foraminifera in these glacial marine deposits also supports a tidewater margin interpretation for the ice sheet. Meltwater was a significant contributor to retreat of the ice sheet and to sedimentation on the continental shelf. The reappearance of ice proximal glacial marine lithofacies and glacial marine foraminifera above the transitional LFA 3 in core CE-08-010 and CE-08-015 suggests minor oscillations of the ice margin during retreat. The inner shelf cores (CE-8-003 and CE-08-004) record ice proximal glacial marine deposition with high sedimentation rates which are again consistent with a tidewater glacial marine environment.

6.2.4 The ice sheet had retreated to inner Donegal Bay by c.17,800 cal. yr BP

Radiocarbon dates obtained from core CE-08-004 indicate ice sheet retreat from the Donegal Bay moraine had occurred by c. 17,800 cal. yr BP. In contrast to previous work (e.g. McCabe et al. 2005), it is inferred on the basis of this date that the moraine pre-dates the Killard Point Stadial (15.6 kyr BP). The Donegal Bay moraine could be interpreted as either marking a re-advance or a longer still stand during retreat which would have taken place sometime between >17,800-19,300 kyr BP.

6.2.5 The drivers of ice sheet retreat are still unclear

The foraminifera data indicate that at least initial ice sheet retreat across the shelf was not associated with the incursion of warmer Atlantic water. Rather the glacial marine indicator species and associated laminated glacial marine sediments point to the importance of meltwater during retreat. The timing of initial retreat from the shelf edge coincides with Heinrich event 2 (as indicated by the date of 23.7 cal kyr BP from the outer shelf core) and was associated with a large iceberg calving event. Hence it is possible that sea level rise associated with H2 (Chiverell et al. 2013) could have triggered initial retreat but this is still speculative.

6.3 Recommendations for future research

6.3.1 Improving core chronologies for the continental shelf

A recommendation for future research would be to try and constrain the timing of deglaciation from the BIIS shelf edge position offshore of NW Ireland by dating a glacial marine deposit overlying a subglacial till. The

cores analysed in this study did not recover a complete subglacial to ice proximal glacimarine sequence on the outer shelf.

6.3.2 Improve our understanding on the forcing behind ice sheet collapse

A higher resolution study of foraminifera abundance from cores near to the shelf edge is necessary to ascertain whether there is a clear insurgence of warmer Atlantic water and therefore an increase in Atlantic and temperate foraminifera taxa.

6.3.3 Reconstructing the dynamics of the BIIS

This study was the first to analyse marine sediment cores within this sector of the BIIS. As a result, there is huge potential to expand this research across the BIIS continental shelves to effectively constrain LGM ice sheet limits and the BIIS pattern of retreat. This will help to develop a robust ice sheet model for the collapse of the BIIS, which will enable a greater understanding of the various controls and feedback processes that govern ice sheet retreat.

References

- Anderson, J.B., Brake, C.F. & Myers, N.C., 1984. Sedimentation on the Ross Sea continental shelf, Antarctica. *Marine Geology*, 57(1-4), 295–333.
- Austin, W. E., Bard, E., Hunt, J. B., Kroon, D., & Peacock, J. D. 1995. The 14C age of the Icelandic Vedde Ash: implications for Younger Dryas marine reservoir age corrections. *Radiocarbon*, 37(1), 53-62.
- Ballantyne, C.K., Mccarroll, D. & Stone, J.O., 2007. The Donegal ice dome, northwest Ireland: dimensions and chronology. *Journal of Quaternary Science* 22, 773-783.
- Benetti, S., Dunlop, P. & Cofaigh, C.Ó., 2010. Glacial and glacially-related features on the continental margin of northwest Ireland mapped from marine geophysical data. *Journal of Maps*, 6(1), 14–29.
- Bond, G.C. & Lotti, R., 1995. Iceberg discharges into the north atlantic on millennial time scales during the last glaciation. *Science (New York, N.Y.)*, 267(5200), 1005–1010.
- Boulton, G.S., 1990. Sedimentary and sea level changes during glacial cycles and their control on glacial marine facies architecture. *Geological Society, London, Special Publications*, 53(1), 15–52.
- Boulton GS, Peacock JD, Sutherland DG. 1991. Quaternary. In *Geology of Scotland*, 3rd edn, Craig GY (ed.). The Geological Society: London; 503–543.
- Bowen, D. Q., Rose, J., McCabe, A. M., & Sutherland, D. G. 1986. Correlation of quaternary glaciations in England, Ireland, Scotland and Wales. *Quaternary Science Reviews*, 5, 299-340.
- Bowen, D. Q., Phillips, F. M., McCabe, A. M., Knutz, P. C., & Sykes, G. A. 2002. New data for the last glacial maximum in Great Britain and Ireland. *Quaternary Science Reviews*, 21(1), 89-101.
- Bradwell, T., Stoker, M. S., Golledge, N. R., Wilson, C. K., Merritt, J. W., Long, D., Everest, J.D., Hestvik, O.B., Stevenson, A.G., Hubbard, A.L., Finlayson, A.G & Mathers, H. E. 2008. The northern sector of the last British Ice Sheet: maximum extent and demise. *Earth-Science Reviews*, 88(3), 207-226.
- Charlesworth JK. 1924. The glacial geology of the north-west of Ireland. *Proceedings of the Royal Irish Academy B* 36: 174–314.
- Charlesworth. J. K. 1973. Stages in dissolution of the last ice-sheet in Ireland and Irish sea region. *Proceedings of the Royal Irish Academy Section B-Biological Geological and Chemical Science* 73(5): 79-86.
- Chiverrell, R.C. & Thomas, G.S.P., 2010. Extent and timing of the Last Glacial Maximum (LGM) in Britain and Ireland: a review. *Journal of Quaternary Science*, 25(4), 535–549.
- Chiverrell, R. C., Thrasher, I. M., Thomas, G. S., Lang, A., Scourse, J. D., van Landeghem, K. J., Mccarroll, D., Clark, C.D., Ó Cofaigh, C., Evans, D.J.A & Ballantyne, C. K. 2013. Bayesian modelling the retreat of the Irish Sea Ice Stream. *Journal of Quaternary Science*, 28(2), 200-209.
- Clark, J., McCabe, A., Schnabel, C., Clark, P. U., Freeman, S., Maden, C., & Xu, S. 2009. 10Be chronology of the last deglaciation of County Donegal, northwestern Ireland. *Boreas*, 38(1), 111-118.
- Clark, C. D., Hughes, A. L., Greenwood, S. L., Jordan, C., & Sejrup, H. P. 2012. Pattern and timing of retreat of the last British-Irish Ice Sheet. *Quaternary Science Reviews*, 44, 112-146.

- Clark, J., McCabe, A. M., Bowen, D. Q., & Clark, P. U., 2012. Response of the Irish Ice Sheet to abrupt climate change during the last deglaciation. *Quaternary Science Reviews*, 35, 100–115.
- Clark, P. U., Dyke, A. S., Shakun, J. D., Carlson, A. E., Clark, J., Wohlfarth, B., Mitrovica, J.X., Hostetler, S.W., & McCabe, A. M. 2009. The last glacial maximum. *science*, 325(5941), 710-714.
- Coastal and Marine Ecological Classification Standard. 2013. *Shell Hash (Substrate Subclass*. [Online]. [Accessed 15 January 2014] Available from: <http://www.cmecscatalog.org>
- Cowan, E. A., Cai, J., Powell, R. D., Clark, J. D., & Pitcher, J. N. 1997. Temperate glacimarine varves: an example from Disenchantment Bay, southern Alaska. *Journal of Sedimentary Research*, 67(3).
- Cowan, E. A., Seramur, K. C., Cai, J., & Powell, R. D. 1999. Cyclic sedimentation produced by fluctuations in meltwater discharge, tides and marine productivity in an Alaskan fjord. *Sedimentology*, 46(6), 1109-1126.
- Domack, E. W., & Lawson, D. E. 1985. Pebble fabric in an ice-rafted diamicton. *The Journal of Geology*, 577-591.
- Dowdeswell, J. a., Whittington, R.J. & Marienfeld, P., 1994. The origin of massive diamicton facies by iceberg rafting and scouring, Scoresby Sund, East Greenland. *Sedimentology*, 41(1), 21–35.
- Dowdeswell, J.A., Elverhøi, A. & Spielhagen, R., 1998. Glacimarine sedimentary processes and facies on the polar North Atlantic margins. *Quaternary Science Reviews*, 17(1-3), 243–272.
- Dowdeswell, J. a. & Cofaigh, C.O., 2002. Glacier-influenced sedimentation on high-latitude continental margins: introduction and overview. *Geological Society, London, Special Publications*, 203(1), 1–9.
- Dowdeswell, J. A., & Elverhøi, A. 2002. The timing of initiation of fast-flowing ice streams during a glacial cycle inferred from glacimarine sedimentation. *Marine Geology*, 188(1), 3-14.
- Dowdeswell, J.A., Cofaigh, C.Ó. & Pudsey, C.J., 2004. Thickness and extent of the subglacial till layer beneath an Antarctic paleo-ice stream. *Geology*, 32(1), 13-16.
- Dunlop, P., Shannon, R., McCabe, M., Quinn, R., & Doyle, E. 2010. Marine geophysical evidence for ice sheet extension and recession on the Malin Shelf: New evidence for the western limits of the British Irish Ice Sheet. *Marine Geology*, 276(1), 86-99.
- Elverhøi, A. et al., 1989. Glaciomarine sedimentation in epicontinental seas exemplified by the northern Barents Sea. *Marine Geology*, 85(2-4), 225–250.
- Evans, D.J.A., and Benn, D.I. 2004 A practical guide to the study of glacial sediments. London: Hodder Education.
- Evans, D. J. A., Phillips, E. R., Hiemstra, J. F., & Auton, C. A. 2006. Subglacial till: formation, sedimentary characteristics and classification. *Earth-Science Reviews*, 78(1), 115-176.
- Evans, J. & Pudsey, C.J., 2002. Sedimentation associated with Antarctic Peninsula ice shelves: implications for palaeoenvironmental reconstructions of glacimarine sediments. *Journal of the Geological Society*, 159(3), 233–237.
- Evans, J., Pudsey, C. J., Ó Cofaigh, C., Morris, P., & Domack, E. 2005. Late Quaternary glacial history, flow dynamics and sedimentation along the eastern margin of the Antarctic Peninsula Ice Sheet. *Quaternary Science Reviews*, 24(5), 741-774.

- Eyles, N., Eyles, C.H. & Miall, A.D., 1983. Lithofacies types and vertical profile models; an alternative approach to the description and environmental interpretation of glacial diamict and diamictite sequences. *Sedimentology*, 30(3), 393–410.
- Feyling-Hanssen, R.W., 1972. The Pleistocene/Holocene boundary in marine deposits from the Oslofjord area. *Boreas*, 1(3), 241–246.
- George, T.N. & Oswald, D.H., 1957. The Carboniferous rocks of the Donegal syncline. *Quarterly Journal of the Geological Society*, 113(1-4), 137–183.
- Gilbert, R., Nielsen, N., Desloges, J. R., & Rasch, M. 1998. Contrasting glaciomarine sedimentary environments of two arctic fiords on Disko, West Greenland. *Marine Geology*, 147(1), 63–83.
- Greenwood, S.L. & Clark, C.D., 2009. Reconstructing the last Irish Ice Sheet 2: a geomorphologically-driven model of ice sheet growth, retreat and dynamics. *Quaternary Science Reviews*, 28(27-28), 3101–3123.
- Grobe, H. 1987. A simple method for the determination of ice-rafted debris in sediment cores. *Polarforschung*, 57(3), 123–126.
- Haapaniemi, A. I., Scourse, J. D., Peck, V. L., Kennedy, H., Kennedy, P., Hemming, S. R., Furze, M.F.A., Pienkowski, A.J., Austin, W.E.N., Walden, J., Wadsworth, E. & Hall, I. R. 2010. Source, timing, frequency and flux of ice-rafted detritus to the Northeast Atlantic margin, 30–12 ka: Testing the Heinrich precursor hypothesis. *Boreas*, 39(3), 576–591.
- Heroy, D.C. & Anderson, J.B., 2007. Radiocarbon constraints on Antarctic Peninsula Ice Sheet retreat following the Last Glacial Maximum (LGM). *Quaternary Science Reviews*, 26(25-28), 3286–3297.
- Hillenbrand, C.-D., Baesler, a. & Grobe, H., 2005. The sedimentary record of the last glaciation in the western Bellingshausen Sea (West Antarctica): Implications for the interpretation of diamictites in a polar-marine setting. *Marine Geology*, 216(4), 191–204.
- Hogan, K. A., Dowdeswell, J. A., Noormets, R., Evans, J., & Ó Cofaigh, C. 2010a. Evidence for full-glacial flow and retreat of the Late Weichselian Ice Sheet from the waters around Kong Karls Land, eastern Svalbard. *Quaternary Science Reviews*, 29(25), 3563–3582.
- Hogan, K. A., Dowdeswell, J. A., Noormets, R., Evans, J., Ó Cofaigh, C., & Jakobsson, M. 2010b. Submarine landforms and ice-sheet flow in the Kvitøya Trough, northwestern Barents Sea. *Quaternary Science Reviews*, 29(25), 3545–3562.
- Howe, J.A., Stoker, M.S. & Woolfe, K.J., 2001. Deep-marine seabed erosion and gravel lags in the northwestern Rockall Trough, North Atlantic Ocean. *Journal of the Geological Society*, 158(3), 427–438.
- Howe, J. A., & Pudsey, C. J. 1999. Antarctic circumpolar deep water: a Quaternary paleoflow record from the northern Scotia Sea, South Atlantic Ocean. *Journal of Sedimentary Research*, 69(4).
- Howe, J. A., Stoker, M. S., Masson, D. G., Pudsey, C. J., Morris, P., Larter, R. D., & Bulat, J. 2006. Seabed morphology and the bottom-current pathways around Rosemary Bank seamount, northern Rockall Trough, North Atlantic. *Marine and Petroleum Geology*, 23(2), 165–181.
- Hubbard, A., Bradwell, T., Gollledge, N., Hall, A., Patton, H., Sugden, D., Cooper, R. & Stoker, M. 2009. Dynamic cycles, ice streams and their impact on the extent, chronology and deglaciation of the British–Irish ice sheet. *Quaternary Science Reviews*, 28(7), 758–776.

- Jennings, A. E., Hald, M., Smith, M., & Andrews, J. T. 2006. Freshwater forcing from the Greenland Ice Sheet during the Younger Dryas: evidence from southeastern Greenland shelf cores. *Quaternary Science Reviews*, 25(3), 282-298.
- Jennings, A. E., Walton, M. E., Ó Cofaigh, C., Kilfeather, A., Andrews, J. T., Ortiz, J. D., De Vernal, A. & Dowdeswell, J. A. 2014. Paleoenvironments during Younger Dryas-Early Holocene retreat of the Greenland Ice Sheet from outer Disko Trough, central west Greenland. *Journal of Quaternary Science*, 29(1), 27-40.
- Kaplan, M. R. 1999. Retreat of a tidewater margin of the Laurentide ice sheet in eastern coastal Maine between ca. 14 000 and 13 000 14C yr BP. *Geological Society of America Bulletin*, 111(4), 620-632.
- Kilfeather, A. A., Cofaigh, C. Ó., Lloyd, J. M., Dowdeswell, J. A., Xu, S., & Moreton, S. G. 2011. Ice-stream retreat and ice-shelf history in Marguerite Trough, Antarctic Peninsula: Sedimentological and foraminiferal signatures. *Geological Society of America Bulletin*, 123(5-6), 997-1015.
- Knight, J. & McCabe, A. M., 1997. Drumlin evolution and ice sheet oscillations along the NE Atlantic margin, Donegal Bay, western Ireland. *Sedimentary Geology*, 111(1-4), 57-72.
- Knutz, P.C., Zahn, R. & Hall, I.R., 2007. Centennial-scale variability of the British Ice Sheet: Implications for climate forcing and Atlantic meridional overturning circulation during the last deglaciation. *Paleoceanography*, 22(1), p.n/a–n/a.
- Kurtz, D.D. & Anderson, J.B., 1979. Recognition and Sedimentologic Description of Recent Debris Flow Deposits from the Ross and Weddell Seas, Antarctica. *SEPM Journal of Sedimentary Research*, 49(4).
- Lloyd, J. M., Park, L. A., Kuijpers, A., & Moros, M. 2005. Early Holocene palaeoceanography and deglacial chronology of Disko Bugt, west Greenland. *Quaternary Science Reviews*, 24(14), 1741-1755.
- Lloyd, J.M. 2006. Late Holocene environmental change in Disko Bugt, west Greenland: interaction between climate, ocean circulation and Jakobshavn Isbrae. *Boreas*, 35(1), 35-49.
- Mackiewicz, N. E., Powell, R. D., Carlson, P. R., & Molnia, B. F. 1984. Interlaminated ice-proximal glacial marine sediments in Muir Inlet, Alaska. *Marine Geology*, 57(1), 113-147.
- McCabe, A.M., 1986. Glaciomarine Facies Deposited by Retreating Tidewater Glaciers: An Example from the late Pleistocene of Northern Ireland. *Journal of Sedimentary Research*, 56(6).
- McCabe, A. M., Bowen, D. Q., & Penney, D. N. 1993. Glaciomarine facies from the western sector of the last British ice sheet, Malin Beg, County Donegal, Ireland. *Quaternary Science Reviews*, 12(1), 35-45.
- McCabe, M., Knight, J. & McCarron, S., 1998. Evidence for Heinrich event 1 in the British Isles. *Journal of Quaternary Science*, 13(6), 549-568.
- McCabe, A.M. & Clark, P.U., 2003. Deglacial chronology from County Donegal, Ireland: implications for deglaciation of the British-Irish ice sheet. *Journal of the Geological Society*, 160(6), 847-855.
- McCabe, A. M., Clark, P.U. & Clark, J., 2005. AMS 14C dating of deglacial events in the Irish Sea Basin and other sectors of the British-Irish ice sheet. *Quaternary Science Reviews*, 24(14-15), 1673-1690.
- McCabe, A. M., Clark, P.U. & Clark, J., 2007. Radiocarbon constraints on the history of the western Irish ice sheet prior to the Last Glacial Maximum. *Geology*, 35(2), p.147.

- Mitchell, G.F., Penny, L.F., Shotton, F.W., and West, R.G., 1973, A correlation of Quaternary deposits in the British Isles: Geological Society [London] Special Report 4, 1–99.
- Mix, A. C., Bard, E., & Schneider, R. 2001. Environmental processes of the ice age: land, oceans, glaciers (EPILOG). *Quaternary Science Reviews*, 20(4), 627-657.
- Ó Cofaigh, C., Lemmen, D. S., Evans, D. J. A., & Bednarski, J. 1999. Glacial landform–sediment assemblages in the Canadian High Arctic and their implications for late Quaternary glaciation. *Annals of Glaciology*, 28(1), 195-201.
- Ó Cofaigh, C., & Dowdeswell, J. A. 2001. Laminated sediments in glacialmarine environments: diagnostic criteria for their interpretation. *Quaternary Science Reviews*, 20(13), 1411-1436.
- Ó Cofaigh, C., Dowdeswell, J. A., & Grobe, H. 2001. Holocene glacialmarine sedimentation, inner Scoresby Sund, East Greenland: the influence of fast-flowing ice-sheet outlet glaciers. *Marine Geology*, 175(1), 103-129.
- Ó Cofaigh, C., Dowdeswell, J. A., Allen, C. S., Hiemstra, J. F., Pudsey, C. J., Evans, J., & Evans, D. J. A. 2005. Flow dynamics and till genesis associated with a marine-based Antarctic palaeo-ice stream. *Quaternary Science Reviews*, 24(5), 709-740.
- Ó Cofaigh, C., Evans, J., Dowdeswell, J. A., & Larter, R. D. 2007. Till characteristics, genesis and transport beneath Antarctic paleo-ice streams. *Journal of Geophysical Research: Earth Surface*, 112(F3).
- Ó Cofaigh, C., & Evans, D. J. 2007. Radiocarbon constraints on the age of the maximum advance of the British–Irish Ice Sheet in the Celtic Sea. *Quaternary Science Reviews*, 26(9), 1197-1203.
- Ó Cofaigh, C., Dunlop, P. & Benetti, S., 2012. Marine geophysical evidence for Late Pleistocene ice sheet extent and recession off northwest Ireland. *Quaternary Science Reviews*, 44, 147–159.
- Ó Cofaigh, C. Ó., Dowdeswell, J. A., Jennings, A. E., Hogan, K. A., Kilfeather, A., Hiemstra, J. F., Noormets, R., Evans, J., McCarthy, D.J., Andrews, J.T., Lloyd, J.M. & Moros, M. 2013. An extensive and dynamic ice sheet on the West Greenland shelf during the last glacial cycle. *Geology*, 41(2), 219-222.
- Olausson, E. 1982. The Pleistocene/Holocene boundary in southwestern Sweden, Sveriges Geologiska Undersökning, C 346 (1982), p. 107
- Ottesen, D. & Dowdeswell, J. A., 2006. Assemblages of submarine landforms produced by tidewater glaciers in Svalbard. *Journal of Geophysical Research*, 111(F1).
- Park, R. G. 1997. Foundations of structural geology. Chapman & Hall, London. p. 192.
- Peck, V. L., Hall, I. R., Zahn, R., Elderfield, H., Grousset, F., Hemming, S. R., & Scourse, J. D. 2006. High resolution evidence for linkages between NW European ice sheet instability and Atlantic Meridional Overturning Circulation. *Earth and Planetary Science Letters*, 243(3), 476-488.
- Peck, V. L., Hall, I. R., Zahn, R., Grousset, F., Hemming, S. R., & Scourse, J. D. 2007. The relationship of Heinrich events and their European precursors over the past 60ka BP: a multi-proxy ice-rafted debris provenance study in the North East Atlantic. *Quaternary Science Reviews*, 26(7), 862-875.
- Polyak, L. & Solheim, A., 1994. Late- and postglacial environments in the northern Barents Sea west of Franz Josef Land Physiographic features. 13(2), 197–207.

- Pudsey, C. J., Murray, J. W., Appleby, P., & Evans, J. 2006. Ice shelf history from petrographic and foraminiferal evidence, Northeast Antarctic Peninsula. *Quaternary Science Reviews*, 25(17), 2357–2379.
- Reimer, P., 2013. IntCal13 and Marine13 Radiocarbon Age Calibration Curves 0–50,000 Years cal BP. *Radiocarbon*, 55(4), 1869–1887.
- Sacchetti, F., Benetti, S., Georgiopoulou, A., Shannon, P. M., O'Reilly, B. M., Dunlop, P., Quinn, R., & Ó Cofaigh, C. 2012. Deep-water geomorphology of the glaciated Irish margin from high-resolution marine geophysical data. *Marine Geology*, 291, 113–131.
- Sacchetti, F., Benetti, S., Ó Cofaigh, C., & Georgiopoulou, A. 2012. Geophysical evidence of deep-keeled icebergs on the Rockall Bank, Northeast Atlantic Ocean. *Geomorphology*, 159, 63–72.
- Salvi, C., Busetti, M., Marinoni, L., & Brambati, A. 2006. Late Quaternary glacial marine to marine sedimentation in the Pennell Trough (Ross Sea, Antarctica). *Palaeogeography, Palaeoclimatology, Palaeoecology*, 231(1), 199–214.
- Scourse, J.D., Haapaniemi, A. I., Colmenero-Hidalgo, E., Peck, V. L., Hall, I. R., Austin, W. E., Knutz, P. C., and Zahn, R. 2009. Growth, dynamics and deglaciation of the last British–Irish ice sheet: the deep-sea ice-rafted detritus record. *Quaternary Science Reviews*, 28(27–28), 3066–3084.
- Shanmugam, G., 2000. 50 years of the turbidite paradigm (1950s–1990s): deep-water processes and facies models—a critical perspective. *Marine and Petroleum Geology*, 17(2), 285–342.
- Stevens, R.L., 1990. Proximal and distal glacialmarine deposits in southwestern Sweden: contrasts in sedimentation. *Geological Society, London, Special Publications*, 53(1), 307–316.
- Stuiver, M. Reimer, P.J. and R. Reimer. 1986. *CALIB Radiocarbon Calibration*. Available: <http://calib.qub.ac.uk/calib/>.
- Synge, F., 1969. The Wurm ice limit in the west of Ireland. In: Wright Jr., H.E. (Ed.), *Quaternary Geology and Climate*. National Academy of Sciences, Washington, D.C., 89–92.
- Synge, F.M., 1978. Pleistocene events. In: Davies, G.L., Stephens, N. (Eds.). *Ireland*, Methuen and Co Ltd., London, 115–180.
- Talling, P.J., 2013. Hybrid submarine flows comprising turbidity current and cohesive debris flow: Deposits, theoretical and experimental analyses, and generalized models. *Geosphere*, 9(3), 460–488.
- van der Meer, J. J. M., 1993. Microscopic evidence of subglacial deformation. *Quaternary Science Reviews*, 12(7), 553–587.
- Warren WP. 1992. Drumlin orientation and the pattern of glaciation in Ireland. *Sveriges Geologiske Undersökelse 81*: 359–366.
- Wilson, L.J. & Austin, W.E.N., 2002. Millennial and sub-millennial-scale variability in sediment colour from the Barra Fan, NW Scotland: implications for British ice sheet dynamics. *Geological Society, London, Special Publications*, 203(1), 349–365.

Appendices

Appendix 1: Foraminifera taxonomic list

Astronium spp
Bolivina (Brasilina) spp
Cassidulina laevigata
Cassidulina reniforme
Cibicides lobatulus
Cyclogyra spp
Dentalina spp
Elphidium excavatum
Elphidium excavatum forma clavata
Elphidium magellanicum
Elphidium margeratasium
Elpdium spp
Fissurina spp
Glabratella milletti
Globulina spp
Lagena spp
Millionella
Nonion labradoricum

Nonion obiculare
Nonionella turgida
Nonion spp
Ooalina mello
Parafissurina spp
Pyrgo williamsoni
Pyrgo spp
Quinqueloculina agglutinate
Quinqueloculina seiminulum
Quinquequoculina spp
Reophax spp
Rosalina spp
Triloculina trihedral
Virgulina spp
Molluscs
Pteropod
Molluscs spp

Appendix 2: Foraminifera counts of core CE-08-003

Sample depth (cm)	Cassidulina reniforme	Elphidium excavatum forma clavata	Elphidium excavatum	Elpidium spp	Astronium spp	Bolivina (Brasilina) spp	Cassidulina laevigata	Cibicides lobatulus	Cyclogyra spp	Dentalina spp	Elphidium magellanicum	Elphidium margeratasium	Fissurina spp	Glabrata milleti	Globulina spp	Lagena spp	Millionella
162-163	13	5	5	3	0	1	5	40	0	0	4	2	4	7	0	1	3
179-180	11	5	2	7	0	0	2	29	0	0	3	0	4	7	0	0	8
424-425	124	23	9	45	0	8	1	3	8	0	11	0	3	0	0	0	0
441-442	126	29	10	34	1	9	0	0	1	0	9	0	2	0	0	3	0
458-459	183	46	3	7	0	5	0	5	0	0	15	0	2	0	0	1	0
475-476	170	32	7	40	0	3	0	9	2	0	4	0	3	0	2	3	0
492-493	196	30	9	10	0	3	0	8	0	0	14	0	2	0	0	0	0
509-510	167	53	13	13	0	10	0	1	2	0	14	1	0	0	0	0	0

Appendix 3: Foraminifera counts of core CE-08-003 continued

Nonion labradoricum	Nonion obiculare	Nonionella turgida	Nonion spp	Ooalina mello	Parafissurina spp	Pyrgo williamsoni	Pyrgo spp	Quinqueloculina agglutinata	Quinqueloculina seiminulum	Quinquequoculina spp	Reophax spp	Rosalina spp	Triloculina trihedra	Virgulina spp	Unidentified spp	Total	Molluscs	Pteropod	Total
0	0	25	0	4	0	0	0	0	16	28	0	20	0	12	0	198	23	241	264
0	0	1	0	1	0	0	0	0	3	19	0	8	0	4	1	115	2	196	198
1	3	0	0	0	2	8	0	3	4	8	1	23	8	3	1	300	0	0	0
4	1	0	3	0	0	24	0	1	2	4	0	30	7	0	0	300	0	0	0
2	1	0	1	0	0	5	3	3	1	4	0	7	3	3	0	300	0	0	0
0	0	0	0	0	0	1	0	6	0	0	0	10	5	0	3	300	0	0	0
2	8	0	2	0	0	0	0	2	0	0	0	5	4	1	4	300	0	0	0
4	1	0	0	0	0	3	0	1	2	0	0	11	3	1	0	300	0	0	0

Appendix 4: Foraminifera counts of core CE-08-010

Sample depth (cm)	Cassidulina reniforme	Elphidium excavatum forma clavata	Elphidium excavatum	Elpidium spp	Astronium spp	Bolivina (Brasilina) spp	Cassidulina laevigata	Cibicides lobatulus	Cyclogyra spp	Dentalina spp	Elphidium magellanicum	Elphidium margaritatum	Fissurina spp	Glabratella milleti	Globulina spp	Lagena spp	Millionella	Nonion labradoricum
258-259	139	1	3	45	0	11	0	6	5	4	11	0	1	0	15	0	3	7
275-276	233	18	12	14	0	2	0	13	0	0	3	0	0	0	0	0	0	2
430-431	156	39	6	14	0	8	0	30	4	0	8	0	2	0	3	2	0	1
447-448	3	2	2	6	0	2	0	3	8	0	1	0	5	0	0	3	0	2
464-465	180	49	10	15	1	3	0	16	0	2	5	0	4	0	0	1	0	2
481-482	187	30	13	21	0	4	0	9	0	0	3	0	8	0	0	0	0	8
498-499	6	0	0	0	0	1	0	0	0	0	0	0	0	0	1	0	0	0
515-516	177	57	8	8	0	1	0	21	0	0	4	0	2	0	2	1	0	1

Appendix 5: Foraminifera counts of core CE-08-010 continued

Nonion obiculare	Nonionella turgida	Nonion spp	Ooalina mello	Parafissurina spp	Pyrgo williamsoni	Pyrgo spp	Quinqueloculina agglutinata	Quinqueloculina seiminulum	Quinquequoculina spp	Reophax spp	Rosalina spp	Triloculina trihedra	Virgulina spp	Unidentified spp	Total
0	0	0	0	0	0	0	0	5	11	0	24	6	3	0	300
1	0	0	0	0	0	0	0	0	0	0	0	1	1	0	300
0	0	0	0	0	1	0	0	6	5	0	11	2	0	2	300
1	0	0	0	0	1	0	0	4	4	0	3	2	1	1	54
0	0	0	0	0	0	0	0	2	0	0	8	2	0	0	300
0	0	0	0	0	2	0	0	0	0	0	7	8	0	0	300
0	0	0	0	0	0	0	0	0	0	0	1	2	0	0	11
0	0	0	0	0	6	0	1	2	0	0	7	2	0	0	300